Cardio-metabolic risk profile of people living with HIV: Is retinal microvascular geometric morphology a marker of effect?

by

Boipelo Mirriam Lepetjia Kgokane

Thesis presented in fulfilment of the requirements for the degree of Master of Science in the Faculty of Medicine and Health Sciences at Stellenbosch University

Supervisor: Prof Hans Strijdom
Co-supervisor: Dr Frans Everson
Co-supervisor: Dr Festus Kamau

April 2022

Declaration:

By submitting this thesis electronically, I declare that the entirety of the work contained therein is my own, original work, that I am the sole author thereof (save to the extent explicitly otherwise stated), that reproduction and publication thereof by Stellenbosch University will not infringe any third-party rights and that I have not previously in its entirety or in part submitted it for obtaining any qualification.

Boipelo Mirriam Lepetjia Kgokane

April 2022

Abstract

Background and Aim

Cardiovascular disease in people living with HIV has become of great concern. HI-viral factors, ART-toxicity and HIV/ART-associated cardiometabolic adverse effects have been implicated in the development of cardiovascular disease. Retinal microvascular geometric features may be potential useful markers of these effects. We aimed to investigate whether altered retinal microvascular geometric features are markers of HIV, ART and/or HIV/ART-associated cardiometabolic effects in a study population from the Western Cape Province.

Methods

The study followed a cross-sectional (HIV-free: n = 88 and HIV+ART: n = 122) and longitudinal (baseline *vs.* 18-month follow-up for HIV+ART only: n = 82) study design. Volunteering participants were recruited from health care clinics. Demographic, lifestyle, socioeconomic and anthropometric data were collected. Fasting blood and urine samples were collected and transported to the National Health Laboratory Services for biochemical analyses. Retinal images were obtained (Canon CR-2 camera) and vessel features quantified (MONA REVA 2.1.1 software). Linear stepwise regression (cross-sectional) and linear mixed model (longitudinal) analyses were applied to elucidate independent associations and statistical significance of $p < 0.05$.

Results

Population characteristics: The study population was relatively young (HIV-free:44.06±11.09 and HIV+ART:40.35±8.94years) and mostly women (HIV-free:80.7% and HIV+ART:63.1%). The baseline median/mean viral load (VL), CD4 cell count and ART-duration were 50 (10 to 675032) copies mRNA/mL, 539.92±237.16 cells/mm^3 and 166 (1 to 707) weeks respectively. **Cardiometabolic results:** Body mass index (BMI) (24.50±6.65 *vs.* 28.25±7.68kg/m^2, $p < 0.001$) was significantly lower in HIV+ART *vs.* HIV-free. ΔBMI in HIV+ART was significantly correlated with average arterial tree diameter ($r = 0.323$, $p < 0.05$), total length of skeletonised tree ($r = 0.355$, $p < 0.01$) and arteriolar branching angle ($r = 0.234$, $p < 0.05$). High density lipoprotein-cholesterol (1.59±0.74 *vs.* 1.39±0.45mmol/L, $p = 0.019$) and gamma-glutamyl transferase (GGT) (43.5 (14 to 494) *vs.* 27.0 (11 to 814)U/L, $p < 0.001$) were significantly higher in HIV+ART *vs.* HIV-free, but decreased in HIV+ART (Baseline *vs.* Follow-up HDL:1.62±0.77 *vs.* 1.44±0.64mmol/L, $p = 0.017$ and GGT:45 (14 to 494) *vs.* 41.50 (14 to 219)U/L, $p = 0.004$). HDL was significantly correlated with central retinal venular equivalent (CRVE) (r =-0.195, $p < 0.01$) and GGT with venular branching optimality ($r = 0.180$, $p < 0.05$). **HIV and ART results:** Cross-sectionally, HIV+ART status independently associated with CRVE (-0.146 (-0.280 to -0.012), $p = 0.033$) and arteriolar and venular mother branch (D0), first daughter branch (D1) and second daughter branch (D2) ($p < 0.05$, respectively). VL (-0.198 (-0.025 to -0.001), $p = 0.037$) and ART-duration (0.188 (0.001 to 0.024), $p = 0.047$) were independently associated with arteriolar-venular ratio (AVR). Longitudinally, VL independently associated with CRVE (0.096 (0.017 to 0.175), $p = 0.018$) and AVR (-0.003 (-0.0006 to 0.000003), $p = 0.046$). CD4 cell count was independently associated with number of branchpoints

(0.042 (-0.002 to 0.086), *p*=0.006) and endpoints (3.0 (0.750 to 5.250), *p*=0.010). HIV duration independently associated with lacunarity (-0.0080 (-0.0150 to -0.0010), *p*=0.036) and fractal analyses (0.011 (0.0001 to 0.021), *p*=0.045). 2nd-line ART was independently associated with CRVE (8.58 (0.35 to 16.81), *p*=0.041) and ART-duration with fractal analysis (-0.022 (-0.037 to -0.008), *p*=0.003).

Discussion and conclusion

HIV+ART appeared to have a more favourable cardiovascular risk profile *vs.* HIV-free. Various markers of HIV/ART and HIV-ART-associated cardiometabolic risk factors were associated with retinal vessel features and associations appeared mostly favourable/cardioprotective. These results indicate that retinal vessel geometric features may be potential markers of the effects of HIV/ART and/or associated cardiometabolic risk factors in the current study population.

[498 words]

Opsomming

Agtergrond en Doelstelling

Kardiovaskulêre siekte in MIV-positiewe individue wek groot kommer. MI-virale faktore, antiretrovirale terapie (ART)-toksisiteit en MIV/ART-geassosieerde kardiometaboliese newe-effekte word geïmpliseer. Retinale mikrovaskulêre geometriese patrone mag potensieël nuttige merkers van hierdie effekte wees. Die doel van hierdie studie was om te ondersoek of veranderinge in retinale mikrovaskulêre geometriese patrone as merkers van MIV, ART en/of MIV/ART-geassosieerde kardiometaboliese effekte in 'n studie populasie van die Wes-Kaap beskou kan word.

Metodes

Die studie het 'n deursnee (MIV-vry: n = 88 en MIV+ART: n = 122) en longitudinale (basislyn *vs.* 18-maande opvolg vir slegs MIV+ART: n = 82) studie-ontwerp gevolg. Vrywillige deelnemers was vanaf gesondheidsorg klinieke gewerf. Demografiese, lewenstyl, sosio-ekonomiese en antropometriese inligting is ingewin. Vastende bloed- en urinemonsters was versamel en na die NHLS vervoer vir biochemiese ontledings. Retinale beelde was vasgelê (Canon CR2-kamera) en bloedvat patrone was gekwantifiseer (MONA REVA 2.1.1 sagteware). Liniêre, stapsgewyse regressie (deursnee studie) en liniêre gemengde model (longitudinale studie) analises was aangewend om onafhanklike assosiasies te ondersoek (statistiese beduidenheid: p<0.05).

Resultate

Populasie eienskappe: Die studie populasie was relatief jonk (MIV-vry:44.06±11.09 en MIV+ART:40.35±8.94 jaar) en het meestal uit vroue bestaan (MIV-vry:80.7% and MIV+ART:63.1%). Die basislyn mediaan/gemiddelde virale lading (VL), CD4 seltelling en ART-duur was onderskeidelik 50 (10 tot 675032) kopieë bRNA/mL, 539.92±237.16 selle/mm^3 and 166 (1 to 707) weke. **Kardiometaboliese resultate:** Liggaam-massa-indeks (BMI) (24.50±6.65 *vs.* 28.25±7.68kg/m^2, p<0.001) was betekenisvol laer in MIV+ART *vs.* MIV-vry. ΔBMI in MIV+ART was betekenisvol gekorreleer met die gemiddelde arteriële boom deursnit (r=0.323, p<0.05), totale lengte van die skelet boom (r=-0.355, p<0.01) en arteriolêre vertakkingshoek (r=0.234, p<0.05). HDL-cholesterol (1.59±0.74 *vs.* 1.39±0.45mmol/L, p=0.019) en GGT (43.5 (14 to 494) *vs.* 27.0 (11 to 814) U/L, p<0.001) was betekenisvol hoër in MIV+ART *vs.* MIV-vry, maar laer in MIV+ART (Basislyn *vs.* Opvolg HDL:1.62±0.77 *vs.* 1.44±0.64mmol/L, p=0.017 en GGT:45 (14 to 494) *vs.* 41.50 (14 tot 219)U/L, p=0.004). HDL het betekenisvol gekorreleer met CRVE (r=-0.195, p<0.01), en GGT met venulêre vertakking (r=0.180, p<0.05). **MIV en ART resultate:** Deursnee studie: MIV+ART status was onafhanklik geassosieer met CRVE (-0.146 (-0.280 tot -0.012), p=0.033), en arteriolêre en venulêre D0, D1 en D2 (p<0.05 onderskeidelik). VL (-0.198 (-0.025 tot -0.001), p = 0.037) and ART-duur (0.188 (0.001 tot 0.024), p=0.047) het onafhanklik met AVR geassosieer. Longitudinale studie: VL was onafhanklik geassosieer met CRVE (0.096 (0.017 tot 0.175), p=0.018) en AVR (-0.003 (-0.0006 tot 0.000003), p=0.046). CD4 telling was onafhanklik geassosieer met die aantal takpunte (0.042 (-0.002 tot 0.086), p=0.006) en eindpunte (3.0 (0.750 to 5.250), p=0.010). MIV-duur was onafhanklik geassosieer met lakunariteit (-0.0080 (-0.0150 tot -0.0010), p=0.036) en fraktale analises (0.011 (0.0001 tot 0.021), p=0.045). Tweede-lyn ART was onafhanklik

geassosieer met CRVE (8.58 (0.35 tot 16.81), *p*=0.041) en ART-duur met fraktale analise (-0.022 (-0.037 tot -0.008), *p*=0.003).

Bespreking en gevolgtrekking

MIV+ART individue blyk oor die algemeen ‘n meer gunstige kardiovaskulêre profiel te toon as mense sonder MIV. Verskeie merkers van MIV/ART en MIV-ART-geassosieerde kardiometaboliese risiko faktore was met retinale bloedvat eienskappe geassosieer, en die assosiasies was meestal gunstig / kardiobeskermend. Hierdie resultate dui daarop dat retinale bloedvat geometriese eienskappe as potensiële merkers van die effekte van MIV/ART en/of geassosieerde kardiometaboliese risiko faktore in die huidige studie populasie beskou kan word.

Dedication

To my late father, I love you always.

Acknowledgements

- To my loving parents, thank you for your unwavering support and encouragement. I thank God for the two of you.
- To my supervisors, thank you for persistently believing in me, for being thoughtful and patient, and for sharing your expertise with me. I am honoured to have been guided by the greatest.
- Thank you, Dr Frans Everson, for being the wind beneath my wings. This could have not been possible without you. I am indebted to you.
- EndoAfrica, thank you for the lovely experience of working with an incredible team.
- To the Division of Medical Physiology, thank you for creating a conducive learning environment. Your kindness and willingness to help allowed me to prosper.
- Thank you to Stellenbosch University, Sankie Strauss, Division of Medical Physiology and Maties football club for your financial assistance.
- To my friends, thank you for being my home away from home, for the laughter, for the banter and for the spontaneous karaoke sessions.
- To my partner in crime, thank you for the emotional support. You made this journey memorable.

Table of contents

List of abbreviations

ABC	: Abacavir
AIDS	: Acquired immunodeficiency syndrome
ART	: Antiretroviral therapy
ATV	: Atazanavir
AVR	: CRAE to CRVE ratio
AZT	: Zidovudine
3TC	: Lamivudine
BMI	: Body mass index
BRAO	: Branch arterial occlusion
CCR5	: C-C chemokine receptor type 5
CD4	: Cluster of differentiation 4
CHD	: Coronary heart disease
CKD	: Chronic kidney disease
CRAE	: Central retinal arteriolar equivalent
CRVE	: Central retinal venular equivalent
CVD	: Cardiovascular disease
CRVO	: Central retinal vein occlusion
CXCR4	: C-X-C chemokine receptor type 4
DBP	: Diastolic blood pressure
D0	: Diameter of mother branch
D1 and D2	: Diameter of daughter branches
d4T	: Stavudine
D*f*	: Fractal dimensions
DNA	: Deoxyribonucleic acid
DRV	: Darunavir
DTG	: Dolutegravir
EDTA	: Ethylenediamine tetra-acetic acid
EFV	: Efavirenz

eGFR	: Estimated glomerular filtration rate
FIs	: Fusion inhibitors
FTC	: Emtricitabine
GGT	: Gamma-glutamyl transferase
Hb	: Haemoglobin
HbA1c	: Glycated haemoglobin
HDL-C	: High-density lipoprotein cholesterol
HIV	: Human immunodeficiency virus
HIV+ART	: HIV positive on ART
hsCRP	: High-sensitivity c-reactive protein
ICAM-1	: Intercellular adhesion molecule-1
IL-6	: Interleukin-6
INSTIs	: Integrase strand transfer inhibitors
LDL-C	: Low-density lipoprotein cholesterol
LMIC	: Low-to-middLe income countries
LPV	: Lopinavir
NCD	: Noncommunicable disease
NHLS	: National Health Laboratory Service
NNRTIs	: Non-nucleoside reverse transcriptase inhibitors
NRTIs	: Nucleoside reverse transcriptase inhibitors
NVP	: Nevirapine
PIs	: Protease inhibitors
PLWH	: People living with HIV
r	: Ritonavir
RNA	: Ribonucleic acid
SBP	: Systolic blood pressure
ssRNA	: Single strand RNA
SA	: South Africa
SSA	: sub-Saharan Africa

TB : Tuberculosis

TDF : Tenofovir

T2DM : Type 2 diabetes mellitus

TNF-α : Tumour necrosis factor alpha

USA : United States of America

WHR : Waist-to-hip ratio

List of figures

List of tables

Chapter 1
Introduction

1.1. Introduction

Cardiovascular disease (CVD) is the leading cause of death worldwide and contribute to over 17.9 million deaths annually (1). Mortality due to CVD is on an upward trend in low-to-middle income countries (LMIC), including countries in sub-Saharan Africa (SSA) (2). Although about 80% of global CVD occurs in developing regions such as Africa, CVD receives less research attention compared to the developed world (3). CVD furthermore increases pressure on health care systems in LMIC as these countries are simultaneously under an even greater burden from communicable diseases such as HIV/AIDS and tuberculosis (4). Early cardiovascular risk assessment is critical to ensure that preventative strategies are employed to curb the burden of CVD (5).

Various risk factors are associated with CVD. Traditional modifiable cardiovascular risk factors include hypertension, smoking, dietary factors (e.g., high fat and salt consumption), obesity and physical inactivity while non-modifiable risk factors include various genetic and biological factors such as gender and age (6,7). Emerging risk factors such as HIV infection and treatment of HIV-infected patients with antiretroviral therapy (ART) play a significant role in the development of CVD (8,9). People living with HIV (PLWH) are estimated to be at a 2-fold increased risk for developing CVD compared to the general population (10,11). This is of great concern in sub-Saharan Africa (SSA) as the region is home to the largest number (19.6 million) of PLWH globally (12). South Africa (SA) in particular has approximately 7.7 million PLWH and more than 5 million of them are on ART (13). Even though the pathophysiology of HIV- and ART-associated CVD is not clearly understood, it is necessary to assess the cardiovascular and cardio-metabolic risk profile of PLWH in SA to mitigate the CVD burden in this particular population (14). Rapid, non-invasive and relatively inexpensive tools such as retinal microvascular imaging have shown to be valuable in cardiovascular research, but more investigation in South African populations are needed (15).

Retinal imaging in PLWH is currently gaining more research interest as HIV- and ART-associated cardiovascular risk factors such as dyslipidaemia, hypertension and diabetes have been associated with various retinal microvascular geometric features such vessel calibre, vessel network features and vessel branching angles (15,16). Retinal microvascular features as markers of HIV- and ART-associated cardiovascular risk in SA may have valuable application, but is still underexplored (17). Therefore, the current study aims to investigate whether retinal features can be used as a marker of effect of CVD risk in PLWH from the Worcester area of SA.

1.2. Cardiovascular disease (CVD)

CVD collectively refers to disease conditions related to the heart and blood vessels (18). Cumulative exposure to cardiovascular risk factors throughout life increases the risk for developing CVD (18–20). Cardiovascular risk factors contribute to the development of CVD through various pathophysiological pathways **(Figure 1.1)**

(21). According to the World Health Organisation (WHO), modifiable lifestyle cardiovascular risk factors such as an unhealthy diet, obesity and smoking, are mostly responsible for the development of CVD globally (5,22).

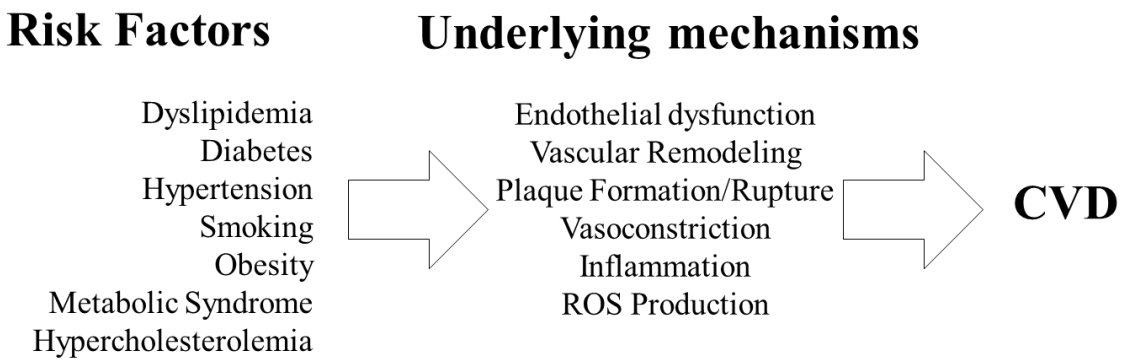

Figure 1.1*. Pathophysiological mechanisms linking cardiovascular risk factors to CVD* (23–25). ***Abbreviations****: CVD: Cardiovascular disease.*

1.3. CVD epidemiology

CVD is the leading cause of death worldwide (5,19,21). The WHO reported 17.9 million global CVD deaths in 2016 (26). More than 75% of these deaths occur in LMIC (21,27). It is estimated that global CVD deaths will increase to 24 million by 2030 (28–30).

SSA is experiencing epidemiological transition with a dual burden of infectious and noncommunicable diseases (NCD) (31) (32). NCD are becoming more common in LMIC with CVD being the biggest contributor to the NCD mortality rate with more than 75% of global CVD deaths (19,32,33). The WHO estimates the CVD burden will double in SSA by 2030 (33–35). The increased burden of CVD in SSA is mostly attributed to risk factors such as hypertension, smoking, and obesity, alcohol use and hypercholesterolaemia (33,36). According to the INTERHEART study, risk factors such as smoking, hypertension, abdominal obesity and diabetes account for about 90% risk of first myocardial infarction in the nine African countries evaluated in their study and about 30% of women in Africa are classified as obese, which is a major cardiovascular risk factor (33). Evidence shows that levels of income, education, urban living and psychosocial stress are strong determinants of cardiovascular risk in SSA (33). It is also estimated that 10.8 million people in Africa suffer from type 2 diabetes mellitus (T2DM), which is a major cardiometabolic risk factor (33). Despite these high rates, research related to cardiovascular risk factors and CVD in Africa is underwhelming compared to developed countries (33,34).

The situation in SA is not different, and the burden of NCD in SA is higher than in many developed countries (33,37). CVD, in particular, is the leading cause of NCD mortality in SA (37% of all NCD and 17% of all deaths in SA) (37–41). According to Statistics SA, the biggest contributors to CVD in SA are heart failure, cardiac arrest and cardiomyopathy (42). SA also has a high prevalence of cardiovascular risk factors such as obesity, high blood pressure (systolic or diastolic), elevated total cholesterol levels and smoking **(Figure 1.2.)** (33,35).

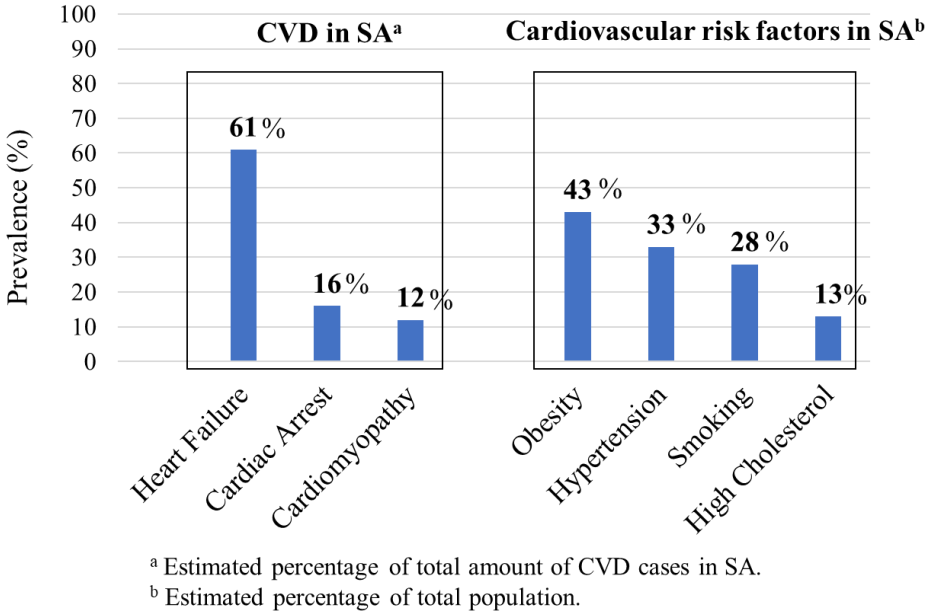

Figure 1.2*. Estimated prevalence of CVDs and major cardiovascular risk factors in SA* (33,35,42).
Abbreviations: *CVD: Cardiovascular disease, SA: South Africa.*

Considering the acceleration of epidemiological transition in SA and that diseases such as CVD and diabetes are on the rise, the health care costs incurred could be devastating to South Africans and the health care system (37,43). Early detection measures to assess and prevent CVD in SA are thus needed.

1.4. Traditional cardiovascular risk factors

Cardiovascular risk factors can be sub-classified into two main categories: Modifiable and non-modifiable cardiovascular risk factors. Modifiable cardiovascular risk factors such as hypertension, an unhealthy lifestyle and diet, obesity, and socioeconomic factors can be mitigated through intervention strategies such as therapeutics and lifestyle modification (5,6,44). On the other hand, non-modifiable cardiovascular risk factors include age, sex and family history (45–50).

1.4.1. Modifiable cardiovascular risk factors

Abnormal lipid profiles such as hypercholesterolaemia, hypertriglyceridaemia and/or high levels of low-density lipoprotein cholesterol (LDL-C) and/or low levels of high-density lipoprotein cholesterol (HDL-C) are associated with increased CVD risk (21,51). The WHO estimates that abnormal blood lipid levels contribute to an estimated 2.6 million deaths each year, this is mostly prevalent in high-income countries (5). Factors that contribute to abnormal lipid levels include, but are not limited to, unhealthy dietary practices that are high in saturated fats/ high calorie and a lack of exercise (5,19).

Diabetes mellitus is a disorder that results from inadequate insulin production or inability of tissues to respond to circulating insulin and is considered a major cardiovascular risk factor (52,53). Research has estimated that a diabetic patient/person is twice at risk of developing CVD compared to a non-diabetic individual (5,53). The South African Heart and Stroke Foundation defines fasting blood glucose levels of < 5.6 mmol/L as the normal,

6-6.9 mmol/L as risk for future diabetes and hyperglycaemia ≥ 7 mmol/L level is classified as diabetes (54). Diabetes has major effects on various body systems as insulin, secreted by pancreatic beta cells, induces glucose uptake in cardiomyocytes, skeletal muscle, and adipose tissue through various signaling pathways (53).

An unhealthy diet is mostly composed of high energy dense foods such as saturated, trans-fats and carbohydrates, as well as, sodium and/or a diet lacking in vitamins and minerals (55–57). An estimated 31% of CVD globally is attributed to a diet high in saturated fats and is rising in high-, middle- and low-income countries (5,53). Also, most populations consume high levels of sodium, a major contributor to hypertension and CVD (5,58,59).

Globally, an estimated 1.46 billion adults are overweight (BMI ≥ 25 kg/m²), about 500 million are obese (BMI ≥ 30 kg/m²) and more than 115 million suffer from obesity-related morbidities (34,60). Also, each year an estimated 2.8 million people die as a result of obesity (5,46). Not only is obesity a health care problem in developed countries, it is now a growing health concern in LMIC, including many African countries (33,34,55,60,61). Adiposity (overweight/obesity) is mainly caused by consuming high energy foods such as fatty foods in combination with low energy expenditure such as exercise (59). Obesity is strongly associated with various cardiovascular risk factors such as inflammation, insulin resistance, diabetes, hypercholesterolaemia and hypertension (53,59,60,62,63).

Hypertension is the biggest contributor to stroke and a major risk factor for heart disease (20,64). In 2008, an estimated 1 billion individuals worldwide had hypertension (systolic ≥ 140 or diastolic ≥ 90 mm Hg) (60). An annual estimation of 7.5 million deaths globally is attributed to hypertension each year (about 12.8% of all deaths each year) (5,21).

Socioeconomic factors such as poverty, stress, social isolation, education level, anxiety and depression have been linked to the rising prevalence of CVD, and mortality risk (85–87). The dimensions of socioeconomic factors are complex and often interrelated (66) (65). For instance, stress can involve emotional, cognitive, behavioural, environmental and physiological processes (67), while poverty can contribute to stress as income represents affordability and is often associated with a better quality of living (65). Levels of education and income are often closely related and are also indicators of general health status (65).

Unhealthy lifestyle in terms of excessive alcohol consumption and tobacco smoking are cardiovascular risk factors. There appears to be a fine balance between alcohol consumption and cardiovascular risk (5). According to the WHO, alcohol consumption of two drinks per day reduces risk of heart disease by 30 %, however, excessive alcohol consumption beyond this limit has adverse cardiovascular effects (5). An estimated 2.3 million deaths per year (3.8 % of global deaths) are attributed to harmful alcohol consumption and is a major concern across all socioeconomic levels (5). Although moderate alcohol consumption often exhibit anti-inflammatory effects (68) and acts as a nervous system suppressant, excessive alcohol use is harmful to a person's health as factors such as lipopolysaccharide and complements activate innate immunity and stimulates Kupffer cells to induce oxidative stress and to produce proinflammatory cytokines such as tumor necrosis

factor alpha (TNF-α) that cause hepatocellular damage resulting in the initiation and promotion of alcoholic liver injury (68). Excessive alcohol use also causes harm to the heart through the development of cardiomyocyte apoptosis, mitochondrial dysfunction, decreased protein synthesis and excitation-contraction coupling dysfunction as a result of an increase in cardiac oxidative and nitrosative stress (69).

Tobacco smoking is also a major health concern and a cardiovascular risk factor (6). Globally, an estimated 1.3 billion people use tobacco and contributes largely to global morbidity and mortality rates estimated to be 6 million people each year (21,35,36). It was furthermore projected that by 2020, 7.5 million people will die each year of tobacco-related complications and 8.3 million by 2030 (5,19,70). Smoking is also responsible for 71 % of lung cancers, 42 % of chronic respiratory disease and about 10 % of CVD (5). Cigarette smoking promotes atherosclerosis influenced through multiple pathways involved in cellular processes such as inflammation, cell migration and proliferation (70).

1.4.2. Non-modifiable cardiovascular risk factors

Non-modifiable cardiovascular risk factors are often related to genetic factors that predispose a person to increased risk for CVD (45,46). Ageing alone, for example, induces the dilation of large arterial walls, especially the intima, and the media exhibit increased collagen content and frayed elastin (46). Aside from the actual ageing of the vasculature over time, secondary age related factors such as a sedentary lifestyle and dietary factors also play a role (71,72).

Other genetic factors such as sex, ethnicity and family history can also impact cardiovascular health (47–50). Men are at increased risk for CVD compared to premenopausal women (73). This difference can be explained by hormones such as oestrogen that protect premenopausal women (50,73,74). Men also have bigger arterial diameter than women, while women have less plaque formation, but more pronounced stenosis (48,50). Aside from physiological differences, men in general are also more likely to engage in risky behaviours such as smoking and excessive alcohol consumption compared to women (50). Additionally, physiological and sociological differences between ethnic groups are often reported in clinical studies and are closely related to differences in cultural practices, social norms, values, behaviours and diets (49,75–77). Another factor, family history of CVD, has shown to increase CVD risk up to 12-times compared to the general population (73).

1.5. HIV/AIDS: Background

Human immunodeficiency virus (HIV) was first recognised in 1981 and isolated in 1983 (78,79). In 1984, two types of viruses (HIV-1 and HIV-2) were identified (80). HIV-1 is thought to have originated in Central Africa and HIV-2 in some parts of Western or Central Africa (81).

HIV is an enveloped virus with a membrane that contains glycoproteins namely gp120 and gp41, matrix protein (p17) and a capsid with p24 antigen (82) (**Figure 1.3**).

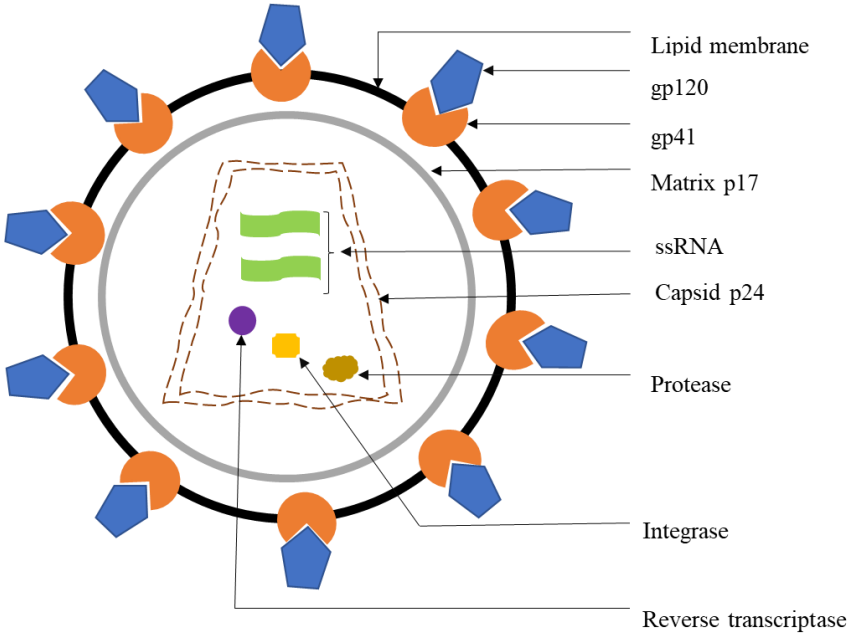

Figure 1.3*. A diagram representing the structure of HI-virus* (82). ***Abbreviations:*** *ssRNA: Single strand ribonucleic acid.*

The capsid contains two identical single stranded ribonucleic acid (ssRNA) and three enzymes (reverse transcriptase, integrase and protease) (82).

HIV is transmitted through body fluids (83). It binds to a primary cellular receptor, CD4 and then to a cellular co-receptor (C-C chemokine receptor type 5 (CCR5) or C-X-C chemokine receptor type 4 (CXCR4)), exposing the gp41 to allow fusion to the host cell membrane (83). Following fusion, entry of the viral matrix into the host cell's cytoplasm takes place and the capsid disintegrates, exposing the viral RNA (83). Reverse transcriptase converts viral RNA into pro-viral DNA (83). The pro-viral DNA migrates into the nucleus of the host cell, where it is inserted into the host DNA by the protein integrase (83). The pro-viral DNA generates viral messenger RNA that migrates into the cytoplasm where the formation of inactive precursor proteins occurs (83). The viral protein protease cleaves the precursor proteins to generate viral particles with an envelope and two strands of newly formed viral RNA (83). Finally, the newly formed HI-virus exits the host cell through its membrane where it can now infect other cells (83). Chronic activation of the host immune system leads to a decrease in CD4+ cell count (84). Severe immunosuppression and constant growth of untreated opportunistic infections leads to AIDS (85). Thus, CD4 cell count and HIV viral load are valuable indicators of HIV disease progression/regression (86).

1.6. HIV epidemiology

HIV/AIDS spread quickly from the early 1980s, causing death globally, in a relatively short period of time (< 40 years) and is currently one of the most prominent diseases in human history (87). At the peak of the global HIV-epidemic in 2003, about 15 000 people became infected each day, about 8000 people died each day and 25 million people became infected with HIV that year (88–90). Also, approximately 3.5 million people worldwide died each year, making HIV/AIDS the 5th leading global burden of disease (88,89). In 2010, the

UNAIDS reported an estimate of 60 million people to have been infected with HIV, 35 million people have died as a result of AIDS since the first description of HIV/AIDS and 35.3 million people were living with HIV (88,89,91). In 2017, it was estimated that 36.9 million people were living with HIV/AIDS, 1.8 million become infected and 1.3 million died from AIDS related causes (12).

In the early 2000s the HIV-epidemic reached its peak in SSA, an estimated 3.4 million people became HIV-infected (700 000 children < 15 years of age) and approximately 2.3 million people died from HIV/AIDS (one in five of all deaths in the region) (88,90,92). In 2017, UNAIDS estimated 19.6 million people were living with HIV in SSA (12).

In 2000, HIV/AIDS was responsible for 25% of deaths in SA and rural as well as financially disadvantaged provinces were mostly affected (e.g. Mpumalanga and KwaZulu-Natal) (39,42,93,94). In 2006, 5.4 million South Africans were infected with HIV (about 11 % of the total population) and 11 % of those infected had AIDS (about 600 000 people) (39,42,93,94). Currently, SA is home to 7.7 million HIV-infected people and more than 5 million people are receiving ART (13). HIV/AIDS is responsible for about 27 % of all deaths in SA (95). Each year, more than 10 million people test for HIV and approximately 85% of PLWH know their status (95). SA currently has the largest HIV population (about 17 % of the global HIV-infected population) and ART programme worldwide (39,42,93,94).

1.7. The HI-virus and CVD

Evidence suggests that PLWH have a two-fold increased risk of developing CVD compared to the general population (10,11). Studies have shown an increased rate of acute myocardial infarction in PLWH compared to their uninfected counterparts (9,10). Furthermore, studies have shown an increased incidence of premature atherosclerosis (independent of traditional CV-risk factors), inflammatory disorders (e.g. macro vascular arteritis), and other complications of the endocardium, myocardium and pericardium in the HIV population (96–99). Although the pathophysiological mechanisms are incompletely understood, evidence suggests that HI-viral factors contribute to the pathogenesis of CVD through chronic immune activation, metabolic dysregulation, inflammation, endothelial dysfunction and oxidative stress (96,100–102).

In addition, cardiovascular risk factors, with or without ART, appear to be highly prevalent in PLWH compared to the general population (73,103). High rates of smoking and dysregulation of glucose metabolism are frequently reported in PLWH (73,103). These CVD risk factors, in combination with HIV viral factors, may increase the release of pro-inflammatory cytokines that may enhance endothelial dysfunction and promote CVD (104). The endothelium is of importance in the regulation of vascular tone (blood pressure), organ perfusion (cellular function) and general homeostasis (24).

Impaired immune function (T-cell dysfunction) inflammatory changes due to HIV infection, related opportunistic infections, and clotting disorders have shown to contribute to microvascular dysfunction and cardiovascular risk (105). Also, HIV-associated hypertension and dyslipidaemia have been associated with microvascular dysfunction (106,107). It has been reported that increased levels of biomarkers such as high sensitivity C-reactive protein (hsCRP), interleukin-6 (IL-6), tumour necrosis factor-alpha (TNF-α), d-dimer,

fibrinogen, intercellular adhesion molecules (intercellular adhesion molecule-1 (ICAM-1) and vascular cell adhesion molecule-1 (VCAM-1)) are present in ART-naïve PLWH compared to those on ART (108). Also, viral proteins such as Tat and Nef have been associated with vascular dysfunction, including the microvasculature (108).

1.8. Antiretroviral therapy: Background

The advent of ART has led to improved prognosis of HIV/AIDS through suppression of viral replication (109). ART drugs mediate their actions by inhibiting key steps in the HIV-lifecycle. Although highly successful in controlling viral replication, ART cannot eradicate the virus or its genetic information from the body (110–112). Due to the effectiveness of ART, HIV is no longer a fatal disease, but a chronic (manageable) disease that requires lifelong treatment (113).

1.9. ART: Drug and drug-classes

There are more than 25 ART drugs currently available which are classified in various drug-classes according to their mechanisms of action on the HIV lifecycle (112,114,115). There are six major classes of ART namely: nucleoside reverse transcriptase inhibitors (NRTIs), non-nucleoside reverse transcriptase inhibitors (NNRTIs), protease inhibitors (PIs), fusion inhibitors (FIs), CCR5 antagonists, and integrase strand transfer inhibitors (INSTIs) (112).

The preferred 1st-line ART for adults comprises of two NRTIs plus a NNRTI or an INSTI. Failing of the 1st-line regimen results in administration of 2nd-line ART consisting of two NRTIs plus atazanavir (ATV)/ritonavir (r) or lopinavir (LPV)/r (**Table 1.1.**). Failing of 1st-line regimen including abacavir (ABC)+lamivudine (3TC) or tenofovir (TDF) results in the use of zidovudine (AZT)+3TC in the 2nd-line and vice versa. If stavudine (d4T) or AZT was used in the 1st-line failing regimen, TDF+3TC (or FTC) +ATV/r or LVP/r should be used in the 2nd-line and if TDF was used in the 1st-line failing regimen, AZT+3TC+ATV/r or LPV/r should be used in the 2nd-line (116).

Table 1.1*. 1st -and- 2nd line ART regimens in adults.*

Preferred 1st-line regimens	TDF+3TC (or FTC) +EFV
Alternative 1st-line regimens	AZT+3TC+EFV (or NVP) TDF+3TC (or FTC) +DTG TDF+3TC (or FTC) +EFV_{400}[a] TDF+3TC (or FTC) +NVP
Failing 1st -line regimens	2NRTIs+EFV (or NVP) 2NRTIs+DTG
Preferred 2nd-line regimen	2NRTIs+ATV/r or LPV/r
Alternative 2nd-line regimens	2NRTIs+DRV/r

[a] EFV at lower dose (400 mg/day). ***Abbreviations****: ATV: atazanavir, 3TC: lamivudine, ABC: abacavir, AZT: zidovudine, d4T: stavudine, DRV: darunavir, DTG: dolutegravir, EFV: efavirenz; FTC: emtricitabine; LPV: lopinavir, NVP: nevirapine, r: ritonavir; TDF: tenofovir*.

1.9.1. NRTIs and associated adverse effects that may increase cardiovascular risk

It has been noted that women are at an increased risk for NRTI-associated adverse health effects, the underlying mechanisms remain poorly understood (117).

Although NRTIs, compared to other drug classes, are less hepatotoxic, NRTIs are associated with peripheral neuropathy, hyperlactataemia and lactic acidosis, ototoxicity, cytopenia, hepatomegaly with steatosis, pancreatitis, myopathy/cardiomyopathy and lipoatrophy (117). To a certain extent, NRTIs inhibit mitochondrial DNA polymerase Y, an enzyme responsible for mitochondrial DNA replication, leading to mitochondrial dysfunction and side effects such as cardiomyopathy (117,118). There is also an association between NRTI use and renal dysfunction, therefore, monitoring renal function during NRTI use is recommended (117). TDF is specifically associated with nephrotoxicity and should be avoided in patients with renal failure (117).

1.9.2. NNRTIS and associated adverse effects that may increase cardiovascular risk

NNRTIs target HIV reverse transcriptase and are metabolised in the liver (112,119). NNRTIs alter lipid profile and increases cardiovascular risk (119–121). There are studies that showed efavirenz may cause an increase in all serum lipids, especially LDL levels (119,121). Also, both efavirenz and nevirapine increase triglyceride levels (121). Over the course of treatment nevirapine and efavirenz increase HDL cholesterol (120). On the other hand, efavirenz is associated with side effects of the central nervous system, as well as prenatal defects (e.g. neural tube defects), rash and dyslipidaemia (119). It appears that NNRTIs have less deleterious effects on glucose metabolism compared to other drug classes (120).

1.9.3. PIs and associated adverse effects that may increase cardiovascular risk

Since their introduction in 1996, PIs have contributed to the dramatic decline in morbidity and deaths caused by HIV/AIDS (87,119). In the lifecycle of HIV, PIs block protease enzymes, preventing cleavage of viral polyproteins and thus inhibiting the ability of virus particles to infect new host cells (112,122). PIs are metabolised in the liver and to a lesser extent in the small intestine, and therefore carry an increased risk for liver toxicity compared to other ART combinations (112,119).

PIs alone, as well as in combination with other ART-classes, are associated with gastrointestinal side effects (nausea, vomiting, diarrhoea, and bloating), alterations of the lipid profile (increased triglyceride, total cholesterol and LDL levels) as well as glucose metabolism in PLWH (87,119,121). Moreover, PIs have been associated with insulin resistance. (119,120). PI-associated insulin resistance and altered glucose and lipid profiles have been associated with chronic inflammation, cellular homeostatic stress responses, and affected (promoting and/or inhibiting) adipocyte storage capacity (87). This process may lead to lipodystrophy, lipotoxicity, a pro-atherogenic lipid profile, increased central body fat distribution and/or a decrease in adipose tissue volume in the legs and arms (87).

1.9.4. INSTIs and associated adverse effects that may increase cardiovascular risk

Literature has shown an association between INTSIs and weight gain, more especially dolutegravir (DTG) (123). An increase in weight and obesity are factors that increase CVD risk and diabetes (124). Although the mechanism of weight gain with the use INSTIs is unknown, literature has shown that INSTIs may influence adipose tissue adipogenesis, fibrosis and insulin resistance (125) while some data showed that pharmacogenetics may have an impact in weight gain on people who switched to an INSTI-based regiment (126).

1.10. ART coverage in SA

In 2002, only 2 % of PLWH in SA received ART, which increased to 37 % in 2009 (42,127,128). Due to the successes of ART programmes, annual HIV/AIDS-related mortality rate in SA decreased by 7.7 % between 2010 and 2011 (39,42,127,128). In 2011, life expectancy in KwaZulu-Natal increased by 11.3 years compared to 2003 when ART was introduced (111). This dramatic upscaling of ART coverage prevented an estimated 505 000 South African deaths per year due to HIV/AIDS around 2010 (42,127,128). SA is currently home to the largest HIV population and government-sponsored ART programme globally (129–131). An annual decrease in new HIV-infections suggests that HIV/AIDS in SA is reaching a mature phase in disease progression (39,42,127,128).

1.11. Markers of cardiovascular risk/disease

The specific contribution of individual cardiovascular risk factors in the development of CVD are difficult to determine since they may differ in intensity, duration and have complex overlapping physiological pathways (132–134). Nonetheless, there are several methods developed to assess and predict cardiovascular risk

including mathematical algorithms and methods that use statistical modelling of traditional cardiovascular risk factor clusters, as well as chemical biomarkers such as high-sensitivity C-reactive protein (hsCRP), tumor necrosis factor alpha (TNF-α) and intercellular adhesion molecule 1 (ICAM-1) (135–142).

Previous studies have shown that cardiovascular risk factors are associated with changes in retinal microvasculature (107,143). Therefore, the use of a non-invasive technique such as retinal imaging has proven to be useful in assessing vascular health *in vivo* (144).

1.12. Retinal microvascular imaging as a tool to assess cardiovascular risk

1.12.1. Background

The pupil provides unique, non-invasive access to observe/assess the retinal microvasculature (144). Retinal examination by shining light at the correct angle through the pupil has been practised for more than a century (144). In 1823, Jan Evangelista Purkyně devised the purkinje images technique for examining the fundus and in 1845, Charles Baggage used that technique to invent the ophthalmoscope (144). In 1851, Herman von Helmholtz reinvented the ophthalmoscope (144). Although Purkyně had already produced retinal vascular drawings, van Trigt published the first retinal images in 1853 (144). In 1891, Gerloff (German ophthalmologist) obtained the first retinal images that showed blood vessels (144). In 1910, Gullstrand invented the first fundus camera and received the Nobel Prize for his invention (144). Currently, the fundus image (a two-dimensional (2D) representation of the 3D structure) is used to evaluate the effects of various cardiovascular risk factors on geometric patterns of retinal micro-vessels **(Figure 1.4**) (144).

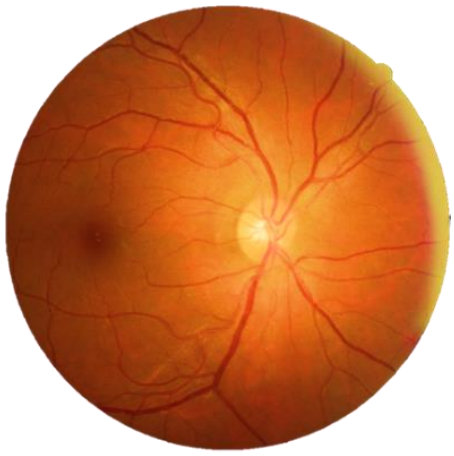

Figure 1.4*. Digital fundal image of retinal microvasculature (captured using Canon CR2 digital camera (Canon Europa NV, The Netherlands).*

Fundoscopy offers a unique opportunity to non-invasively assess vascular disorders in various CVD states (144). Also, systemic and cardiometabolic diseases such as diabetes and hypertension are successfully monitored through their retinal microvasculature effects (144). Therefore, retinal microvascular imaging has a wide range of applications in the clinical research setting (144).

1.13. Retinal imaging and features of interest

Currently, digital images are obtained non-invasively **(figure 1.5)** and analysed by means of semi-automated software to quantify geometric features (145,146).

Figure 1.5*. Obtaining a digital retina image non-invasively using canon CR2 digital camera (Canon Europa NV, The Netherlands). Photo is of the author of this thesis – permission supplied.*

To accurately characterise retinal microvasculature morphology, a number of vascular parameters such as retinal vessel calibre, tortuosity, branching angle and fractal dimension are measured (147). Chronic conditions such as hypertension and diabetes alter vascular structure and morphology. Prognosis of these conditions can be accurately made when retinal microvascular morphological alterations are measured, thereby providing a vital tool for treatment response monitoring. Factors such as autonomic dysregulation of vascular tone, inflammation, oxidative stress and endothelial dysfunction play a significant role in the induction and progression of microvascular geometric morphological changes (147).

Various computerised software programmes are currently available to quantify the complex geometric patterns of retinal micro-vessels. Unfortunately, absolute values obtained from different software programmes are not comparable, as different quantitative algorithms and protocols may be used between programmes (145,148). Also, secondary factors such as pharmacological intervention to induce pupil dilation is utilised in some retinal imaging protocols (149). Nonetheless, comparisons of general trends in effects such as widening or narrowing of vessels between studies is widely accepted (144,150,151).

1.13.1. Retinal vessel calibre

Retinal vessel calibre represents the mean vessel diameter of the six largest arterioles (central arteriolar equivalent (CRAE) and venules (central retinal venular equivalent (CRVE)). These measurements are performed in the zone 0.5- and 1-disc diameter from the optic disc margin. Also, CRAE-to-CRVE ratio (arteriolar-to-venular ratio; AVR) is calculated **(Figure 1.6)** (152–154).

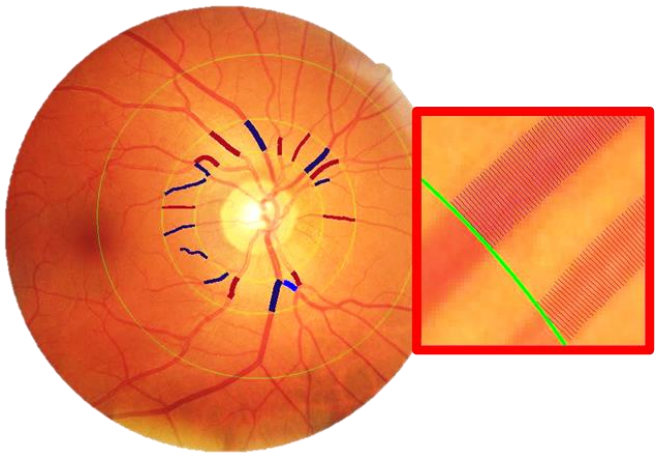

Figure 1.6. *Retinal vessel diameter is determined by means of semi-automated software.*

A more detailed description of the parameters and the protocol followed for the determination of CRAE, CRVE and AVR in the context of the current study are provided in the methods section.

1.13.1.1. Retinal vessel calibre in relation to traditional cardiovascular risk factors, HIV and ART

Various cardiovascular risk factors have previously been associated with retinal vessel calibre. For example, age (155), gender (male) (156), ethnicity (black) (157–159), smoking (160–162), physical activity (163), hypercholesterolaemia (160,164), hyperglycaemia (165,166), superoxide dismutase (SOD) (158) and haematocrit (159) have been positively associated with CRAE, whereas, age (159–161,164,167–170), high body composition (163,171), blood pressure (159–164,167–169,172–174), HDL (161), reactive oxygen species (ROS) (158), Von Willebrand factor (157) and clot lysis (157) have been inversely associated with CRAE.

On the other hand, CRVE has been positively associated with age (155,174), ethnicity (black) (158,159), smoking (159–162,175), body composition (163,171), blood pressure (167), hyperlipidaemia (160), hyperglycaemia (165,166), inflammation (C-reactive protein (170,176) and Interleukin-6 (170)), Von Willebrand factor (157), nephropathy (177), risk for stroke (177), ischaemic heart disease (161) and risk for all-cause mortality (161) and negatively associated with age (159,167,168), physical activity (163), blood pressure (160,172) and HDL (161). AVR has been furthermore positively associated with cardiovascular risk factors such as fibrinogen (157) and negatively associated with age (155), ethnicity (black), blood pressure (168,172), SOD and ROS (158).

Retinal vessel calibres have also been associated with various markers of HIV and ART (159,169,178). AIDS-specific factors such as viral load and increased mortality risk in PLWH have been reported (169). More specific effects of HIV and ART on retinal vessel calibre as reported in literature have been summarised in the following table **(Table 1.2)**.

***Table 1.2**.. Evidence of the effects of HIV, ART and related factors on retinal vessel calibre parameters.*

Study characteristics	Findings
Gangaputra *et al.* (159) (*n* = 1250 HIV-positive participants). United States of America (USA).	• CRAE inversely and CRVE positively associated with history of ART ($p < 0.001$). • CRAE inversely associated with CD4+ T lymphocyte count ($p = 0.04$). • Mortality risk as inversely associated with AVR (12% (95% CI, 2%–21%), p = 0.02). • No associations between viral load and vessel calibres were observed.
Pathai *et al*. (179) Case-control study (*n* = 491 adults ≥30 years (*n* = 242 HIV-infected adults and age- and gender-matched HIV-negative controls (*n* = 249)). SA.	• Age reduced retinal arteriolar and venular diameters in relation to HIV, but not in controls. • ART inversely associated with CRAE independently of age (167.83 µm < 3 years of ART *vs.* 158.89 µm > 6 years, $p = 0.02$). • HIV viral load >10,000 copies/mL inversely associated with CRAE in PLWH on ART (p = 0.05). • HIV-related venular changes were not observed.
Tan *et al.* (15) Case-control study of *n* = 85 patients with HIV and *n* = 251 age-, sex-, and race-matched healthy controls. Singapore.	• HIV viral loads were positively associated with CRAE (P trend = 0.009) and inversely associated with AVR (P trend = 0.025).
Haddow *et al.* (180) Cross-sectional sub study of a larger cohort including 3 demographically matched groups. SA.	• Study group was not associated with AVR • SBP, history of stroke, history of a heart attack and recreational drug use were respectively inversely associated with AVR in the HIV population (adjusted β −0.009 per +10 mm Hg, 95% CI −0.015 to −0.003, $p = 0.002$), (adjusted β −0.070, 95% CI −0.12 to −0.015, $p = 0.01$) and (adjusted β −0.037, 95% CI −0.057 to −0.018, $p = 0.0002$).
Kalyani *et al.* (169) Cross-sectional analyses (*n* = 1242 participants living with HIV) USA.	• CRAE was inversely associated with haematocrit ($p = 0.003$). • CRAE was inversely associated with age ($p = 0.002$), history of hypertension ($p = 0.02$), and history of ART-use ($p = 0.01$). • Larger CRVE was positive associated with smoking ($p = 0.003$). • CRVE was inversely associated with AIDS duration ($p = 0.02$) and history of ART-use ($p = 0.02$). • AVR was inversely associated with haematocrit ($p = 0.001$). • Smaller AVR was inversely associated with hypertension ($p = 0.01$) and smoking ($p = 0.04$).
Jabs et al. (170) A cross-sectional study to evaluate relationships among retinal vascular calibre and biomarkers of systemic inflammation in patients with AIDS in *n* = 454 participants from the USA.	• Elevated CRP, IL-6, and IP-10 were positively associated with CRVE. • Hyperlipidaemia was associated with CRVE (mean difference, −7.5 µm (95% CI, −13.7 to −1.2) $p = 0.02$). • CVD was inversely associated with CRAE (mean difference, −5.2 µm (95% CI, −10.3 to −0.1; $p = 0.05$). • Age was inversely associated with CRAE (slope, −0.26 µm/year (95% CI, −0.46 to −0.06; $p = 0.009$). • IL-6 was positively associated with CRVE (slope, 5.3 µm/standard deviation $\log_{10}$[plasma IL-6 concentration] (95% CI, 2.7 to 8.0; $p < 0.001$).
Edwar et al. (181) *n* = 79 HIV patients beginning ART in Jakarta, Indonesia.	• HIV patients had narrower retinal arteries and higher levels of CMV antibodies than healthy controls. • CRAE decreased over 12 months of ART (p < 0.0001). • CRAE correlated with CMV antibody. • Multivariable models associated CRAE with detectable HIV RNA levels. • Decreases in CRAE in HIV patients responding to ART suggest progressive microvascular change distinct from changes assessed in large vessels.

Results from the aforementioned studies indicate that HIV and ART are predictors of CRAE, CRVE and AVR. Overall, findings suggest that HIV, as indicated by viral load, and associated inflammatory markers such as IL-6, mostly have dilatory effects on CRAE and CRVE, while ART appears to have the opposite effect (15,159,169,170,179,181). Other cardiovascular risk factors such as age, history of stroke and heart disease, hypertension and haematocrit were also associated with vessel calibre in these HIV study populations (15,159,169,170,179,181). Interestingly, the study by Gangaputra *et al.* (2012) showed that a 0.1 decrease in AVR was associated with a 12% increased risk of mortality in their HIV study population (159).

These findings support the hypothesis that HIV and ART have atherogenic effects on vasculature (169,179) and that measurements of retinal vascular calibre could be an innovative and non-invasive method of estimating vascular risk in PLWH (179).

1.13.2. Retinal vessel network features

Retinal vessel network features include fractal dimensions (D_f), vessel tortuosity, vessel segment lengths, number of vessels branch points and vessel endpoints, and lacunarity (147). Most commonly reported features are vessel D_f and vessel tortuosity (**Figure 1.7**).

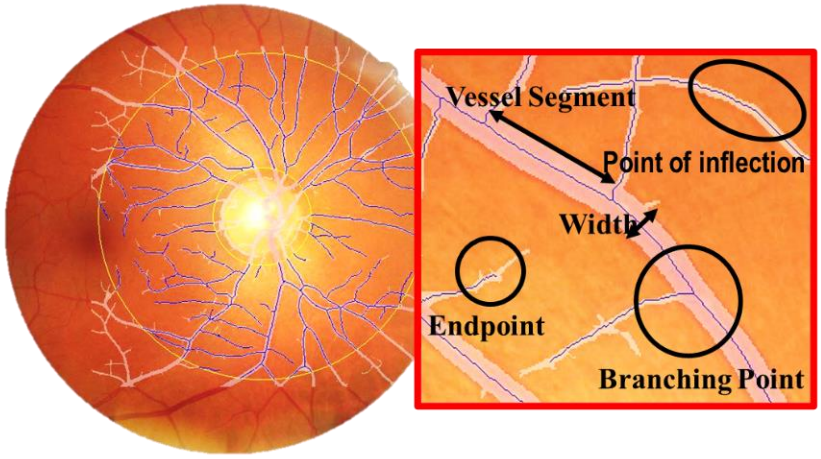

Figure 1.7 *Retinal vessel network features are determined by means of semi-automated software. The blue lines in the retinal image represent the skeletonised tree.*

Retinal vessel fractal dimensions are quantitative measures of microvascular branching patterns, network complexity and network density (182,183). Fractal dimensions were described by the mathematician Benoît Mandelbrot in 1975 in order to describe/quantify irregular patterns in mathematics and in nature that exhibit self-similarity (184). A lower value for fractal dimension reflects a sparser vascular network which is often associated with risk factors such as older age (147).

Vessel tortuosity is mainly a quantitative measure of bending of the vessels (152,185). More specifically, retinal vascular tortuosity is defined as the integral of the curvature square along the path of the vessel

normalised by the total path length (it thus considers the bowing and points of inflection) (147). Vessel tortuosity has been positively associated with cardiovascular risk factors such as hypertension (147).

Vessel lacunarity is a measurement of the lack of network complexity and thus quantifies gap sizes between vessels (186–188). In terms of other features, increased arteriolar length to diameter ratio has been positively associated with older age and elevated systolic blood pressure (189). Vessel network features specifically related to the current study are described in more detail in the Methods Chapter.

1.13.2.1. Retinal vessel network features in relation to traditional cardiovascular risk factors, HIV and ART

Although retinal vessel network features appear to be infrequently reported in clinical research compared to vessel calibres, they have found useful application in cardiovascular risk assessment (152,153,190). Literature has shown that D_f can predict coronary heart disease (CHD) mortality as well as CVD (191) and is also associated with elevated blood pressure (192), increased risk of chronic kidney disease (CKD) (193) and various brain and neurological disorders (194). D_f appears to exhibit a stronger association with hypertension than CRAE (195) and can also be used as a measure to quantify microvascular remodelling (196).

More tortuous vessels, on the other hand, have been associated with various cardiovascular risk factors such as older age (197), hypertension (197), BMI (197,198), diabetes (199), early stages of kidney disease (200) and lower HDL level (197).

Lacunarity has furthermore been positively associated with hypertension (201,202), diabetes (201,203) and cognitive impairment (204).

Although markers of HIV and ART have been associated with retinal network features such as D_f, and to a lesser extent tortuosity and lacunarity (15,205–208), research about retinal network features in HIV positive population is limited. Findings from literature related to retinal vessel network features in HIV populations are summarised in the following table.

***Table 1.3**. Evidence of the effects of HIV, ART, and related factors on retinal vessel network parameters*

Study characteristics	Findings
Tan *et al.* (15). Case-control study (*n* = 85 patients with HIV and *n* = 251 age-, sex-, and race-matched normal healthy controls selected from the Singapore Epidemiology of Eye Disease program were included in this study.	• Arteriole and venule tortuosity were respectively positively associated with HIV status *vs.* control (0.77 × [10^4] *vs.* 0.59 × [10^4], $p < 0.001$) and 0.90 × [10^4] vs. 0.74 × [10^4], $p < 0.001$).
Tan *et al.* (209). Compare retinal vascular parameters between patients with HIV and controls to elicit the relationship between retinal vascular parameters and CD4 counts (*n* = 37 HIV patients with no clinical retinal pathology and *n* = 111 age-gender matched normal healthy controls). Singapore	• HIV was associated with higher total fractal dimension compared to control (1.457 *vs.* 1.439, p = 0.045), higher venular fractal dimension (1.246 *vs.* 1.218, p = 0.004). • HIV was associated with more tortuous arterioles (0.741 *vs.* 0.560 [x105], p < 0.001) and venules (0.883 *vs.* 0.717 [x105], p < 0.001), compared with healthy normal subjects.
Tan *et al.* (207). Investigate whether retinal microvascular changes are predictive of subsequent CD4 /CD8 and haemoglobin (Hb) levels in HIV patients on highly active antiretroviral therapy (HAART). Singapore.	• A decrease in 0.1 unit of Df was also significantly associated with a subsequent 0.67 g/dL decrease in Hb level. (p = 0.028).

Findings from the aforementioned studies indicate that retinal vessel network features may predict the vascular effects of HIV and ART (15). A linear associations between CD4 cell count (a marker of HIV disease progression) and network features were observed (209). Arteriolar D_f has also been associated with HIV-associated haemoglobin levels (207). A higher venous D_f has been associated with smaller cortical volumes and increased cortical atrophy, whereas a higher arterial D_f was associated with the opposite (205). Cortical volume represents amount and size of neurons, dendritic processes and glial cells and cortical atrophy is a degenerative brain and nervous system syndrome that affect eyesight and processing of visual information. Cardiovascular risk factors such as hypertension and diabetes mellitus are associated with cortical thinning (210). From these findings, it appears that higher D_f and more tortuous vessels are associated with HIV and increased cardiovascular risk. In their 2016 study in particular, Tan *et al.* emphasised that retinal vessel network features may be useful in predicting responses to ART in PLWH (207).

1.13.3. Retinal vessel branching

Retinal vessel branching broadly represents the quantification angles (∟) between mother and daughter branches (∟1 to 5) and the vessel diameters of these mother (D0) and daughter branches (D1 and D2) in the bifurcation area just before and after the branch point (**Figure 1.8**) (211).

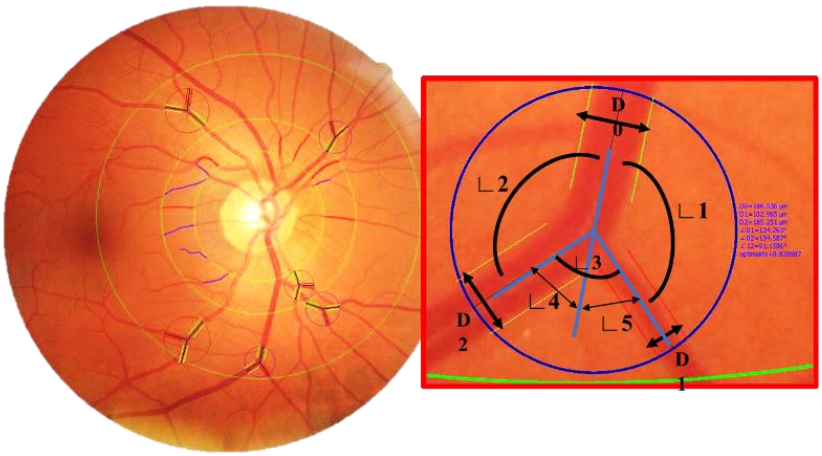

Figure 1.8 *Retinal vessel branching features are determined by means of semi-automated software.*

Out of all the retinal geometric features, retinal vessel branching appears to be most infrequently described in CVD, but is closely related to blood circulation efficiency (212–214). Retinal vessel branching features also appear to have a relationship with other retinal geometric features related to vessel density (147,215). For example, a less dense vessel network may result in wider angles as vessels aim to cover the maximum retinal area (147,215). Branching angles are also closely related to the cost-effectiveness of blood flow in terms of power required for blood circulation and drag experienced during blood flow (211). Different optimum values for branching angles and branching diameters ratios have been proposed by various theoretical studies over the years (216–218). In terms of vessel bifurcation diameters, Murray's law states that for optimal blood flow, the cube of the parent vessel's diameter is equal to the sum of the cubes of the daughters' diameters and that deviation from this may indicate pathology (211). Patton *et al.* (2005) postulated that vascular arteriolar junctional exponents, which is a measure of the relative diameters of parent and daughter branch vessels, in particular, may serve as a good measure of overall altered retinal vascular geometry in CVD (215). Although not well understood, vascular endothelial growth factor (VEGF) appears to play an important role in branching angles during angiogenesis (219,220).

Currently, a clear standardised protocol for the quantification of retinal vessel branching features remains incompletely described, but focus has been given to the first order angle, which is the first angle closest to the optic circle and the analysed zones, subtended between two daughter vessels at each bifurcation (147,211). A single angle or the average of up to 15 angles has previously been used (211). Retinal vessel branching features and the protocol specific to the current study are described in more detail in the Methods Chapter.

1.13.3.1. Retinal vessel branching features in relation to cardiovascular risk factors, HIV and ART

Literature shows retinal vessel branching as a long-term marker for vascular remodeling and cardiovascular risk as changes become more pronounced over a longer period of time (171,211). Systemic vascular disease such as diabetes have been associated with arterial and venous occlusions (known as central and branch arterial occlusions (CRAO, BRAO) and central and branch venous occlusions (CRVA, BRVO)) (144,211,221). Also, cardiac diseases such as atrial fibrillation, valvular disorders, and intracardial thrombosis have been associated with ocular vascular obstruction and occlusion (221).

Retinal vessel angles in relation to cardiac structure and cerebrovascular blood flow have also received increased attention over recent years. A recent study by Huang *et al.* (2020) investigated the associations between cardiac structure and retinal vascular geometry and found that each unit increase in a set of cardiac structure indices was associated with larger retinal arteriolar branching angles (222). On the other hand, Nadal *et al.* (2019) showed that cerebral microcirculation is associated with branching patterns of retinal vessels (223). These changes in retinal arteriolar geometric morphology reflected sub-optimal alterations in cardiac and cerebrovascular structure and blood supply (222,223).

Risk factors such as smoking, hypertension, diabetes, hyperlipidaemia and hypercholesterolaemia, and hyperuricaemia have been associated with ocular vessel occlusion (221,224,225). Furthermore, it has been shown that patients with poor glycaemic control tended to have larger retinal arteriolar branching angle compared to their age- and gender- matched counterparts with good glycaemic control (226). Serum leptin and zeaxanthin levels have also been associated with vessel angle (227).

The effects of HIV and ART on retinal branching parameters appear to be poorly described in the literature. Tan *et al.* (2016) showed that each 1° increase in arteriolar branching angle was significantly associated with a subsequent 3.74 cells/µl decrease in CD4 count and T helper cell levels. The effects of hypertensive retinopathy on vessel branching angles have also been observed in PLWH (228).

Evidence related to the effects of HIV and ART on retinal vessel branching are summarised in the following table.

Table 1.4. *Evidence of the effects of HIV, ART and related factors on retinal branching parameter.*

Study characteristics	**Findings**
Tan *et al.* (207). Investigate whether retinal microvascular changes are predictive of subsequent CD4 /CD8 and haemoglobin (Hb) levels in HIV patients on highly active antiretroviral therapy (HAART) in Singapore.	• Each 1° increase in arteriolar branching angle was significantly associated with a subsequent 3.74 cells/µl decrease in CD4 count (p = 0.001) and T helper cell (Thc) levels (0.14, p = 0.003).
Dunn *et al.* (229). Investigated clinical features of retinal vascular occlusion in an HIV population from the USA.	• PLWH have a small risk of retinal vascular occlusion
Conway *et al.* (230). Observed BRAO and BRVO is associated with HIV-infected people that have cytomegalovirus retinitis in the USA.	• AIDS patients who also had cytomegalovirus retinitis developed BRAO and BRVO

Limited evidence related to the effects of HIV and ART in vessel branching features underscores the need for more research.

1.14. Rationale/motivation

CVD is the leading cause of death worldwide, with approximately 80% of CVD deaths occurring in developing countries such as SA (3). HIV/AIDS also remains a serious disease burden worldwide (87). Although ART has improved the longevity of PLWH, HIV-associated co-morbidities such as CVD appear to affect PLWH disproportionally (109). Although studies have shown that PLWH have a 2-fold increased risk of developing CVD compared to their HIV-free counterparts, CVD receives less research attention in developing countries compared to developed countries (10,11). CVD in PLWH is a major concern in SA in particular, since it is home to the largest HIV population (17% of global HIV population) and government sponsored ART programme in the world (95). Therefore, new, non-invasive, and relatively inexpensive techniques are needed to assess cardiovascular risk in PLWH in SA. As retinal imaging is a non-invasive and relatively inexpensive technique that has proven to be useful in assessing vascular health in the general population and PLWH, it may potentially also be a useful tool to assess cardiovascular risk in PLWH in the SA context (144). Evidence, mostly from the developed countries, has already shown that retinal microvascular geometric features such as retinal calibre, vessel network and retinal vessel branching have application in HIV populations. Data from SA is scanty and thus need for robust studies in PLWH.

1.15. Aims and objectives

The overarching aim of the study is to investigate the association between retinal microvascular geometric morphology, HIV and ART, and related cardiometabolic risk factors in a study population of Worcester, Western Cape, South Africa.

To achieve the above aim, our specific objectives are

1. To recruit study participants with and without HIV residing in the Worcester area.
2. To collect demographic, lifestyle, medical history, and socioeconomic data from each participant.
3. To perform anthropometric and cardiovascular measurements and collect blood and urine samples for subsequent biochemical analyses (lipid profile, liver function, glucose metabolism and renal function).
4. To obtain digital retinal images from all study participants.
5. To analyse retinal microvascular geometric morphology using a semi-automated software to quantify vessel calibre, network, and branching features.
6. To statistically analyse the data to determine whether associations exist between retinal microvascular geometric features and HIV, ART, and HIV- and ART-associated cardiovascular risk factors.

1.16. Conclusion

Although SA is currently still under a high burden of communicable diseases, especially HIV/AIDS, non-communicable diseases such as CVD are becoming more prevalent. CVD is also increasingly becoming a

health concern in PLWH. As HIV affects about one-fifth of the South African population, the cardiovascular effects of HIV and ART in SA needs to be investigated. Quick, inexpensive, and non-invasive techniques such as retinal microvascular imaging may have useful application, but more population-based evidence is needed. In light of the lack of evidence from SA, the current study aims to evaluate whether an association between retinal microvascular geometric features and HIV and ART, and related cardiometabolic risk factors exist. Results from the current study will contribute to a better understanding of the cardiovascular effects of HIV and ART in SA and whether retinal microvascular imaging may be a useful tool in assessing these effects in a South African HIV study population.

Chapter 2

Methods and Materials

2.1. Study background and ethics clearance

The current MSc study was embedded in a larger parent longitudinal study: EndoAfrica, with Prof. Hans Strijdom from Stellenbosch University as the principal investigator (231). The overarching aim of the parent study is to investigate whether HIV-infection and treatment with antiretroviral therapy (ART) is associated with cardiovascular risk by assessing vascular endothelial function and various markers of cardiometabolic risk factors in a study population that resides in the Western Cape Province, South Africa (SA). The parent EndoAfrica study is ongoing, with baseline, and subsequent 18-month and 36-month follow-up assessments completed.

Ethics approval was obtained from the Health Research Ethics Committee (HREC) of Stellenbosch University (HREC protocol number: N19/02/029). The current MSc candidate is registered as a sub-investigator in the approved ethics protocol and participated in all the research activities. Anonymity of study participants was maintained, and data were securely uploaded to and stored in the Research Electronic Data Capture application (REDCap^{TM}) where only authorised researchers were granted access.

2.2. Study overview and design

The current study consists of two sub-studies: (i) a cross-sectional sub-study, which included HIV-negative (HIV-) and HIV-positive on ART (HIV+ART) groups and, (ii) a longitudinal, repeated measures sub-study, which only included a HIV+ART group. We extracted data from the parent study's 18-month follow-up assessments to serve as baseline data for the current study and subsequent data was extracted from 36-month follow-up parent visit to serve as 18 months data for the current study. For a general overview of the current study design and activities, refer to **Figure 2.1.** below.

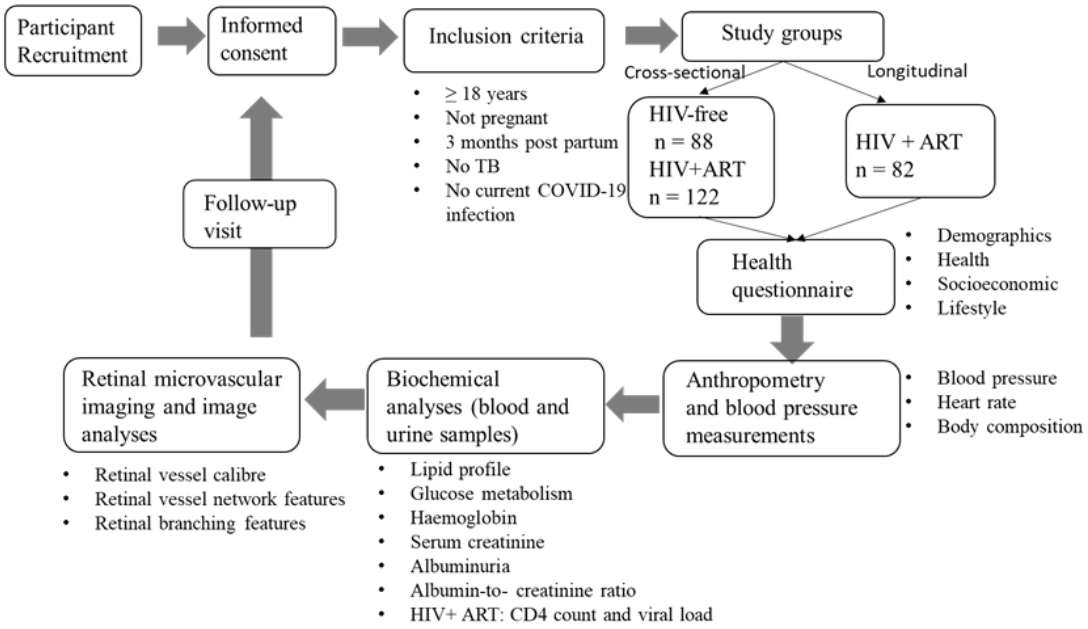

Figure 2.1. *A schematic illustration of the study outline/design.* ***Abbreviations****: TB: Tuberculosis, HIV: Human immunodeficiency virus: ART: Antiretroviral therapy, HIV+ART: Study group consisting of participants that are HIV-positive on ART.*

2.3. Study groups

We categorised the study participants into two groups based on their HIV status: The HIV-negative control group (HIV-negative, *n = 88*), and the HIV-positive group on ART ((HIV+ART), *n* = 122 (cross-sectional), *n* = 82 (longitudinal)). We relied on hospital records for the participants who were on follow-up for HIV and recruited the control counterparts from the same community. We performed rapid antibody screening tests using BioSURE™ HIV self-test (Midstream Estate, South Africa) on all new recruits with unconfirmed HIV status.

2.4. Participant recruitment, informed consent, and inclusion/exclusion criteria.

Volunteering study participants previously enrolled in the parent study hailed from the Worcester community (Western Cape, SA). Informed consent was obtained from all volunteering study participants for both baseline and follow-up visits before any research activities were conducted. The inclusion criteria required the participants to be 18 years or older, not pregnant (confirmed with a Church and Dwight, Co., Inc, New Jersey, pregnancy test), minimum 3 months post-partum, without tuberculosis or current/recent SARS-COV-2 infection (screened for symptoms and fever before arriving at clinic and at clinical visit).

2.5. Health Questionnaire

On the day of clinical visit, we used a comprehensive health questionnaire to obtain information on medical background (e.g., history of diabetes, hypertension, heart disease and tuberculosis), demographics (e.g., age (years), gender (male or female) and ethnicity (black, coloured, white)), lifestyle (e.g., smoking (yes or no)

and alcohol consumption (yes or no)), and socioeconomic status such as level of education completed (none, primary school, high school, adult basic education training, or college/University/Other tertiary institution), employment status (unemployed and employed) and total household income (less than R1000, R1000-R4999, R5000-R9.999, R10000-R20000 and more than R20000).

2.6. Anthropometric and cardiovascular measurements

The following anthropometric variables were measured and recorded: based on previously published international standardised protocols (232) body weight in kg (Omron HN288 digital scale, Kyoto, Japan), height in cm (Seca 213 stadiometer, Hamburg, Germany), waist and hip circumferences in cm (measuring tape). BMI (kg/m^2) and waist-to-hip ratio (WHR) were additionally calculated. Subsequently, systolic, and diastolic blood pressure (SBP and DBP, mmHg) and heart rate (bpm) of each participant were determined (Omron M6 automatic digital monitor, Kyoto, Japan) in a seated position, three times at 5 minutes intervals and the mean SBP, DBP and heart rate calculated.

2.7. Biochemical analyses

Fasting blood was collected in vacutainers (BD Vacutainers®, Franklin lakes, New Jersey) and urine in urine pods (JOYLAB™, Auckland, New Zealand) from each participant and sent to the National Health Laboratory Service (NHLS, Tygerberg Hospital) for further biochemical analyses as described in **(Figure 2.2)** below.

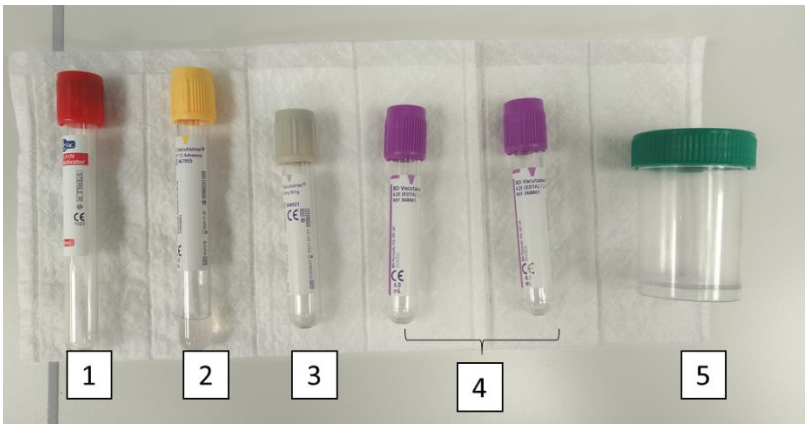

Figure 2.2*. Examples of collection containers used for samples sent to the NHLS for biochemical analyses.*

Description: 1. (1 x 6mL) Lithium heparin (clot activator) tube for determination of high-sensitivity C reactive-protein (hsCRP) **2.** (1 x 7mL) Citrate dextrose (clot activator) tube for fasting lipogram, serum creatinine and gamma-glutamyl transferase (GGT) quantification. **3.** (1 x 5mL) Potassium oxalate (anticoagulant) and sodium fluoride tube for fasting glucose quantification **4.** (2 x 5mL) Ethylenediamine tetra-acetic acid (EDTA) (anticoagulant) tube for haemoglobin (Hb), glycated haemoglobin (hbA1c), viral load and CD4 cell count determination. **5.** Urine pod for urine samples for urine creatinine, albuminuria, and albumin-to-creatinine ratio determinations.

The various biochemical analyses performed at the NHLS are summarised below, (**Table 2.1.**).

***Table 2.1**. NHLS assay and cut-off standards for biochemical analyses.*

	Variable	NHLS analysers	NHLS Cut-off standards
1.	Lipid Profile	Cobas® 301/501 analyser (Roche/Hitachi cobas® c systems, Basel, Switzerland)	• Normal: TC < 5 mmol/L. • Normal: HDL > 1.2 mmol/L for women and > 1.0 mmol/L for men. • Normal: LDL < 3 mmol/L. • Normal: TG < 1.7 mmol/L (233).
2.	Fasting glucose and HbA1c	Hemolysate application on a cobas® 311/501 analyser (Roche/Hitachi cobas® c systems, Basel, Switzerland).	• Normal: Fasting glucose level < 5.6 mmol/L. • Normal: Hba1c levels between 4% and 5.6% (54).
3.	GGT	CObas® 311/501 analyser (Roche/Hitachi cobas® c systems, Basel, Switzerland)	• Normal: GGT levels < 60 U/L for men and < 40 U/L for women (234).
4.	hsCRP	IMMAGE® Immunochemistry Systems and Calibrator 5 Plus assay kit (LOD: 0.02 mg/dL; Beckman Coulter, Inc., CA, USA).	• Normal <1.0 to 3.0 mmol/L (235).
5.	Serum and Urine creatinine. Albuminuria. ACR.	Cobas® 311/501 analyser (Roche/Hitachi cobas® c systems, Basel, Switzerland).	• Serum creatinine normal levels: 0.7-1.3 mg/dL for men and 0.6-1.1 mg/dL for women. • Albuminuria normal levels: 0-8 mg/dL. • ACR normal levels: < 30 mg/mmol creatinine (236).
6.	Viral Load	COBAS® AmpliPrep/COBAS® TaqMan® HIV-1 Test, v2.0. (Risch-Rotkreuz, Switzerland)	• Acceptable levels: < 20 to 75 copies mRNA/mL (116).
7.	CD4 cell count	Flow cytometry (FC 500 MPL analyser) with MXP software (Backman Coulter, Brae, CA, US).	• Acceptable levels: 500-1500 cells/mm^3 (116).

2.8. Retinal Imaging

Retinal images were captured with a Canon CR2 digital camera (Canon Europa NV, The Netherlands) following the setup shown in **(Figure 2.3)** below.

Figure 2.3*. A visualisation of the retinal imaging setup. Photos are of the author of this thesis – permission supplied.*

The participant was seated in front of the camera and a dark cloth was placed over the participant's head to create a dark environment to ensure pupillary dilation without use of mydriatic drugs. The camera was positioned in line with the pupil of the eye and after obtaining a clear focus of the retina, a digital image was captured. Digital images of both the left and right eye were captured, but only the image with the best quality (either left or right) was analysed for each participant. Left vs. right images do not statistically differ. All images were analysed the same way and according to standardised protocol. All calculations were done by software to remove bias and human error.

2.9. Retinal image analysis

The digital retinal images were subsequently analysed using semi-automated computerised software (MONA REVA 2.1.1 developed at the Flemish Institute for Technological Research (VITO); https://mona.health) with edge-detection technology. The software quantified the following geometric features respectively:

1. Vessel calibre
2. Vessel network features
3. Vessel branching.

2.9.1. Retinal vessel calibre

Retinal vessel calibre represents the mean diameter of the 6 largest arterioles and 6 largest venules respectively in the zone 0.4 – and 1 – disc diameter from the optic disc margin.

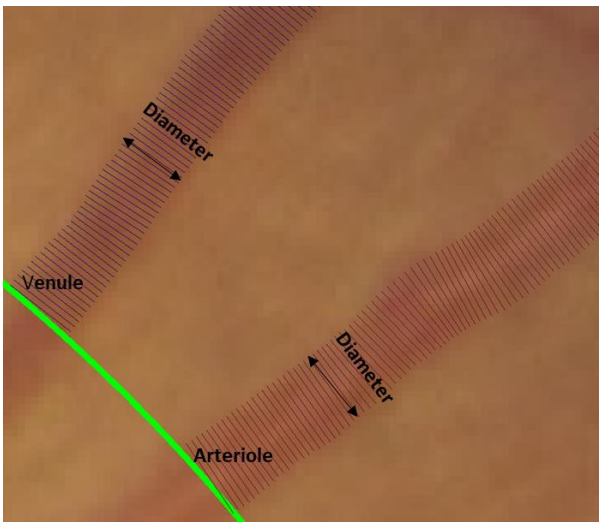

***Figure 2.4**. Determination of retinal vessel calibre.*

Classification of arterioles and venules and the edge-detection by the semi-automated software is confirmed by the grader and corrected where necessary to distinguish the differences between venules and arterioles. The following characteristics are evaluated to assist the grader in distinguishing between arterioles and venules:

- Arterioles are lighter in colour compared to venules.
- Venules are generally straighter compared to arterioles.
- The mean diameter of arterioles is generally smaller compared to that of venules.

Retinal calibre parameters included in the current study are defined in **(Table 2.2)** as previously described.

***Table 2.2**. Retinal vessel calibre endpoints defined for the current study.*

	Variable	Definition
1.	Central retinal arteriolar equivalent (CRAE) (µm)	The mean diameter of the 6 largest arterioles 0.5- and 1-disc diameter from the optic disc margin.
2.	Central retinal venular equivalent (CRVE) (µm)	The mean diameter of the 6 largest venules 0.5- and 1-disc diameter from the optic disc margin.
3.	CRAE/CRVE ratio (arteriolar-venular ratio; AVR)	CRAE-to-CRVE ratio calculated

2.9.2. Retinal vessel network

Retinal vessel network analyses quantify the density and complexity of the total vessel network in the zone 1.5 times optic disc diameters from the optic disc margin.

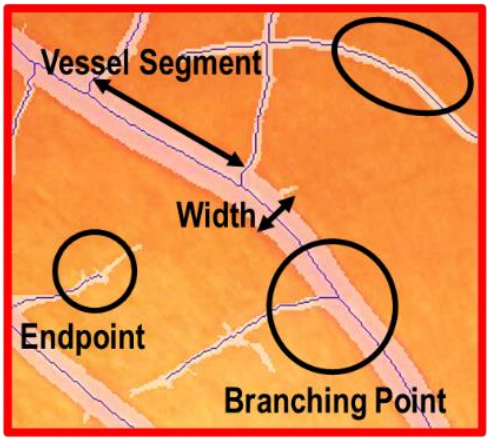

Figure 2.5*. Quantification of retinal vessel network features. Vessel segment is a section between the start and end of a branch and the width is measured from side to side. Branching point is where the vessel divides into multiple branches and an endpoint is where the vessel completes.*

The grader evaluated the automated analyses and corrected possible misclassifications such as areas with wrong edge detection and missed detection of vessels to improve the quality of the analyses.

Vessel network features of interest for the current study are described in **(Table 2.3)** as previously defined.

***Table 2.3**. Defined retinal vessel network features for the current study.*

	Variable	Definition
1.	Average tree diameter (µm)	The average diameter of all the vessels observed in the area for analysis. Larger values indicate lesser flow-resistance and larger blood volume transport.
2.	Total length of skeletonised tree (mm)	Total length of vessel skeletonised tree as indicated in figure 1.7 page 15.
3.	Segmented tree area (mm^2)	Total area covered by vessel tree segments in the zone for analysis.
4.	Number of endpoints and branchpoints and endpoints	Represents the number of times vessels ended and branched off into smaller vessels. A larger value indicates a better vessel distribution and retinal perfusion.
5.	Lacunarity (segmented and skeletonised)	Evaluates the lack of network complexity and thus focuses on the gap sizes between vessels. Larger values represent bigger spaces in a pattern and indicates a less complex geometric pattern.
6.	Fractal analysis (Segmented and skeletonised)	Measure of vascular branching complexity (Larger values represented more complex network patterns).
7.	Fourier fractal (Enhanced)	Measure of simple patterns that may underlie a more complex pattern or system of patterns. Larger values represent complexity in patterns.
8.	Tortuosity (index and of branching segments)	Calculates as the actual length between two points divided by the shortest distance between the two points. .

2.9.3. Retinal vessel branching

Retinal vessel branching features are markers of blood flow efficiency and were determined for arterioles and venules respectively in the zone further than 0.5-disc diameter from the optic disc.

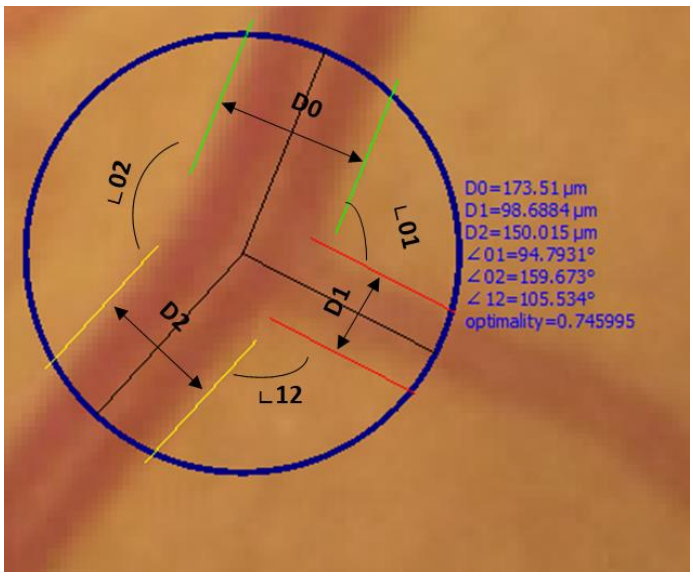

Figure 2.6*. Quantification of retinal vessel network features.*

The average of branching feature of the first order branches of the two largest arterioles and the two largest venules (according to calibre measurements) were determined, respectively.

The mother branch was presented as D0, the big daughter branch was presented as D2, and the small daughter branch was presented as D1. The angle between D0 and D1 and D2 were measured respectively, as well as the angle between D1 and D2. Vessel branching features of interest for the current study for arterioles and venules are summarised in **(Table 2.4)** as previously described.

Table 2.4*. Retinal arterioles and venules branching features evaluated for the current study.*

	Variable	Definition
1.	D0 (µm)	Mean diameter of the mother vessels.
2.	D1 (µm)	Mean diameter of smallest daughter vessels.
3.	D2 (µm)	Mean diameter of largest daughter vessels.
4.	Mean branching angle (°)	Mean of ∟3 (optimum is 72°)
5.	Mean optimality	Deviation from the junctional exponent optimal value (=3).
6.	Mean branching coefficient	The square of the sums of the diameters of the daughter vessels and the parent vessel.
7.	Mean asymmetry ratio	The square of the diameter of daughter vessel 2 divided by the square of diameter of daughter vessel 1.
8.	Mean angular asymmetry	The square of ∟5 divided by the square of ∟4.

2.10. Statistical analyses

2.10.1. Power analyses:

Power analysis was performed (G-power) using historical data from the EndoAfrica study (HIV-free and HIV+ART participants from Worcester) and using CRVE as the parameter of interest (previously associated with HIV-status). The suggested sample size for HIV-free and HIV+ART respectively is $n = 28$ for each group (80% confidence at $\alpha = 0.05$). According to these criteria, a sample size of 75 for each group would give a more than 90% certainty to observe a significant difference in CRVE between study groups.

2.10.2. Statistical analyses to obtain results:

The COVID-19 pandemic interrupted recruitment of HIV-negative participants. It was therefore decided that comparisons between the HIV+ART participants to HIV-negative participants were to be performed cross-sectionally, while the effects of HIV and ART in the HIV+ART group to be conducted longitudinally **(Figure 2.7)**.

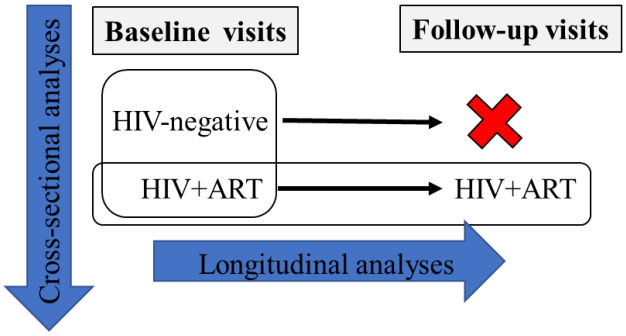

Figure 2.7*. Between-groups effects (cross-sectional design: HIV-negative vs. HIV+ART) and within-group group effects (Longitudinal: HIV+ART at baseline vs. follow-up visit) of HIV and ART evaluated during the current study.*

All statistical analyses were performed using IBM® SPSS® software (version 25, New York, NY, USA) by the MSc candidate, and verified by supervisors and a professional biostatistician. Data distributions for all the continuous variables were evaluated using Shapiro-Wilk tests, evaluating data histograms and Q-Q plots. Baseline population characteristics were presented as mean ± standard deviation (SD) and median (range: minimum to maximum) for parametric and non-parametric continuous variables, respectively. Categorical variables were presented as number (*n*, % of the study group).

Unadjusted comparisons for HIV-free *vs.* HIV+ART and Baseline *vs.* Follow-up

To determine the differences in variable outcomes between HIV-negative and HIV+ART, independent sample t-tests were performed for parameters with a normal distribution and Mann-Whitney tests for parameters with a skewed data distribution. To evaluate the differences in variable outcomes in HIV+ART at baseline *vs.*

follow-up, dependent sample t-tests were performed for variables with a normal data distribution and a Wilcoxon test was performed for variables with a skewed data distribution.

Relationship between variable outcomes:

To determine the relationship between continuous variables, Spearman correlations were performed and reported the Spearman Rho correlation coefficient as r. To evaluate the relationship between categorical variable outcomes, a Chi-square or Pearson Chi-square tests were performed with Bonferroni post-hoc corrections when more than 2 comparisons were made.

Independent associations:

Cross-sectional analyses: To determine independent associations between independent and dependent variable outcomes (retinal vessel features), multiple linear stepwise regression analyses were performed. Multiple linear stepwise regression analyses were preferred due to the large number of variables in our relatively small study population size as multiple stepwise regression analyses take all possible confounding factors into account, but only adjust for significant confounders in analyses. Variables with skewed data distribution were $\log_{10}$-transformed. Results were reported as the standardised β coefficient (95% confidence interval (95%CI)) with R, R^2 and adjusted R^2 for each analysis.

Longitudinal repeated measures analyses: Linear mixed model regression analysis was applied to determine the longitudinal effects of markers of HIV and ART on variable outcomes in the HIV+ART study group only. For each analysis, participants were nested in each visit and participants at each time point were included as random effects factor variables with random intercept to account for possible inter-individual variation while adjusting for selected covariates (Age, sex, smoking, alcohol consumption, employment, BMI, DBP and timepoint). Variables with skewed data distribution were $\log_{10}$-transformed. Estimated effects are expressed as a change (parametric data) or a % change (non-parametric data) for each SD increment change with a 95% confidence interval.

Markers of HIV and ART: For cross-sectional and longitudinal statistical analyses markers of HIV and ART included viral load, CD4 cell count, HIV-duration (< 5 years *vs.* ≥ 5 years), ART-duration (weeks), ART-type (1^{st} line *vs.* 2^{nd} line).

Statistical Significance: The significant threshold for all statistical analysis was set at $p < 0.05$.

Chapter 3

Cross-sectional results

Results in the current chapter represent cross-sectional statistical analyses and compares HIV-free and HIV+ART study groups. Also, independent associations between HIV+ART *vs*. HIV-free and markers of HIV (viral load, CD4 cell count and HIV-duration) and ART (ART-duration and ART-type) were elucidated in linear stepwise regression analyses. The description of regression results focusses mostly on the significant associations between dependent variable outcomes (retinal vessel features) and markers of HIV and ART, as well as cardiometabolic variables that were significantly different between study groups, although all the results are presented in the data tables.

3.1. Population characteristics

3.1.1. Demographic, lifestyle, and socio-economic population characteristics

The cross-sectional part of the present study assessed a total number of 210 study participants (HIV-free: n = 88 and HIV+ART: n = 122). The mean±SD age for HIV+ART was significantly younger (p = 0.011) and consisted of significantly fewer participants of mixed ancestry (p = 0.002) compared to HIV-free. Level of education was also lower in HIV+ART *vs*. HIV-free (p = 0.001). No other significant differences were observed (**Table 3.1.**).

Table 3.1*. Demographic, lifestyle, and socio-economic population characteristics.*

Variable [a]	HIV-free (n = 88)	HIV+ART (n = 122)	*P*-value
Age (years)	44.06±11.09	40.35±8.94	0.011
Sex (Women, *n* (%))	71 (80.7%)	77 (63.1%)	0.006
Ethnicity (Mixed, *n* (%))	83(94.3%)	97(79.5%)	0.002
Smoking status (Yes, *n* (%))	55 (62.5%)	65 (53.3%)	0.162
Alcohol consumption (Yes, *n* (%))	34 (38.6%)	55 (45.1%)	0.351
Employment (unemployed, *n* (%))	49 (55.7%)	50 (41%)	0.108
Level of education (≤ primary school completed, *n* (%))	70 (79.5%)	80 (65.6%)	0.001

[a]Data represented as mean±SD or *n* (% of group) for HIV-free (n = 88) and HIV+ART (n = 122).

3.1.2. Body composition population characteristics

The mean BMI for HIV-free was in the overweight range. The mean BMI for HIV+ART was significantly lower than HIV-free ($p < 0.001$) and in the normal weight range. After stratifying study participants according to the WHO BMI categories, a significant inverse association between BMI and HIV+ART *vs*. HIV-free was

observed (p = 0.002). Although waist-to-hip ratio did not significantly differ between study groups, both waist (p = 0.006) and hip circumferences (p < 0.001) were significantly lower in HIV+ART compared to HIV-free (**Table 3.2.**).

Table 3.2*. Body composition population characteristics.*

Variable[a]	HIV-free (*n* = 88)	HIV+ART (*n* = 122)	*p*-value
Body Mass Index (BMI, kg/m^2)	28.25±7.68	24.50±6.65	< 0.001
Weight (kg)	72.50±21.41	64.78±16.85	0.006
Body composition (BMI classification)			
Underweight (BMI < 18.5 kg/m^2, *n* (%))	6 (6.8%)	20 (16.4%)	0.002
Normal weight (BMI 18.5 to < 25 kg/m^2, *n* (%))	26 (29.5%)	52 (42.6%)	
Overweight (BMI 25 to < 30 kg/m^2, *n* (%))	22 (25%)	28 (23%)	
Obese (BMI > 30 kg/m^2, *n* (%))	34 (38.6%)	22 (18%)	
Waist-to-hip ratio	0.89 (0.71 to 1.19)	0.92 (0.71 to 29.33)	0.171
Elevated (>0.95/>0.90 women/men)	54 (61.4%)	81 (66.4%)	0.453
Waist circumference (cm)	93.77±17.16	87.54±14.44	0.006
Hip circumference (cm)	104.23±15.70	95.90±13.43	< 0.001

[a]Data represented as mean±SD, median (range) or *n* (% of group) for HIV-free (*n* = 88) and HIV+ART (*n* = 122).

3.1.3. Fasting lipid and glucose population characteristics

HDL cholesterol was significantly higher in HIV+ART compared to HIV-free (p = 0.019). Although the mean triglyceride levels did not differ between HIV+ART compared to HIV-free, significantly more participants in HIV+ART compared to HIV-free presented with elevated triglyceride levels (p = 0.042). HbA1C was also significantly lower in HIV+ART compared to HIV-free (p = 0.047). No other significant differences were observed. (**Table 3.3.**).

Table 3.3. *Fasting lipid and glucose population characteristics.*

Variable [a]	HIV-free (*n* = 88)	HIV+ART (*n* = 122)	*p*-value
Lipid Profile			
Total Cholesterol (mmol/L)	4.51±0.98	4.59±1.00	0.569
Elevated (≥ 5 mmol/L, *n* (%))	21 (23.9%)	37 (30.3%)	0.301
High-Density Lipoprotein Cholesterol (HDL, mmol/L)	1.39±0.45	1.59±0.74	0.019
Decreased (≤ 1.2/1.0 mmol/L women/men, *n* (%))	31 (35.2%)	33 (27%)	0.204
Low-Density Lipoprotein Cholesterol (LDL, mmol/L))	2.57±0.83	2.43±0.85	0.231
Elevated (≥ 3 mmol/L, *n* (%))	21 (24.1%)	27 (22.3%)	0.758
Triglycerides (mmol/L)	1.22±0.67	1.27±0.92	0.616
Elevated (≥ 1.7 mmol/L, *n* (%))	14 (15.9%)	34 (27.9%)	0.042
Glucose Homeostasis			
Fasting glucose (mmol/L)	4.97±1.85	5.07±2.10	0.714
Elevated (≥ 5.6 mmol/L, *n* (%))	6 (6.8%)	10 (8.2%)	0.710
Glycated Haemoglobin (HbA1c, %)	5.58±1.00	5.32±0.90	0.047
Elevated (≥ 5.9%, *n* (%))	12 (13.6%)	9 (7.4%)	0.136

[a]Data represented as mean±SD or *n* (% of group) for HIV-free (*n* = 88) and HIV+ART (*n* = 122).

3.1.4. Hb, liver function (GGT) and kidney function (serum creatinine, urine albumin, albumin-to-creatinine ratio and eGFR levels)

The liver enzyme GGT was significantly higher in HIV+ART compared to HIV-free ($p < 0.001$) and significantly more study participants in HIV+ART presented with and elevated GGT levels compared to HIV-free ($p < 0.001$). eGFR was also significantly higher in HIV+ART compared to HIV-free ($p = 0.020$). No other significant differences were observed (**Table 3.4.**).

Table 3.4*. Hb, GGT, serum creatinine, albuminuria, albumin-to-creatinine ratio and eGFR population characteristics.*

Variable[a]	HIV-free (*n* = 88)	HIV+ART (*n* = 122)	*p*-value
Haemoglobin (g/dL)	13.53±1.48	13.5±1.68	0.894
Decreased (Women: < 12.0, men: < 13.0 g/dL, *n* (%))	15 (17%)	25 (20.5%)	0.530
hsCRP (mg/L)	5.55 (0.10 to 89)	4.50 (0.10 to 55.8)	0.906
Elevated (> 3mg/L)	55 (64%)	73 (60.3%)	0.597
Liver function			
γ-Glutamyl transferase (U/L)	27.0 (11 to 814)	43.5 (14 to 494)	< 0.001
Elevated (≥ 40/≥ 60 U/L women/men, *n* (%))	20 (22.7%)	62 (50.8%)	< 0.001
Kidney Function			
Serum creatinine (μmol/L)	62.68±14.73	65.48±20.90	0.257
Albuminuria (mg/L)	8.5 (1.1 to 496)	8.25 (0.0 to 988.2)	0.396
Albumin-to-creatinine ratio (mg/mmol)	0.7 (0.10 to 35.9)	1.7 (0.0 to 123.5)	0.563
Increased (> 3 mg/mmol, *n* (%))	13 (15.1%)	23 (18.9%)	0.483
eGRF (mL/minute/1.73 m^3)	107.38±15.69	112.55±15.88	0.020
Decreased (< 90 mL/minute/1.73 m^3, *n* (%)) [e]	9 (10.2%)	7 (5.7%)	0.226

[a]Data represented as mean±SD, median (range) or *n* (% of group) for HIV-free (*n* = 88) and HIV+ART (*n* = 122).

3.1.5. Blood pressure and heart rate

SBP ($p < 0.001$), DBP ($p < 0.001$), heart rate ($p = 0.032$) and the frequency of hypertension (SBP >140 mmHg or DBP >90 mmHg, $p = 0.001$) were significantly lower in HIV+ART *vs.* HIV-free (**Table 3.5.**).

Table 3.5*. Blood pressure and heart rate population characteristics.*

Variable[a]	HIV-free (*n* = 88)	HIV+ART (*n* = 122)	*p*-value
Systolic Blood Pressure (mmHg)	130.96±20.30	120.89±18.12	< 0.001
Elevated (> 140 mmHg), *n* (%)	26 (29.5%)	19 (15.6%)	0.015
Diastolic Blood pressure (mmHg)	89.30±13.62	82.69±12.25	< 0.001
Elevated (> 90 mmHg), *n* (%)	41 (46.6%)	29 (23.8%)	0.001
Hypertension (SBP > 140 mmHg or DBP >90 mmHg), *n* (%)	44 (50%)	34 (27.9%)	0.001
Heart Rate (bpm)	70.06±11.74	73.74±12.61	0.032

[a]Data represented as mean±SD or *n* (% of group) for HIV-free (*n* = 88) and HIV+ART (*n* = 122).

3.1.6. HIV and ART population characteristics

The median viral load in HIV+ART was within the WHO recommended range (< 1000 copies mRNA/mL) for successful viral suppression (237). The mean CD4 cell count in HIV+ART was above WHO recommended cut-off of 250 cells/mm^3 (237).

Most participants were on first-line ART (TDF + 3TC (or FTC) + EFV) (86.8%) with the median ART duration 149 weeks (range:1 to 566 weeks). The median viral load (p = 0.036) and ART-duration (p < 0.001) were significantly lower and mean CD4 cell count significantly higher (p = 0.002) for participants that were in 1st-line ART compared to 2nd-line ART.

HIV duration (< 5 years *vs.* ≥ 5 years) had no effect on median viral load values, however, mean CD4 cell count was significantly higher (p = 0.028) and median ART-duration was significantly lower in HIV-duration of < 5 years compared to ≥ 5 years (p < 0.001). No other significant differences were observed (**Table 3.6.**).

Table 3.6. *HIV and ART population characteristics.*

Variable[a]	**HIV+ART (*n* = 122)**	**Viral load** (copies mRNA/mL)	**CD4 cell count** (cells/mm^3)	**ART-duration**
HIV+ART		50 (10 to 675032)	539.92±237.16)	166 (1 to 707)
ART-type				
1st line therapy	105 (86.8%)	50 (10 to 222342)	563.42±238.06	149 (1 to 566)
2nd line therapy	16 (13.2%)	348 (10 to 675032)	388.94±180.06	430.29 (157 to 707)
***p*-value**		**0.036**	**0.002**	**< 0.001**
HIV-duration				
< 5 years	56 (46.3%)	32 (10 to 222342)	591.98±253.72)	105 (1 to 314)
≥ 5 years	65 (53.7%)	50 (10 to 675032)	442.35±215.75	290 (12 to 707)
***p*-value**		**0.179**	**0.028**	**< 0.001**

[a]Data represented as mean±SD, median (range) or *n* (% of group) for HIV+ART (n = 122).

Viral load and CD4 cell count were inversely correlated (Spearman's correlation coefficient r = 0.275; p = 0.003). ART duration was not significantly correlated with viral load (p = 0.893) and CD4 count (p = 0.101).

3.1.7. Retinal vessel calibre population characteristics.

The mean CRVE in HIV+ART was significantly lower compared to HIV-free (p = 0.004). No other significant differences were observed between groups in terms of CRAE and AVR (**Table 3.7.**).

Table 3.7. *Retinal vessel calibre population characteristics.*

Variable[a]	**HIV-free (*n* = 80)**	**HIV+ART (*n* = 112)**	***p*-value**
Central retinal arteriolar equivalent (CRAE, μm)	151.57±16.69	147.06±14.75	0.055
Central retinal venular equivalent (CRVE, μm)	232.47±25.41	222.18±22.12	0.004
CRAE/CRVE ratio (AVR)	0.66±0.06	0.66±0.07	0.355

[a]Data represented as mean±SD for HIV-free (n = 80) and HIV+ART (n = 112).

3.1.8. Retinal vessel network population characteristics

No significant differences were observed between study groups in terms of retinal vessel network features (**Table 3.8.**).

Table 3.8. *Retinal vessel network population characteristics.*

Variable[a]	HIV-free (*n* = 79)	HIV+ART (*n* = 98)	*p*-value
Segment tree area (mm^2)	4.63±1.00	4.50±0.82	0.366
Total length of skeletonised tree (mm^2)	60.71±12.63	59.74±10.25	0.582
Fractal analysis - segmented	1.34±0.02	1.34±0.02	0.898
Fractal analysis – skeleton	0.62±0.03	0.63±0.03	0.425
Fourier fractal – enhanced	2.43±0.13	2.43±0.13	0.892
Lacunarity – segmented	1.04±0.02	1.05±0.02	0.980
Lacunarity – skeleton	0.93±0.02	0.93 ± 0.02	0.777
Number of branch points	46.32±15.44	45.13±12.46	0.582
Number of end points	62.87±9.20	63.49±8.07	0.640
Average arterial tree diameter (µm)	75.86±7.16	75.37±6.29	0.634
Retinal area (mm^2)	62.61±11.64	61.77±8.36	0.589
Number of arterial tree branch segments/tree area (mm^2)	9.97±2.16	10.01±1.89	0.903
Tortuosity index	0.90±0.01	0.90±0.01	0.550
Average tortuosity of branch segments	0.91±0.01	0.91±0.01	0.344
Average length of branch segments (mm)	0.72±0.11	0.72±0.09	0.933

[a]Data represented as mean±SD or median (range) for HIV-free (*n* = 79) and HIV+ART (*n* = 98).

3.1.9. Retinal vessel branching population characteristics

Arteriolar D0, D1 and D2 were wider in HIV+ART compared to HIV-free ($p < 0.001$). Similarly, venular D0 ($p = 0.001$), D1 ($p < 0.001$) and D2 ($p = 0.001$) were wider in HIV+ART compared to HIV-free. Venular branching optimality ($p = 0.001$) and mean branching coefficient ($p = 0.009$) were significantly lower and mean asymmetry ratio was significantly higher ($p = 0.024$) in HIV+ART compared to HIV-free. No other significant differences were observed (**Table 3.9**).

Table 3.9. *Retinal vessel branching population characteristics.*

Variable[a]	HIV-free (*n* = 80)	HIV+ART (*n* = 112)	*p*-value
Arteriolar features			
D0 (µm)	121.53±13.63	135.60±16.18	< 0.001
D1 (µm)	87.95±11.90	100.67±13.98	< 0.001
D2 (µm)	108.71 (82.46 to 147.53)	121.24 (94.19 to 1144.08)	< 0.001
Branch angle °	89.47±15.96	90.71 ± 14.06	0.577
Branch optimality	0.83±0.05	0.84±0.04	0.061
Mean branching coefficient	2.62±0.41	2.62±0.48	0.939
Mean asymmetry ratio	0.68±0.13	0.69±0.14	0.433
Mean angular asymmetry	43.93 (-47.99 to 96.83)	38.33 (-34.64 to 104.86)	0.190
Venular features			
D0 (µm)	158.31±19.08	168.22±20.37	0.001
D1 (µm)	94.34±15.45	107.83±18.22	< 0.001
D2 (µm)	141.45±19.15	151.55±20.45	0.001
Branch angle °	84.21±9.93	86.22±10.95	0.189
Branch optimality	0.78±0.04	0.80±0.04	0.001
Branching coefficient	3.60±1.02	3.23±0.87	0.009
Mean asymmetry ratio	0.49±0.16	0.54±0.17	0.024
Mean angular asymmetry	46.19±22.21	48.75±22.41	0.433

[a]Data represented as mean±SD for HIV-free (*n* = 80) and HIV+ART (*n* = 112).

3.1.10. Relationship between cardiometabolic variables and retinal vessel features

To evaluate whether cardiometabolic variable outcomes were associated with retinal vessel features, Spearman correlations were applied in the total study population. Significant correlation coefficients between cardiometabolic and retinal vessel variables in the total study population are indicated in bold. Additionally, significant correlation coefficients of variables that were also significantly different between HIV-free and HIV+ART are indicated in grey. These variables indicated in grey are of particular interest as they may indicate a possible cardiometabolic involvement in differences observed in retinal vessel variables between groups.

HDL-cholesterol and HbA1c (significantly higher and significantly lower in HIV+ART *vs.* HIV free, respectively: **Table 3.3.**), were respectively negatively and positively correlated with CRVE (as observed in HIV+ART *vs.* HIV-free: **Table 3.7.**). ART-duration was also inversely correlated with CRVE.

Similarly, a significant inverse correlation between blood pressure (SBP and DBP significantly lower in HIV+ART *vs.* HIV-free: **Table 3.5.**) and various arteriolar branching vessel diameters and venular D1 were observed. Also, a significant inverse correlation between ART-duration and arteriolar D1 was observed

Positive correlations between heart rate (Significantly higher in HIV+ART *vs.* HIV-free: **Table 3.5.**) and arteriolar D2 and venular D0, D1, D2 and branching optimality (significantly higher in HIV+ART vs. HIV-free: **Table 3.9.**) were observed.

GGT (significantly higher in HIV+ART *vs.* HIV-free: **Table 3.4.**) was positively correlated with venular branching optimality (Also significantly higher in HIV+ART *vs.* HIV-free: **Table 3.9.**) and eGFR (significantly higher in HIV+ART *vs.* HIV-free: **Table 3.4.**) was positively correlated with venular D1. Age (significantly higher in HIV-free *vs.* HIV+ART: **Table 3.1.**) was inversely correlated with venular D1, branching coefficient and angular ratio. All correlations are reported in **Table 3. 10.**

*T**able 3.10**. Spearman correlation between cardiometabolic and retinal vessel feature variable outcomes for the total study population (Chapter 3).*

	Age	BMI	Waist	WHR	TC	HDL	LDL	TG	FG	HbA1c	Hb	hsCRP	GGT	ACR	eGFR	SBP	DBP	HR	CD4	VL	ART-d
CRAE	-0.116	0.049	0.013	-0.017	0.037	-0.105	**0.145***	-0.036	-0.062	**0.174***	-0.011	**0.201****	**-0.183***	0.082	0.103	**-0.219****	**-0.167***	-0.022	0.129	-0.107	-0.048
CRVE	-0.042	0.126	0.092	0.017	-0.014	**-0.194****	0.115	0.037	-0.108	**0.245****	0.104	**0.284****	-0.127	**0.152***	-0.016	-0.070	-0.009	0.030	-0.077	0.075	**-0.196***
AVR	-0.059	-0.101	-0.111	-0.044	0.027	0.085	0.012	-0.061	0.018	-0.059	-0.121	-0.075	-0.050	-0.038	0.079	**-0.192****	**-0.220****	-0.095	**0.191***	**-0.227***	0.133
Average arterial tree diameter	-0.135	0.014	-0.019	-0.038	-0.030	-0.117	0.063	0.016	-0.046	**0.189***	-0.092	**0.298****	-0.127	0.039	0.094	-0.147	-0.098	0.112	-0.049	0.011	-0.150
Total length of skeletonised tree	-0.077	-0.078	-0.051	0.018	-0.037	-0.031	0.000	-0.061	-0.005	0.062	0.111	-0.015	-0.060	0.046	0.036	**-0.180***	**-0.160***	-0.046	0.045	-0.061	-0.047
Segment tree area	**-0.178***	-0.049	-0.036	0.025	-0.069	**-0.154***	0.050	-0.046	-0.072	**0.156***	0.046	**0.170***	-0.126	0.077	0.109	**-0.300****	**-0.239****	0.003	0.056	0.000	-0.152
Number of branch points	-0.082	-0.018	-0.030	0.013	-0.097	-0.110	-0.025	-0.066	0.063	0.080	0.097	0.068	-0.060	0.027	0.036	**-0.151***	-0.121	-0.034	0.024	0.118	-0.035
Number of end points	-0.066	-0.070	-0.062	0.041	-0.110	-0.033	-0.034	**-0.157***	-0.033	0.027	0.062	-0.004	-0.073	-0.025	0.105	**-0.207****	**-0.166***	0.036	-0.038	0.069	0.060
Lacunarity - segmented	-0.031	-0.025	-0.018	0.051	-0.078	-0.089	0.006	-0.034	0.044	0.073	0.066	0.044	-0.057	0.086	-0.004	-0.076	-0.098	-0.046	0.048	0.013	-0.125
Lacunarity - skeletal	0.044	0.036	0.064	0.013	0.134	0.082	0.061	0.049	-0.048	-0.060	-0.008	-0.067	0.092	-0.068	-0.005	0.084	0.090	0.071	-0.098	-0.022	0.119
Fractal analysis – segmented	**-0.148***	-0.069	-0.082	-0.039	-0.097	**-0.154***	0.038	-0.060	-0.070	0.123	-0.075	**0.241****	-0.098	0.103	0.106	**-0.270****	**-0.252****	0.073	0.019	0.075	-0.195
Fractal analysis – skeletonised	0.066	0.018	0.031	-0.009	0.070	0.146	-0.020	-0.001	-0.043	**-0.205****	-0.031	**-0.249****	-0.036	-0.134	-0.034	**0.209****	**0.177***	-0.038	0.046	0.057	0.125
Fourier fractal – enhanced	**-0.434****	-0.025	-0.034	-0.104	-0.113	-0.053	-0.076	-0.136	**-0.194****	**-0.248****	0.006	-0.026	0.020	0.029	**0.250****	**-0.203****	-0.066	-0.036	0.008	-0.032	-0.096
Tortuosity index	0.029	-0.018	0.001	0.036	-0.039	0.046	-0.024	-0.004	0.037	-0.002	**0.215****	-0.119	0.025	-0.102	-0.081	0.070	-0.003	**-0.280****	-0.033	-0.094	0.046
Average tortuosity of branch segr	-0.036	-0.037	0.006	0.030	-0.061	0.073	-0.107	-0.018	-0.027	0.001	**0.246****	-0.115	0.071	-0.043	0.017	0.012	-0.060	**-0.255****	-0.024	-0.122	0.016
A-D0	-0.096	-0.029	0.059	**0.201****	**0.146***	0.075	0.118	-0.059	0.013	0.035	0.083	0.083	0.057	0.140	0.085	**-0.198****	**-0.194****	0.111	-0.062	-0.001	-0.125
A-D1	-0.112	-0.025	0.064	**0.179***	0.082	0.090	0.047	-0.027	0.008	0.018	0.103	0.108	0.096	**0.156***	0.038	**-0.152***	-0.126	0.083	-0.086	0.012	**-0.198***
A-D2	-0.042	-0.008	0.087	**0.256****	0.135	0.064	0.113	-0.037	0.074	0.043	0.120	0.138	0.087	**0.154***	0.083	**-0.165***	**-0.171***	**0.161***	-0.066	-0.011	-0.070
A-Angle	0.035	0.085	0.064	0.053	0.092	-0.046	0.083	0.058	0.102	-0.026	0.081	-0.009	-0.046	-0.058	0.009	-0.058	-0.012	0.113	-0.155	0.177	0.051
A-Optimality	0.052	0.051	0.100	0.132	0.015	0.021	0.016	0.035	0.070	0.026	0.075	0.130	0.099	0.062	-0.060	-0.008	0.014	0.077	-0.036	-0.075	-0.089
A-branching coefficient	0.080	0.021	0.020	0.085	0.078	-0.043	0.084	0.027	0.097	0.015	0.036	0.013	-0.012	-0.025	0.042	0.037	-0.009	0.119	0.036	0.027	0.092
A-Angle ratio	-0.070	0.003	-0.007	-0.079	-0.063	0.052	-0.082	-0.006	-0.061	-0.022	-0.043	-0.043	0.034	0.027	-0.028	-0.007	0.041	-0.124	-0.005	-0.045	-0.099
A-Anglular Asymmetry	0.120	-0.012	0.006	0.007	0.141	0.059	0.105	0.050	0.020	-0.040	0.091	-0.109	-0.122	-0.071	-0.101	0.114	0.050	-0.081	0.034	-0.014	**0.199***
V-D0	-0.012	0.015	0.115	**0.185***	0.082	-0.042	0.083	0.104	-0.061	0.091	**0.257****	0.140	0.044	**0.235****	0.078	-0.119	-0.075	**0.159***	**-0.201***	0.140	-0.099
V-D1	**-0.169***	-0.022	0.000	0.090	0.033	0.077	0.022	-0.037	-0.041	-0.015	-0.002	0.138	0.045	0.108	**0.153***	**-0.209****	-0.133	**0.182***	-0.130	0.145	-0.088
V-D2	0.029	-0.028	0.083	**0.188****	0.133	-0.023	0.119	**0.161***	-0.002	**0.148***	**0.261****	0.111	0.125	**0.248****	0.032	-0.096	-0.069	**0.188****	**-0.229***	0.149	-0.045
V-Angle	-0.050	0.011	0.017	0.077	0.048	-0.120	0.078	0.002	0.136	0.073	0.018	0.039	0.007	0.057	0.090	0.062	0.081	0.037	0.045	0.042	-0.112
V-Optimality	-0.075	-0.083	-0.054	0.061	0.098	0.089	0.062	0.035	0.100	0.039	-0.045	-0.017	**0.180***	0.012	0.054	-0.115	-0.120	**0.200****	-0.036	0.033	-0.024
V-branching coefficient	**0.180***	0.005	0.051	0.037	0.060	-0.059	0.048	0.122	0.066	0.124	**0.170***	-0.023	0.002	0.084	-0.129	**0.160***	0.125	-0.014	-0.091	-0.055	0.047
V-Angle ratio	**-0.163***	0.030	-0.015	-0.062	-0.058	0.074	-0.063	**-0.161***	-0.031	-0.113	**-0.180***	0.022	-0.050	-0.041	0.115	**-0.151***	-0.105	0.024	0.114	0.022	-0.032
V-Anglular Asymmetry	0.010	0.044	0.049	0.036	-0.026	-0.121	0.065	0.053	0.111	0.094	0.004	0.011	0.040	-0.055	-0.093	0.058	0.035	-0.029	-0.029	-0.179	-0.065

Data expressed as Spearman Rho correlation coefficient (*r*) with *p < 0.05 and **p < 0.01.

Abbreviations: A: Arteriole, AVR: CRAE/CRVE, D0: branch parent width, D1: branch smaller branch, D2: branch larger branch, CRAE: Central retinal arteriole equivalent, CRVE: Central retinal venular equivalent, V: Venule.

3.2. Independent associations between independent variables and retinal vessel features

3.2.1. Independent associations with retinal vessel calibre features.

To identify whether HIV disease progression was associated with retinal vessel calibre, we determined the association between viral load and CRAE, CRVE and AVR.

No markers of HIV or ART were significantly associated with CRAE in the total study population and HIV+ART. In terms of variables that were significantly different between study groups, GGT (p = 0.002) and DBP (p = 0.022) were inversely associated with CRAE, whereas HbA1c (p = 0.008) was positively associated with CRAE in the total study population. GGT (p = 0.023) and HbA1c (p = 0.011) were also positively and negatively associated with CRAE respectively in the HIV+ART study population. Other significant results are reported in (**Table 3.11.)**.

Table 3.11*. Significant associations with CRAE.*

Independent variable and study population	Standardised coefficient β (95% CI)	*p*-value
Total study population[a]		
GGT (U/L)	-0.222 (-0.359 to -0.086)	0.002
HbA1c (%)	0.188 (0.049 to 0.328)	0.008
Smoking (Yes)	-0.171 (-0.306 to -0.035)	0.014
Waist-to-hip ratio	-0.166 (-0.302 to -0.030)	0.017
hsCRP (mg/L)	0.160 (0.023 to 0.297)	0.022
DBP (mmHg)	-0.157 (-0.291 to -0.023)	0.022
ACR (mg/mmol)	0.147 (0.009 to 0.284)	0.036
HIV+ART study population[b]		
HbA1c (%)	0.243 (0.851 to 6.324)	0.011
GGT (U/L)	-0.213 (-5.843 to -0.433)	0.023
LDL cholesterol (mmol/L)	0.189 (0.094 to 5.491)	0.043

[a]R = 0.430; R^2 = 0.185; Adj R^2 = 0.154. [b]R = 0.363, R^2 = 0.132; Adj R^2 = 0.107.

HIV+ART status (*vs.* HIV-free) was inversely associated with CRVE in the total study population (p = 0.033). Markers of HIV and ART were not significantly associated with CRVE in the HIV+ART study population. HDL (significantly different between study groups) was inversely associated with CRVE in the total study population (p = 0.001) and HIV+ART (p = 0.043). Other significant results are reported in (**Table 3.12.).**

***Table 3.12**. Significant associations with CRVE.*

Independent variable and study population	Standardised coefficient β (95% CI)	*p*-value
Total study population[a]		
hsCRP (mg/L)	0.243 (0.111 to 0.375)	< 0.001
HDL cholesterol (mmol/L)	-0.227 (-0.363 to -0.090)	0.001
Hb (g/dL)	0.214 (0.071 to 0.357)	0.004
Sex (Women)	0.171 (0.026 to 0.317)	0.021
ACR (mg/mmol)	0.168 (0.036 to 0.301)	0.013
HIV+ART *vs.* HIV-free	-0.146 (-0.280 to -0.012)	0.033
Smoking (Yes)	-0.132 (-0.262 to 0.002)	0.046
HIV+ART study population[b]		
HDL cholesterol (mmol/L)	0.285 (0.134 to 8.134)	0.043
hsCRP (mg/L)	0.231 (2.283 to 10.336)	0.002
ACR (mg/mmol)	0.187 (0.131 to 0.402)	< 0.001

[a]R = 0.478; R^2 = 0.229; Adj R^2 = 0.199. [b]R = 0.429; R^2 = 0.190; Adj R^2 = 0.168.

Markers of HIV and ART were not significantly associated with AVR in the total study population, but viral load was inversely associated (p = 0.037) and ART-duration was positively associated (p = 0.047) with AVR respectively in the HIV+ART study population. DBP and HDL (significantly different between study groups) were negatively (p = 0.003) and positively (p = 0.010) associated with AVR respectively in the total study population. Other significant results are reported in (**Table 3.13.).**

***Table 3.13**. Significant associations with AVR.*

Independent variable and study population	Standardised coefficient β (95% CI)	*p*-value
Total study population[a]		
DBP (mmHg)	-0.216 (-0.356 to -0.077)	0.003
HDL cholesterol (mmol/L)	0.185 (0.045 to 0.324)	0.010
HIV+ART study population[b]		
Viral load (copies mRNA/mL)	-0.198 (-0.025 to -0.001)	0.037
ART duration (weeks)	0.188 (0.001 to 0.024)	0.047

[a]R = 0.272; R^2 = 0.074; Adj R^2 = 0.064; [b]R = 0.275; R^2 = 0.075; Adj R^2 = 0.058.

3.2.2. Significant associations between independent variables and retinal vessel network features.

To identify whether HIV disease progression was associated with retinal vessel network features, we determined the association between viral load and vessel complexity and density.

Markers of HIV and ART were not significantly associated with retinal vessel length and diameter network features in either the total or the HIV+ART study population. HbA1c (significantly different between study groups) was positively associated with total length of skeletonised tree ($p = 0.001$) and the segmented tree area ($p < 0.001$) in the total and HIV+ART study population. GGT (significantly different between study groups) was inversely associated with segmented vessel tree area ($p = 0.034$). Other significant results are reported in (**Table 3.14.**).

Table 3.14*. Significant associations between independent variables and retinal vessel length and diameter network features.*

Retinal vessel network feature and study population	Independent variables	Standardised coefficient β (95% CI)	*p*-value
Average arterial tree diameter (µm)			
Total study population[a]	**hsCRP** (mg/L)	0.277 (0.133 to 0.422)	< 0.001
	Age (years)	-0.146 (-0.291 to -0.002)	0.048
HIV+ART study population[b]	**hsCRP** (mg/L)	0.261 (0.410 to 2.868)	0.009
	Age (years)	-0.241 (-2.746 to -0.288)	0.016
Total length of skeletonised tree (mm^2)			
Total study population[c]	**HbA1c** (%)	0.253 (0.108 to 0.398)	0.001
HIV+ART study population[d]	**HbA1c** (%)	0.311 (1.257 to 5.117)	0.001
	Smoke (Yes)	-0.274 (-4.743 to -0.867)	0.005
	Education (≥ Secondary School)	0.249 (0.637 to 4.460)	0.010
Segment tree area (mm^2)			
Total study population[e]	**HbA1c** (%)	0.361 (0.219 to 0.503)	< 0.001
	Smoke (Yes)	-0.192 (-0.334 to -0.051)	0.008
	GGT (U/L)	-0.151 (-0.290 to -0.011)	0.034
HIV+ART study population[f]	**HbA1c** (%)	0.402 (0.183 to 0.477)	< 0.001
	Smoke (Yes)	-0.329 (-0.418 to -0.122)	< 0.001
	Education (≥ Secondary School)	0.232 (0.045 to 0.336)	0.011

[a]$R = 0.297$; $R^2 = 0.088$; Adj $R^2 = 0.078$. [b]$R = 0.334$; $R^2 = 0.112$; Adj $R^2 = 0.093$. [c]$R = 0.253$; $R^2 = 0.064$; Adj $R^2 = 0.058$. [d]$R = 0.445$; $R^2 = 0.198$; Adj $R^2 = 0.172$. [e]$R = 0.393$; $R^2 = 0.155$; Adj $R^2 = 0.140$. [f]$R = 0.522$; $R^2 = 0.272$; Adj $R^2 = 0.249$.

Markers of HIV and ART were not significantly associated with number of vessel branch points, end points or lacunarity in the total and HIV+ART study populations. In terms of variables that were significantly different between study groups, HbA1c was positively associated with number of branch ($p = 0.041$) and end points ($p = 0.047$) in the total study population, SBP was inversely associated with number of end points ($p = 0.015$) and HDL cholesterol was positively associated ($p = 0.022$) with lacunarity in the total population, but inversely associated ($p = 0.034$) in the HIV+ART study population. Other significant results are reported in (**Table 3.15.**).

Table 3.15. *Significant associations between independent variables and vessel network features related to number of vessel branch points, end points and lacunarity.*

Retinal vessel network feature and study population	Independent variables	Standardised coefficient β (95% CI)	*p*-value
Number of branch points			
Total study population[a]	**HbA1c** (%)	0.155 (0.006 to 0.303)	0.041
HIV+ART study population	No associations		
Number of end points			
Total study population[b]	**SBP** (mmHg)	-0.183 (-0.329 to -0.036)	0.015
	HbA1c (%)	0.149 (0.002 to 0.295)	0.047
HIV+ART study population[c]	**Sex** (Women)	-0.215 (-3.350 to -0.124)	0.035
Lacunarity - segmented			
Total study population	No associations		
HIV+ART study population[d]	**HDL cholesterol** (mmol/L)	-0.234 (-0.008 to -0.001)	0.022
Lacunarity - skeletal			
Total study population	No associations		
HIV+ART study population[e]	**HDL cholesterol** (mmol/L)	0.217 (0.001 to 0.008)	0.034

[a]R = 0.155; R^2 =0.024; Adj R^2 = 0.018. [b]R = 0.230; R^2 = 0.053; Adj R^2 = 0.042. [c]R = 0.215; R^2 = 0.046; Adj R^2 = 0.036. [d]R = 0.234; R^2 = 0.055; Adj R^2 = 0.045. [e]R = 0.217; R^2 = 0.047; Adj R^2 = 0.037.

Markers of HIV and ART were not significantly associated with vessel network fractal features in the total and HIV+ART study populations. SBP was inversely associated with fractal analyses of vessel segments in the total (p = 0.002) and HIV+ART (p = 0.003) study populations, but positively associated with fractal analyses of the skeletonised vessel tree (p = 0.032) in HIV+ART. DBP was positively associated with fractal analyses of the skeletonised vessel tree in the total study population (p = 0.038). eGFR was inversely associated with enhanced Fourier fractal in HIV+ART (p = 0.015). Other significant results are reported in (**Table 3.16.**).

Table 3.16. *Significant associations between independent variables and retinal vessel network fractal features.*

Retinal vessel network feature and study population	Independent variables	Standardised coefficient β (95% CI)	*p*-value
Fractal analysis – segmented			
Total study population[a]	**SBP** (mmHg)	-0.232 (-0.375 to -0.090)	0.002
	hsCRP (mg/L)	0.222 (0.080 to 0.365)	0.002
HIV+ART study population[b]	**SBP** (mmHg)	-0.288 (-0.011 to -0.002)	0.003
	hsCRP (mg/L)	0.263 (0.002 to 0.010)	0.007
Fractal analysis – skeletonised			
Total study population[c]	**hsCRP** (mg/L)	-0.256 (-0.401 to -0.112)	0.001
	DBP (mmHg)	0.152 (0.008 to 0.296)	0.038
HIV+ART study population[d]	**hsCRP** (mg/L)	-0.337 (-0.017 to -0.005)	0.001
	SBP (mmHg)	0.206 (0.001 to 0.013)	0.032
Fourier fractal – enhanced			
Total study population[e]	**Age** (years)	-0.477 (-0.607 to -0.348)	0.001
	Sex (Women)	0.204 (0.074 to -0.333)	0.002
HIV+ART study population[f]	**Age** (years)	-0.520 (-0.090 to -0.041)	< 0.001
	Sex (Women)	0.277 (0.013 to 0.057)	0.002
	eGFR (mL/minute/1.73 m^3)	-0.211 (0.051 to 0.002)	0.032

[a]R = 0.325, R^2 0.106; Adj R^2 =0.095. [b]R = 0.410; R^2 = 0.168; Adj R^2 = 0.150. [c]R = 0.292; R^2 = 0.085; Adj R^2 =0.075. [d]R = 0.413; R =0.171; Adj R^2 = 0.153. [e]R = 0.514; R^2 = 0.264; Adj R^2 = 0.256. [f]R = 0.563; R^2 = 0.316; Adj R^2 = 0.294.

Markers of HIV and ART were not significantly associated with vessel network tortuosity features. Heart rate (significantly different between study groups) was inversely associated with tortuosity index (p = 0.003) in the total study population. Other significant results are reported in (**Table 3.17.**).

Table 3.17*. Significant associations between independent variables and retinal vessel network tortuosity features.*

Retinal vessel network feature and study population	Independent variables	Standardised coefficient β (95% CI)	*p*-value
Tortuosity index			
Total study population[a]	**Heart rate** (bpm)	-0.205 (-0.345 to -0.065)	0.004
	Hb (g/dL)	0.263 (0.118 to 0.407)	< 0.001
	Triglycerides (mmol/L)	-0.231 (0.376 to 0.086)	0.002
HIV+ART study population	No association		
Average tortuosity of branch segment			
Total study population[b]	**Hb** (g/dL)	0.277 (0.133 to 0.421)	< 0.001
	Triglycerides (mmol/L)	-0.260 (-0.404 to 0.115)	0.001
HIV+ART study population[c]	**Hb** (g/dL)	0.299 (0.001 to 0.005)	0.003

[a]R = 0.377; R^2 = 0.142; Adj R^2 = 0.127. [b]R = 0.382; R^2 = 0.146; Adj R^2 = 0.131. [c]R = 0.299; R^2 =0.089, Adj R^2 = 0.080.

3.2.3. Significant associations between independent variables and retinal branching angle features

To identify whether HIV disease progression was associated with retinal branching angle features, we determined the association between viral load and branching angles and vessel diameters.

HIV+ART status (*vs.* HIV-free) was positively associated with D0, D1 and D2 ($p < 0.001$, respectively) in the total study population. No markers of HIV or ART in the HIV+ART group were associated with arteriolar branching diameters in the bifurcation area. GGT was inversely associated with D0 ($p = 0.048$), and waist circumference positively associated with D1 ($p = 0.002$) in the total study population. DBP was positively associated with D2 in HIV+ART ($p = 0.013$). Other significant results are reported in (**Table 3.18.**).

Table 3.18. *Significant associations between independent variables and* ***arteriolar*** *branching diameters in the bifurcation area.*

Retinal vessel branching feature and study population	Independent variables	Standardised coefficient β (95% CI)	*p*-value
D0 (µm)			
Total study population[a]	**HIV+ART *vs.* HIV-free**	0.469 (0.340 to 0.598)	< 0.001
	Waist-to-hip ratio	0.155 (0.032 to 0.278)	0.014
	Triglycerides (mmol/L)	-0.235 (-0.368 to -0.102)	0.001
	LDL cholesterol (mmol/L)	0.227 (0.100 to 0.353)	0.001
	Hb (g/dL)	0.178 (0.051 to 0.305)	0.006
	ACR (mg/mmol)	0.157 (0.031 to 0.283)	0.015
	GGT (U/L)	-0.140 (-0.278 to -0.001)	0.048
HIV+ART study population[b]	**LDL cholesterol** (mmol/L)	0.245 (0.943 to 6.994)	0.011
	Triglycerides (mmol/L)	-0.243 (-6.952 to -0.901)	0.011
D1 (µm)			
Total study population[c]	**HIV+ART *vs.* HIV-free**	0.467 (0.342 to 0.592)	< 0.001
	Waist circumference (cm)	0.201 (0.072 to 0.329)	0.002
	Triglycerides (mmol/L)	-0.237 (-0.365 to -0.108)	0.000
	Waist-to-hip ratio	0.156 (0.032 to 0.281)	0.014
	Hb (g/dL)	0.130 (0.005 to 0.256)	0.042
HIV+ART study population[d]	**Triglycerides** (mmol/L)	-0.254 (-0.178 to -0.922)	0.009
	LDL cholesterol (mmol/L)	0.202 (0.197 to 5.453)	0.035
D2 (µm)			
Total study population[e]	**HIV+ART *vs.* HIV-free**	0.328 (0.192 to 0.464)	< 0.001
HIV+ART study population[f]	**DBP** (mmHg)	0.237 (0.005 to 0.045)	0.013

[a]R = 0.570; R^2 = 0.325; Adj R^2 = 0.299. [b]R = 0.309, R^2= 0.095; Adj R^2 = 0.078 [c]R = 0.548; R^2 = 0.300; Adj R^2 = 0.281. [d]R = 0291; R^2 =0.085; Adj R^2 = 0.068. [e]R = 0.328; R^2 = 0.107; Adj R^2 = 0.103. [f]R = 0.237; R^2 = 0.056; Adj R^2 = 0.047.

Markers of HIV and ART were not significantly associated with arteriolar branching angle features in the total and HIV+ART study populations. Heart rate was positively associated with mean branching coefficient (p = 0.017 and p = 0.008) and inversely associated with mean branching asymmetry ratio (p = 0.040 and p = 0.016) in the total and HIV+ART study population, respectively. HbA1c was inversely associated with mean angular asymmetry in HIV+ART (p = 0.040). Other significant results are reported in (**Table 3.18.**).

Table 3.19*. Significant associations between independent variables and* ***arteriolar*** *branching angle features.*

Retinal vessel branching feature and study population	Independent variables	Standardised coefficient β (95% CI)	*p*-value
Branch angle			
Total study population	No associations		
HIV+ART population[a]	**Heart rate** (bpm)	0.242(0.154 to 5.9480	0.009
	Viral load (copies mRNA/mL)	0.233(0.224 to 5.817)	0.012
Branch optimality			
Total study population	No associations		
HIV+ART study population[b]	**Albuminuria** (mg/L)	0.195 (0.001 to 0.016)	0.043
Mean branching coefficient			
Total study population[c]	**Heart rate** (bpm)	0.173 (0.032 to 0.315)	0.017
HIV+ART study population[d]	**Heart rate** (bpm)	0.251 (0.031 to 0.209)	0.008
Mean asymmetry ratio			
Total study population[e]	**Heart rate** (bpm)	-0.148 (-0.289 to -0.007)	0.040
	Alcohol consumption (Yes)	0.146 (0.005 to 0.287)	0.043
HIV+ART study population[f]	**Heart rate** (bpm)	-0.230 (-0.056 to -0.006)	0.016
Mean angular asymmetry			
Total study population	No associations		
HIV+ART study population[g]	**HbA1c** (mmol/L)	-0.209 (-0.158 to -0.004)	0.040

[a]R = 0.341; R^2 = 0.116; Adj R^2 = 0.099. [b]R = 0.195; R^2 = 0.038; Adj R^2 = 0.029. [c]R = 0.173; R^2 = 0.030; Adj R^2 = 0.025. [d]R = 0.251; R^2 = 0.063; Adj R^2 = 0.054. [e]R = 0.207; R^2 = 0.043; Adj R^2 = 0.033. [f]R = 0.230; R^2 = 0.053; Adj R^2 = 0.044. [g]R = 0.207; R^2 = 0.043; Adj R^2 =0.033.

In venular parameters, HIV+ART status (*vs*. HIV-free) was positively associated with D0, D1 and D2 in the total study population ($p < 0.001$, respectively). CD4 cell count was inversely associated with D0 ($p = 0.025$), and viral load positively associated ($p = 0.046$) with D1 in HIV+ART. GGT was inversely associated with D0 in the total ($p = 0.009$) and HIV+ART ($p = 0.001$) study populations. SBP was inversely associated ($p = 0.009$) and BMI positively associated ($p = 0.028$) with D1 in the total study population. HbA1c positively associated with D1 in HIV+ART ($p = 0.015$). Other significant results are reported in (**Table 3.20.**).

***Table 3.20**. Significant associations between independent variables and **venular** branching diameters in the bifurcation area.*

Retinal vessel branching feature and study population	Independent variables	Standardised coefficient β (95% CI)	*p*-value
D0 (µm)			
Total study population[a]	**ACR** (mg/mmol)	0.274 (0.143 to 0.405)	< 0.001
	Hb (g/dL)	0.340 (0.203 to 0.476)	< 0.001
	HIV+ART *vs.* HIV-free	0.337 (0.199 to 0.476)	< 0.001
	Hip circumference (cm)	0.137 (0.001 to 0.273)	0.049
	GGT (U/L)	-0.187 (-0.331 to -0.047)	0.009
	hsCRP (mg/L)	0.147 (0.016 to 0.278)	0.028
	Serum creatinine (µmol/L)	-0.142 (-0.273 to -0.010)	0.035
HIV+ART study population[b]	**ACR** (mg/mmol)	0.282 (0.104 to 9.362)	0.002
	Hb (g/dL)	0.259 (0.102 to 8.944)	0.005
	GGT (U/L)	-0.314 (-0.238 to -2.565)	0.001
	CD4 cell count (cells/mm3)	-0.211 (-0.021 to -0.562)	0.025
	hsCRP (mg/L)	0.187 (0.012 to 7.384)	0.038
D1 (µm)			
Total study population[c]	**HIV+ART *vs.* HIV-free**	0.344 (0.207 to 0.481)	< 0.001
	ACR (mg/mmol)	0.182 (0.051 to 0.314)	0.007
	SBP (mmHg)	-0.184 (-0.321 to -0.047)	0.009
	BMI (kg/m^2)	0.156 (0.017 to 0.294)	0.028
HIV+ART study population[d]	**Viral load** (copies mRNA/mL)	0.187 (0.059 to 6.772)	0.046
	HbA1c (mmol/L)	0.232 (0.846 to 7.620)	0.015
	Age (Years)	-0.205 (-7.131 to -0.331)	0.032
D2 (µm)			
Total study population[e]	**Hb** (g/dL)	0.246 (0.116 to 0.376)	< 0.001
	ACR (mg/mmol)	0.253 (0.122 to 0.384)	< 0.001
	HIV+ART *vs.* HIV-free	0.243 (0.113 to 0.373)	< 0.001
	LDL cholesterol (mmol/L)	0.175 (0.044 to 0.306)	< 0.001
HIV+ART study population[f]	**Albuminuria** (mg/L)	0.285 (0.147 to 9.510)	0.002
	Hb (g/dL)	0.217 (0.051 to 8.114)	0.019

[a]R = 0.508; R^2 = 0.258; Adj R^2 = 0.230. [b]R = 0.475; R^2 = 0.225; Adj R^2 = 0.188. [c]R = 0.446; R^2 = 0.199; Adj R^2 = 0.182. [d]R = 0.339; [2]R = 0.115; Adj R^2 = 0.089. [e]R = 0.453; R^2 = 0.205; Adj R^2 = 0.188. [f]R = 0.356; R^2 = 0.126; Adj R^2 = 0.110.

Various markers of HIV and ART were associated with venular branching angle features. In the total study population, HIV+ART status (*vs.* HIV-free) was positively associated with branching optimality (p = 0.019) and inversely associated with mean branching coefficient (p = 0.007) and mean asymmetry ratio (p = 0.025). In HIV+ART, HIV duration ≥ 5 years was positively associated with mean branching coefficient (p = 0.004) and mean angular asymmetry (p = 0.014) and inversely associated with mean asymmetry ratio (p = 0.001).

2nd-line ART (*vs.* 1st-line ART) was negatively associated with mean branching coefficient ($p = 0.002$) and positively associated with mean asymmetry ratio ($p = 0.034$). Viral load ($p = 0.011$) and ART duration ($p = 0.049$) were inversely associated with mean angular asymmetry.

GGT was positively associated with branching optimality in the total ($p = 0.026$) and HIV+ART ($p = 0.006$) study populations and HDL cholesterol inversely associated with mean angular asymmetry in HIV+ART ($p = 0.030$). Other significant results are reported in (**Table 3.21.**).

***Table 3.21**. Significant association between independent variables and **venular** branching angle features.*

Retinal vessel branching feature and study population	Independent variables	Standardised coefficient β (95% CI)	*p*-value
Branch angle			
Total study population	No associations		
HIV+ART study population[t]	**Albuminuria** (mg/L)	0.231 (0.185 to 4.576)	0.016
	Age (Years)	-0.279 (-4.370 to -0.212)	0.026
Branch optimality			
Total study population[u]	**HIV+ART *vs.* HIV-free**	0.176 (0.029 to 0.323)	0.019
	GGT (U/L)	0.168 (0.021 to 0.315)	0.026
HIV+ART study population[v]	**GGT** (U/L)	0.262 (0.003 to 0.018)	0.006
Mean branching coefficient			
Total study population[w]	**HIV+ART *vs.* HIV-free**	-0.191 (-0.331 to -0.052)	0.007
	Hb (g/dL)	0.173 (0.034 to 0.313)	0.015
HIV+ART study population[x]	**HIV duration** (≥ 5 years)	0.275 (0.079 to 0.399)	0.004
	ART type (2nd-line)	-0.294 (-0.419 to -0.093)	0.002
	Age (Years)	0.286 (0.086 to 0.412)	0.003
Mean asymmetry ratio			
Total study population[y]	**Hb** (g/dL)	-0.183 (-0.323 to -0.043)	0.011
	HIV+ART *vs.* HIV-free	0.161 (0.021 to 0.300)	0.025
HIV+ART study population[z]	**HIV duration** (≥ 5 years)	-0.235 (-0.070 to -0.008)	0.014
	Hb (g/dL)	-0.174 (-0.059 to 0.001)	0.057
	Age (Years)	-0.257 (-0.074 to -0.011)	0.008
	ART type (2nd-line)	0.209 (0.003 to 0.067)	0.034
Mean angular asymmetry			
Total study population	No associations		
HIV+ART study population[aa]	**HIV duration** (≥ 5 years)	0.366 (3.528 to 12.869)	0.001
	Viral load (copies mRNA/mL)	-0.232 (-9.219 to -1.197)	0.011
	HDL cholesterol (mmol/L)	-0.199 (-8.493 to -0.431)	0.030
	ART duration (weeks)	-0.209 (-9.331 to -0.023)	0.049

[t]R = 0.288; R^2 = 0.083; Adj R^2 = 0.066. [u]R = 0.281; R^2 = 0.079; Adj R^2 = 0.069. [v]R = 0.262; R^2 = 0.068; Adj R^2 = 0.060. [w]R = 0.259; R^2 = 0.067; Adj R^2 = 0.057. [x]R = 0.433; R^2 = 0.188; Adj R^2 = 0.164. [y]R = 0.245; R^2 = 0.060; Adj R^2 = 0.050. [z]R. = 0.424; R^2 = 0.180; Adj R^2 = 0.148. [aa]R = 0.407; R^2 = 0.166; Adj R^2 = 0.134.

Chapter 4

Longitudinal results

The current chapter presents longitudinal, repeated measures data from the HIV+ART study group of the current study. Too few HIV-free participants were recruited at follow-up to do meaningful/reliable longitudinal statistical analyses. Only participants who completed baseline and 18-month follow-up visits were included. This chapter aims to evaluate the possible temporal changes in retinal vessel features in the HIV+ART study population and whether the main effects of markers of HIV and ART are associated with these changes.

4.1. Population characteristics

4.1.1. Demographic, lifestyle, and socio-economic population characteristics (baseline *.vs.* follow-up)

A total number of n = 82 HIV+ART study participants completed baseline and 18-month follow-up visits. The study population was relatively young, with a mean±SD age at baseline of 41.13±9.04 years. Age significantly increased over time to 42.89 ± 8.95 ($p < 0.001$). Significantly more participants were unemployed at follow-up compared to baseline ($p = 0.007$). The proportion of study participants for gender, ethnicity, smoking status, alcohol consumption and level of education did not significantly differ across time (**Table 4.1.**).

Table 4.1*. Demographic, lifestyle, and socio-economic population characteristics (baseline vs. follow-up).*

Variable[a]	Timepoint 1	Timepoint 2	*P*-value
Age (years)	41.1±9.0	42.89±9.0	< 0.001
Gender (Female, *n* (%))	49 (59.8%)	49 (59.8%)	0.874
Ethnicity (Mixed ancestry, *n* (%))	69 (84.1%)	69 (84.1%)	0.828
Smoking status (Yes, *n* (%))	41 (50%)	42 (51.2%)	0.974
Alcohol consumption (Yes, *n* (%))	38 (46.3%)	39 (47.6)	0.879
Employment (Unemployed, *n* (%))	27 (32.9%)	39 (47.6%)	0.007
Level of education (≥ Secondary school *n* (%))	18 (22%)	18 (22%)	0.948

[a]Data represented as mean±SD or n = (% of group at timepoint) for n = 82 HIV+ART study participants.

4.1.2. Body composition population characteristics (baseline *.vs.* follow-up)

The mean BMI of the HIV+ART study population was within the normal range at baseline and did not significantly differ at Timepoint 2. Also, most participants (~50%) were in the normal body weight range. Although waist-to-hip ratio did not significantly differ between timepoints, both waist ($p < 0.001$) and hip ($p = 0.001$) circumferences were significantly lower at Timepoint 2 *vs.* Timepoint 1 (**Table 4.2.**).

Table 4.2. *Body composition population characteristics (baseline vs. follow-up).*

Variable[a]	Timepoint 1	Timepoint 2	*P*-value
Weight (kg)	64.97±16.75	66.29±17.79	0.022
Body Mass Index (BMI, kg/m^2)	24.27±6.36	24.56±6.55	0.318
Underweight (BMI < 18.5 kg/m^2, *n* (%))	13 (15.9%)	14 (17.1%)	0.889
Normoweight (BMI 18.5 to < 25 kg/m^2, *n* (%))	38 (46.3%)	37 (45.1%)	
Overweight (BMI 25 to < 30 kg/m^2, *n* (%))	14 (17.1%)	17 (20.7%)	
Obese (BMI > 30 kg/m^2, *n* (%))	17 (20.7%)	14 (17.1%)	
Waist-to-hip ratio	0.94±0.09	0.93±0.09	0.223
Elevated (> 0.95/> 0.90 women/men)	66 (81.5%)	57 (69.5%)	0.076
Waist circumference (cm)	92.51±14.93	88.87±14.57	< 0.001
Hip circumference (cm)	98.47±14.28	95.60±13.02	0.001

[a]Data represented as mean±SD or *n* = (% of group at timepoint) for *n* = 82 HIV+ART study participants

4.1.3. Fasting lipid and glucose population characteristics (baseline *.vs.* follow-up)

HDL cholesterol significantly decreased at Timepoint 2 *vs.* Timepoint 1 ($p = 0.017$) and significantly less study participants had elevated triglyceride levels at Timepoint 2 *vs.* Timepoint 1 ($p = 0.048$). HbA1c levels at Timepoint 2 were significantly higher compared to Timepoint 1 ($p < 0.001$) and significantly more participants presented with elevated HbA1c at Timepoints 2 *vs.* Timepoint 1 ($p = 0.024$). Other fasting lipid and glucose characteristics are presented in (**Table 4.3.)**.

Table 4.3. *Fasting lipid and glucose population characteristics (baseline vs. follow-up).*

Variable[a]	Timepoint 1	Timepoint 2	*P*-value
Lipid Profile			
Total Cholesterol (mmol/L)	4.72±0.97	4.56±0.99	0.091
Elevated (≥ 5 mmol/L, *n* (%))	26 (31.7%)	18 (22%)	0.159
High-Density Lipoprotein Cholesterol (HDL, mmol/L)	1.62±0.77	1.44±0.64	0.017
Decreased (≤ 1.2/1.0 mmol/L women/men, *n* (%))	33 (27%)	26 (31.7%)	0.221
Low-Density Lipoprotein Cholesterol (LDL, mmol/L)	2.52±0.87	2.56±0.80	0.657
Elevated (≥ 3 mmol/L, *n* (%))	19 (23.5%)	22 (27.5)	0.556
Triglycerides (mmol/L)	1.02 (0.46 to 8.03)	1.08 (0.46 to 6.25)	0.556
Elevated (≥ 1.7 mmol/L, *n* (%))	34 (41.5%)	22 (26.8%)	0.048
Glucose Homeostasis			
Fasting glucose (mmol/L)	4.90±0.96	4.80±0.71	0.325
Elevated (≥ 5.6 mmol/L, *n* (%))	10 (12.2%)	8 (9.8%)	0.617
Glycated Haemoglobin (HbA1c, %))	5.22±0.37	5.45±0.55	< 0.001
Elevated (≥ 5.9%, *n* (%))	3 (3.7%)	11 (13.6%)	0.024

[a]Data represented as mean±SD or *n* = (% of group at timepoint) for *n* = 82 HIV+ART study participants.

4.1.4. Hb, hsCRP, GGT and markers of kidney function (serum creatinine, albuminuria, albumin-to-creatinine ratio and eGFR) population characteristics (baseline *.vs.* follow-up)

Inflammation as indicated by hsCRP was significantly higher ($p = 0.011$) and GGT ($p = 0.004$) and eGRF ($p < 0.001$) significantly lower at Timepoint 2 *vs.* Timepoint 1. Significantly more study participants presented with decreased eGRF at Timepoint 2 compared to Timepoint 1 ($p = 0.010$). No other significant differences were observed (**Table 4.4.**).

Table 4.4*. Hb, GGT, serum creatinine, albuminuria, albumin-to-creatinine ratio and eGFR population characteristics (baseline vs. follow-up).*

Variable[a]	Timepoint 1	Timepoint 2	*P*-value
Haemoglobin (g/dL)	13.75±1.68	13.93±1.71	0.110
Decreased (< 12.0/< 13.0 g/dL women/men, *n* (%))	12.(14.6%)	9 (11.2%)	0.502
hsCRP (mg/L)	3.7 (1.0 to 55.8)	6.0 (2.0 to 80.6)	0.011
Elevated (> 3mg/L)	47 (58%)	56 (71.8%)	0.069
γ-Glutamyl transferase (U/L)	45 (14 to 494)	41.50 (14 to 219)	0.004
Elevated (≥ 40/≥ 60 U/L women/men), *n* (%)	41 (50%)	36 (43.9%)	0.434
Serum creatinine (μmol/L)	66.91±23.68	68.56±15.73	0.518
Urine albumin (mg/L)	8.80 (0.5 to 547.2)	8.90 (0.05 to 3570)	0.161
Albumin-to-creatinine ratio (mg/mmol)	0.7 (0.2 to 65.4)	0.7 (0.01 to 305.2)	0.483
Elevated (> 3 mg/mmol), *n* (%)	18 (22%)	14 (17.3%)	0.453
eGRF (mL/minute/1.73 m^3)	112 (24 to 1501)	109 (68 to 1522)	< 0.001
Decreased (< 90 mL/minute/1.73 m^3), *n* (%)	5 (6.1%)	16 (19.5%)	0.010

[a]Data represented as mean±SD or *n* = (% of group at timepoint) for *n* = 82 HIV+ART study participants

4.1.5. Blood pressure and heart rate population characteristics (baseline *.vs.* follow-up)

DBP was significantly higher at Timepoint 2 compared to Timepoint 1 ($p = 0.010$). SBP and heart rate did not significantly differ across timepoints, respectively (**Table 4.5.**).

Table 4.5*. Blood pressure and heart rate population characteristics (baseline vs. follow-up).*

Variable[a]	Timepoint 1	Timepoint 2	*P*-value
Systolic Blood Pressure (mmHg)	120.11±18.26	122.63±17.95	0.120
Elevated (> 140 mmHg, *n* (%))	12 (14.6%)	10 (12.2%)	0.647
Diastolic Blood pressure (mmHg)	81.77±12.50	84.53±11.38	0.013
Elevated (> 90 mmHg, *n* (%))	17 (20.7%)	22 (26.8%)	0.359
Hypertension (SBP > 140 mmHg or DBP > 90 mmHg, *n* (%))	17 (20.7%)	22 (26.8%)	0.359
Heart Rate (bpm)	74.49±12.94	76.44±13.32	0.201

[a]Data represented as mean±SD or *n* = (% of group at timepoint) for *n* = 82 HIV+ART study participants.

4.1.6. HIV and ART population characteristics (baseline *.vs.* follow-up)

Median viral load and mean CD4 cell count values were within acceptable ranges according to WHO standards (1000 copies mRNA/mL and 300 cells/mm^3) at both timepoints and did not significantly differ between timepoints. Most participants were on South Africa's 1st-line fixed dose combination ART. The median duration of ART use at baseline was more than 3 years and significantly increased at Timepoint 2 compared to Timepoint 1 ($p < 0.001$). More than half of the study participants (57.3%) were more than 5 years diagnosed HIV-positive at baseline compared to more than 70% at Timepoint 2 (**Table 4.6.**).

Table 4.6*. HIV and ART population characteristics (baseline vs. follow-up).*

Variable[a]	Timepoint 1	Timepoint 2	*P*-value
Viral load (copies mRNA/mL)	50 (10 to 675032)	50 (10 to 460853)	0.192
CD4 count (cells/mm^3)	511.3±228.9	517.3 ± 216.8	0.866
ART type (1st-line, *n* (%))	68 (84%)	60 (75.9%)	0.206
ART duration (weeks)	183 (0 to 707)	270 (12 to 782)	< 0.001
HIV duration (≥5 years, *n* (%))	47 (57.3%)	58 (70.7%)	0.073

[a]Data represented as mean±SD or *n* = (% of group at timepoint) for *n* = 82 HIV+ART study participants

4.1.7. Retinal vessel calibre population characteristics (baseline *.vs.* follow-up)

Retinal vessel calibre variable outcomes did not significantly differ between Timepoint 1 and Timepoint 2 (**Table 4.7.**).

Table 4.7*. Retinal vessel calibre population characteristics (baseline vs. follow-up).*

Variable[a]	Timepoint 1	Timepoint 2	*P*-value
Central retinal arteriolar equivalent (CRAE, μm)	144.17±14.33	140.50±13.86	0.308
Central retinal venular equivalent (CRVE, μm)	218.74±19.45	219.28±19.41	0.568
CRAE/CRVE ratio (AVR)	0.66±0.67	0.66±0.06	0.166

[a]Data represented as mean±SD or *n* = (% of group at timepoint) for *n* = 72 HIV+ART study participants.

4.1.8. Retinal vessel network population characteristics (baseline *.vs.* follow-up)

Retinal vessel network features did not significantly differ between timepoints (**Table 4.8.**).

Table 4.8*. Retinal vessel network population characteristics (baseline vs. follow-up).*

Variable[a]	Timepoint 1	Timepoint 2	*P*-value
Average arterial tree diameter (µm)	73.50±5.08	73.67±4.98	0.827
Total length of skeletonised tree (mm^2)	58.15±7.84	57.28±7.37	0.269
Segment tree area (mm^2)	4.27±0.58	4.21±0.54	0.193
Number of branch points	42.81±10.41	41.65±10.04	0.288
Number of end points	62.62±8.66	62.23±9.06	0.284
Lacunarity – segmented	1.04±0.02	1.04±0.02	0.314
Lacunarity – skeletonised	0.94±0.02	0.94±0.02	0.623
Fractal analysis - segmented	1.33±0.02	1.33±0.02	0.301
Fractal analysis – skeleton	0.63±0.03	0.63±0.03	0.639
Fourier fractal – enhanced	2.43±0.13	2.44±0.14	0.113
Tortuosity index	0.90±0.01	0.90±0.01	0.497
Average tortuosity of branch segments	0.91±0.01	0.91±0.01	0.102

[a]Data represented as mean±SD or *n* = (% of group at timepoint 1) for *n* = 58 and n = (% of group at timepoint 2) for *n* = 66 HIV+ART study participants.

4.1.9. Retinal vessel branching population characteristics (baseline *.vs.* follow-up)

Retinal vessel branching features did not significantly differ between timepoints (**Table 4.9.**).

Table 4.9*. Retinal vessel branching population characteristics (baseline vs. follow-up).*

Variable[a]	Timepoint 1	Timepoint 2	*P*-value
Arteriolar features			
D0 (µm)	138.05±17.18	137.74±16.51	0.756
D1 (µm)	101.79±14.55	102.07±14.18	0.702
D2 (µm)	123.6 (84 to 144)	123.6 (84 to 166.54)	0.360
Branch angle (°)	90.73±13.86	90.31±14.17	0.620
Branch optimality	0.84±0.04	0.84±0.04	0.713
Mean branching coefficient	2.66±0.55	2.62±0.58	0.204
Mean asymmetry ratio	0.68±0.14	0.70±0.15	0.135
Mean angular asymmetry	41.64 (-38.71 to 105.89)	42.30 (-38.71 to 105.89)	0.325
Venular features			
D0 (µm)	171.98±20.84	172.95±21.02	0.369
D1 (µm)	109.45±20.70	109.12±22.41	0.788
D2 (µm)	156.53±20.64	157.20±20.71	0.546
Branch angle (°)	86.21±10.28	86.06±8.96	0.809
Branch optimality	0.81±0.04	0.81±0.04	0.504
Mean branching coefficient	3.30±0.93	3.32±0.93	0.715
Mean asymmetry ratio	0.53±0.17	0.53±0.17	0.735
Mean angular asymmetry	48.68±22.39	49.04±22.83	0.743

[a]Data represented as mean±SD or *n* = (% of group at timepoint) for *n* = 72 HIV+ART study participants.

4.2. Independent associations between independent variables and retinal vessel features (baseline and follow-up)

4.2.1. Independent associations of retinal vessel calibre (baseline and follow-up)

To identify whether HIV disease progression was associated with retinal vessel calibre, we determined the association between viral load and CRAE, CRVE and AVR.

Each 1000 copies mRNA/mL increase in viral load was associated with a 0.096 µm increase in CRVE and a 0.0003 increment decrease in AVR. 2nd-line ART *vs.* 1st-line ART was associated with an 8.58 µm increase in CRVE.

Each 12.5 mmHg increase in DBP was associated with a 40.9 µm decrease in CRAE and a 0.013 decrease in AVR. Each 19.45 µm increase in CRVE was associated with a 6.38 µm increase in CRAE and each 14.33 increment increase in CRAE was associated with an 8.99 increase in CRVE (**Table 4.10.**). For full data tables for each retinal calibre feature, please see **Supplementary Tables 1.1. to 1.3.**

***Table 4.10**. Significant associations with retinal vessel calibre features (baseline and follow-up).*

Retinal vessel branching feature[a]	Independent variables	Change (95% CI)	*p*-value
CRAE (µm)	**DBP** (mmHg)	-40.9 (-70.5 to -11.5)	0.007
	CRVE (µm)	6.38 (4.32 to 8.42)	< 0.001
CRVE (µm)	**CRAE** (µm)	8.99 (5.98 to 12.01)	< 0.001
	Viral load (copies mRNA/mL)	0.096 (0.017 to 0.175)	0.018
	ART type (2^{nd} -line)	8.58 (0.35 to 16.81)	0.041
AVR	**DBP** (mmHg)	-0.013 (-0.025 to 0.0013)	0.019
	Viral load (copies mRNA/mL)	-0.0003 (-0.0006 to 0.000003)	0.046

[a]Estimates expressed as change for each increment change in confounding factors (Age: 9.04 years, BMI: 6.36 kg/m^2, DBP: 12.5 mmHg, CRAE: 14.33, CRVE: 19.45, CD4 count: 250 cells/mm^3, virial load: 1000 copies mRNA/mL and ART duration: 166.98).

4.2.2. Independent associations of retinal network features (baseline and follow-up)

To determine whether HIV disease progression was associated with retinal vessel network, we determined the association between viral load and vessel complexity and density.

Each 250 cells/mm^3 increment increase in CD4 cell count was associated with a 3.50 increment increase in number of branchpoints and a 3.00 increment increase in number of endpoints. Each 1000 copies mRNA/mL increment increase in viral load was associated with a 0.0006 increment decrease in Fourier fractal (enhanced) and a 0.00006 increment decrease in average tortuosity of branch segment. HIV duration (≥ 5 years) was associated with a 0.008 decrease in lacunarity (skeletonised), and a 0.011 increment increase in fractal analysis (skeletonised). Each 166.98 weeks increment increase in ART exposure was associated with a 0.022 increment increase in Fractal analysis (skeletonised). Timepoint 2 *vs.* Timepoint 1 (18 months) was associated with a 0.041 increment increase in Fourier fractal (enhanced)

Each increment increase in BMI was associated with a 0.0064 increment increase in lacunarity (segmented) and fractal analysis (segmented), respectively and 0.025 increment increase in Fourier fractal (enhanced). Each 12.5 mmHg increment increase in DBP was associated with 0.0013 increment increase in fractal analysis (segmented). Other significant associations are reported in **Table 4.11.** For full data tables for each retinal vessel feature, please see **Supplementary Tables 1.4. to 1.15.**

***Table 4.11**. Significant associations with retinal vessel network features (baseline and follow-up).*

Retinal vessel branching feature[a]	Independent variables	Change (95% CI)	*p*-value
Average arterial tree diameter (µm)	No significant associations		
Total length of skeletonised tree (mm^2)	No significant associations		
Segment tree area (mm^2)	No significant associations		
Number of branch points	**CD4 cell count** (cells/mm^3)	3.50 (1.00 to 6.00)	0.006
Number of end points	**Viral load** (copies mRNA/mL)	0.042 (-0.002 to 0.086)	0.059
	CD4 cell count (cells/mm^3)	3.0 (0.750 to 5.250)	0.010
Lacunarity - segmented	**Sex** (Women)	-0.009 (-0.016 to -0.001)	0.019
	Smoking (Yes)	0.009 (0.0010 to 0.0160)	0.020
	BMI (kg/m^2)	0.00636 (0.00064 to 0.00636)	0.036
Lacunarity - skeletonised	**Sex** (Women)	0.011 (0.0030 to 0.0190)	0.006
	Smoking (Yes)	-0.010 (-0.0180 to -0.0010)	0.021
	HIV duration (≥ 5 years)	-0.0080 (-0.0150 to -0.0010)	0.036
Fractal analysis – segmented	**BMI** (kg/m^2)	0.0064 (0.0064 to 0.0127)	0.021
	DBP (mmHg)	0.0013 (-0.0125 to 0.0013)	0.018
Fractal analysis – skeletonised	**Smoking** (Yes)	-0.020 (-0.032 to -0.007)	0.002
	ART duration (weeks)	0.022 (-0.037 to -0.008)	0.003
	HIV duration (≥ 5 years)	0.011 (0.0001 to 0.021)	0.045
Fourier fractal – enhanced	**Age** (years)	-0.045 (-0.072 to -0.027)	< 0.001
	Sex (Women)	0.082 (0.038 to 0.126)	< 0.001
	BMI (kg/m^2)	0.02544 (0.00064 to 0.05088)	0.033
	Viral load (copies mRNA/mL)	-0.00061 (-0.00122 to -0.00003)	0.043
	Timepoint (Timepoint 2 *vs.* 1)	0.041 (0.001 to 0.080)	0.046
Tortuosity index	**Employment** (Yes)	0.005 (0.00010 to 0.010)	0.040
Average tortuosity of branch segment	**Viral load** (copies mRNA/mL)	-0.000064 (-0.000128 to 0.000003)	0.022

[a]Estimates expressed as change for each increment change in confounding factors (Age: 9.04 years, BMI: 6.36 kg/m^2, DBP: 12.5 mmHg, CRAE: 14.33, CRVE: 19.45, CD4 count: 250 cells/mm^3, virial load: 1000 copies mRNA/mL and ART duration: 166.98).

4.2.3. Associations of vessel branching features (baseline and follow-up)

To identify whether HIV disease progression was associated with retinal branching features, we determined the association between viral load and branching angles and vessel diameters.

HIV duration (≥ 5 years) was associated with a 7.15 µm decrease in arteriolar D0, a 7.33 µm decrease in arteriolar D1 and an 11.8 increment increase in mean venular angular asymmetry. Timepoint 2 *vs*. Timepoint

1 (18 months) was associated with a 0.125 increment increase in arteriolar mean branching coefficient and a 0.037 increment increase in arteriolar mean asymmetry ratio

Each 6.36 kg/m^2 increment increase in BMI was associated with a 3.12 ° increase in arteriolar branching angle and a 0.006 increment increase in arteriolar branch optimality. Other significant associations are reported in **Table 4.12**. For full data tables for each retinal vessel branching feature, please see **Supplementary Tables 1.16. to 1.31.**

***Table 4.12**. Significant associations with retinal vessel branching features (baseline and follow-up).*

Retinal vessel branching feature[a]	Independent variables	Change (95% CI)	*p*-value
Arteriolar			
D0 (µm)	**Smoking** (Yes)	-9.110 (-16.167 to -2.052)	0.013
	HIV duration (≥ 5 years)	-7.154 (-14.189 to -0.120)	0.046
D1 (µm)	**Smoking** (Yes)	-6.052 (-11.900 to -0.204)	0.043
	HIV duration (≥ 5 years)	-7.329 (-13.048 to -1.611)	0.012
D2 (µm)	**Smoking** (Yes)	-8.002% (-13.679 to -1.951)	0.011
	Alcohol consumption (Yes)	6.025% (0.109 to 12.291)	0.046
Branching angle (°)	**BMI** (kg/m^2)	3.116 (-0.064 to 6.296)	0.054
Branch optimality	**BMI** (kg/m^2)	0.006 (-0.006 to 0.019)	0.050
Mean branching coefficient	**Timepoint** (Timepoint 2 *vs.* 1)	0.125 (-0.111 to 0.361)	0.043
Mean asymmetry ratio	**Timepoint** (Timepoint 2 *vs.* 1)	0.0370 (0.0001 to 0.0740)	0.049
Mean angular asymmetry	No significant associations		
Venular			
D0 (µm)	No significant associations		
D1 (µm)	No significant associations		
D2 (µm)	No significant associations		
Branching angle (°)	No significant associations		
Branch optimality	No significant associations		
Mean branching coefficient	**Age** (years)	0.235 (0.018 to 0.443)	0.034
Mean asymmetry ratio	**Age** (years)	-0.0452 (-0.0814 to -9.041)	0.027
	Employment (Yes)	-0.052 (-0.103 to -1.001)	0.045
Mean angular asymmetry	**HIV duration** (≥ 5 years)	11.804 (3.024 to 20.584)	0.009

[a]Estimates expressed as change for each increment change in confounding factors (Age: 9.04 years, BMI: 6.36 kg/m^2, DBP: 12.5 mmHg, CRAE: 14.33, CRVE: 19.45, CD4 count: 250 cells/mm^3, virial load: 1000 copies mRNA/mLand ART duration: 166.98).

4.2.4. Temporal relationship between cardiometabolic and retinal vessel calibre variable outcomes

To evaluate whether changes (Δ) in cardiometabolic variables over time (18-months) were associated with changes in retinal vessel features over time, Spearman correlations were applied. Although no statistical significantly change in retinal vessel features over an 18-month time period were observed, various changes in cardiometabolic variables over an 18-month period were significantly correlated with changes in retinal vessel features **(Table 4.13)**. The correlations between retinal vessel features and cardiometabolic variables that significantly changed over an 18-month period of time (baseline *vs.* follow-up visit) were of special interest and included age (increased: **Table 4.1.**), waist circumference (decrease: **Table 4.1.**), HbA1c (increase: **Table 4.3.**), hsCRP (increase: **Table 4.4.**), GGT (decrease: **Table 4.4.**), eGFR (decrease: **Table 4.4.**) and DBP (increase: **Table 4.5.**).

ΔAge (mean: 1.79 years) between baseline and follow-up was not significantly correlated with any changes in retinal vessel features. ΔWaist circumference was positively correlated with Δarteriolar branching angle. ΔHbA1c was positively correlated with ΔCRVE and Δvenular D1. ΔhsCRP was inversely correlated with Δarteriolar D1 and positively correlated with Δvenular branching coefficient. ΔGGT was not significantly correlated with any changes in retinal vessel features. ΔeGFR was positively correlated with Δfractal analyses (skeletonised) and inversely associated with ΔFourier fractal (enhanced) features. ΔDBP was not significantly correlated with any changes in retinal vessel features. Other significant correlations are reported in **Table 4.13.**

***Table 4.13**. Spearman-correlation between change (between baseline and follow-up) in cardiometabolic and retinal vessel feature variable outcomes for HIV+ART (Chapter 4).*

	ΔAge	ΔBMI	ΔWaist	ΔWHR	ΔTC	ΔHDL	ΔLDL	ΔTG	ΔFG	ΔHbA1c	ΔHb	ΔhsCRP	ΔGGT	ΔACR	ΔeGFR	ΔSBP	ΔDBP	ΔHR	ΔCD4	ΔVL	ΔART-d
ΔCRAE	0.092	-0.141	-0.113	**0.235***	-0.035	-0.171	0.116	-0.049	0.164	0.177	-0.008	-0.036	-0.158	-0.130	0.046	**-0.368****	-0.202	0.123	-0.108	0.162	0.011
ΔCRVE	0.008	-0.070	-0.003	0.034	-0.029	-0.200	0.027	0.103	0.082	**0.316****	0.056	0.193	0.011	-0.055	-0.025	**-0.238***	-0.065	0.176	-0.081	0.215	0.029
ΔAVR	0.054	-0.115	-0.092	0.046	-0.010	0.053	0.096	-0.208	0.044	-0.054	-0.109	-0.175	-0.202	-0.047	0.222	-0.168	-0.196	-0.079	-0.026	-0.110	-0.014
ΔAverage arterial tree diameter	0.086	**0.323***	0.061	**0.277***	0.237	-0.108	0.199	0.103	0.163	0.007	-0.204	0.036	0.053	-0.005	-0.065	-0.066	0.084	0.030	0.073	-0.020	-0.163
ΔTotal length of skeletonised tree	-0.039	**-0.355****	-0.155	0.015	-0.199	0.046	**-0.282***	-0.075	-0.028	0.034	0.109	0.047	-0.158	-0.136	-0.162	-0.234	-0.230	-0.027	-0.236	0.207	-0.213
ΔSegment tree area	-0.046	-0.170	0.027	0.034	-0.156	-0.093	-0.120	0.000	0.092	0.108	0.106	0.121	-0.230	-0.182	-0.079	**-0.268***	-0.134	-0.019	-0.163	**0.249***	-0.190
ΔNumber of branch points	0.095	-0.115	0.052	-0.270	-0.234	-0.050	-0.192	0.013	-0.031	-0.034	0.032	-0.048	-0.072	-0.210	-0.187	**-0.271***	-0.135	0.147	0.177	0.224	-0.051
ΔNumber of end points	0.163	-0.255	-0.081	-0.221	-0.251	0.049	-0.256	-0.263	0.009	0.014	0.015	-0.074	-0.072	0.030	-0.081	-0.042	0.127	0.167	-0.091	**0.273***	0.063
ΔLacunarity - segmented	-0.063	-0.261	-0.042	-0.098	-0.111	-0.047	-0.046	0.017	0.025	-0.055	0.100	-0.027	-0.019	-0.072	-0.149	-0.246	-0.199	0.167	0.003	0.185	-0.104
ΔLacunarity - skeletal	0.012	**0.293***	0.214	0.140	0.101	-0.162	0.137	0.098	-0.030	0.004	0.034	0.072	0.071	-0.012	0.046	0.187	0.168	-0.173	-0.077	-0.216	0.182
ΔFractal analysis – segmented	-0.116	0.060	-0.101	0.157	-0.157	-0.140	-0.015	-0.015	0.208	0.025	-0.108	0.070	0.001	-0.168	-0.165	**-0.366****	-0.156	0.039	-0.038	0.077	-0.046
ΔFractal analysis – skeletonised	-0.153	-0.008	0.013	-0.136	-0.052	0.035	0.020	-0.009	-0.003	-0.068	0.082	-0.139	0.094	0.101	**0.276***	0.242	0.083	-0.163	0.005	-0.225	-0.044
ΔFourier fractal – enhanced	-0.048	0.056	0.022	0.008	0.035	-0.139	0.045	0.096	0.237	-0.213	-0.090	0.091	0.143	0.110	**-0.359****	0.034	0.132	0.131	0.126	-0.119	0.223
ΔTortuosity index	-0.055	0.087	0.011	-0.192	0.055	-0.051	0.092	0.073	-0.052	-0.239	0.011	-0.195	-0.063	-0.032	0.073	0.211	0.235	-0.064	0.091	-0.183	0.041
ΔAverage tortuosity of branch segmer	-0.147	-0.011	0.177	-0.042	0.060	0.034	0.049	0.025	0.064	0.049	0.044	-0.042	-0.140	-0.142	0.023	0.188	0.117	0.027	-0.032	**-0.288***	-0.038
ΔA-D0	0.111	-0.110	0.001	0.095	-0.085	-0.100	-0.003	-0.018	0.128	0.021	0.144	-0.230	-0.106	-0.019	0.182	-0.160	-0.076	-0.179	0.067	-0.055	0.198
ΔA-D1	0.097	-0.074	0.024	0.070	-0.110	-0.076	-0.130	-0.049	0.111	-0.054	-0.074	**-0.284***	-0.145	0.063	0.087	-0.139	-0.036	-0.080	0.070	-0.055	0.140
ΔA-D2	0.180	-0.019	0.064	0.084	-0.070	-0.086	-0.006	-0.014	0.053	0.090	0.056	-0.067	-0.152	-0.061	0.187	-0.202	-0.029	-0.046	0.080	-0.003	0.191
ΔA-Angle	-0.063	**0.234***	**0.260***	-0.089	0.165	-0.054	0.212	0.183	0.085	0.158	-0.183	0.096	0.092	-0.147	-0.104	0.007	0.029	0.092	0.086	-0.005	0.062
ΔA-Optimality	0.079	0.138	0.137	-0.004	0.048	0.064	-0.036	-0.082	-0.095	0.024	-0.155	0.031	-0.088	-0.062	-0.041	-0.046	0.047	0.137	-0.044	0.044	-0.011
ΔA-branching coefficient	0.065	0.049	0.043	0.059	0.004	0.053	0.098	-0.067	-0.002	0.095	0.057	0.228	-0.003	-0.081	0.082	-0.031	0.014	0.057	0.103	-0.046	-0.016
ΔA-Angle ratio	-0.069	0.032	-0.019	-0.050	0.009	0.011	-0.097	0.015	-0.030	-0.086	-0.067	-0.221	0.026	0.043	-0.007	0.098	0.020	-0.084	-0.093	0.012	-0.032
ΔA-Anglular Asymmetry	-0.209	0.070	0.167	-0.142	0.003	0.060	-0.036	0.094	0.012	0.190	0.035	0.033	0.129	-0.008	-0.182	**0.256***	0.209	0.005	-0.058	0.039	-0.177
ΔV-D0	0.103	-0.082	-0.075	0.164	-0.059	-0.065	-0.016	-0.041	0.140	**0.284***	0.026	0.034	-0.016	0.086	-0.142	-0.070	0.016	0.099	-0.091	0.143	0.080
ΔV-D1	0.095	-0.036	-0.073	0.179	-0.095	-0.066	-0.093	-0.003	0.187	0.013	-0.117	-0.203	0.058	0.034	-0.080	-0.064	-0.004	0.054	-0.166	0.154	-0.015
ΔV-D2	0.141	-0.058	-0.081	0.126	0.030	-0.033	0.084	-0.029	0.148	0.227	0.018	0.069	-0.026	0.212	-0.073	-0.014	0.070	0.047	-0.083	0.184	0.036
ΔV-Angle	-0.045	-0.107	0.117	-0.026	-0.029	0.035	-0.035	-0.067	-0.046	0.179	-0.138	0.184	0.138	0.068	-0.114	-0.061	-0.089	0.228	0.091	0.067	-0.059
ΔV-Optimality	0.202	0.035	0.074	-0.031	0.020	0.018	0.026	0.008	0.094	-0.119	-0.109	-0.161	0.011	0.106	0.081	-0.020	0.054	-0.102	-0.063	0.050	-0.048
ΔV-branching coefficient	0.008	-0.078	0.046	-0.080	**0.289***	0.157	**0.255***	0.012	-0.094	0.103	**0.272***	**0.274***	-0.086	0.177	0.024	0.186	0.156	0.044	-0.003	-0.079	0.009
ΔV-Angle ratio	0.007	0.057	0.071	0.018	-0.214	-0.124	-0.215	-0.028	0.085	-0.039	-0.206	-0.233	0.103	-0.130	0.082	-0.102	-0.066	-0.041	-0.068	0.039	0.003
ΔV-Anglular Asymmetry	0.209	-0.205	-0.103	0.068	-0.061	-0.220	0.020	0.176	-0.070	-0.101	-0.064	-0.011	-0.001	0.122	-0.036	-0.075	-0.073	-0.102	-0.023	0.127	-0.006

Data expressed as Spearman Rho correlation coefficient (*r*) with *$p < 0.05$ and **$p < 0.01$.

Abbreviations: A: Arteriole, AVR: CRAE/CRVE, D0: branch parent width, D1: branch smaller branch, D2: branch larger branch, CRAE: Central retinal arteriole equivalent, CRVE: Central retinal venular equivalent, V: Venule

Chapter 5

Discussion

The overarching aim of the study is to investigate the association between retinal microvascular geometric morphology, HIV and ART, and related cardiometabolic risk factors in a study population of Worcester, Western Cape, South Africa. Various significant associations were observed. Due to the large number of variable outcomes, results are summarised in figures and discussed respectively in 3 sections below.

5.1. Discussion: Retinal vessel calibre findings

Our results showed that markers of HIV and ART were mostly associated with CRVE and less associated with CRAE. The associations between HIV, ART and retinal vessel calibre features are summarised in (**Figure 5.1)**.

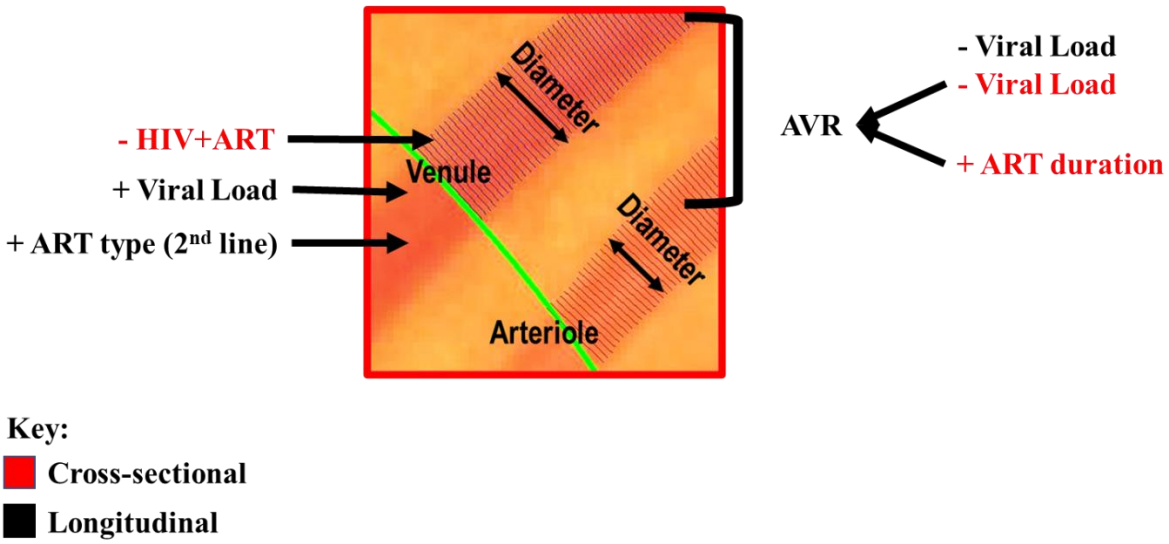

Figure 5.1*. Summary of main results for retinal vessel calibre.*

While CRAE was statistically unaffected by markers of HIV and ART, various markers of HIV and ART were associated with CRVE. Since CRVE is a factor that is used to calculate AVR (AVR = CRAE/CRVE), it follows that variables associated with CRVE also had statistical effects on AVR. These results suggest that retinal venules appear to be more susceptible to, and may also serve as markers of, effects of HIV and ART in the current study population.

Specifically, HIV+ART compared to HIV-free, cross-sectionally, was inversely associated with CRVE. Longitudinally, HIV disease progression, indicated by viral load and the use of 2nd-line ART was positively associated with CRVE. Our findings support those of Gangaputra *et al.* (159) who showed that ART use was positively associated with CRVE, but are in contrast to those of Kalyani *et al.* (169) who found a history of ART use was inversely associated with CRVE. Pathai *et al*. (179), on the other hand, did not observe any significant HIV-related venular changes in a South African study population. Also, Kalyani *et al.* (169) found

an inverse association between HIV duration and CRVE, whereas the current study did not observe an association between HIV duration and CRVE.

Our data show that markers of HIV and ART were not significantly associated with CRAE. These findings are in contrast to other studies. Gangaputra *et al.* (159) found that CRAE was inversely associated with ART use and CD4 cell counts, Pathai *et al*. (179) demonstrated an inverse association between ART use and viral load with CRAE, Tan *et al.* (15) showed a positive association between viral load and CRAE, Kalyani *et al.* (169) found a positive association between ART use and CRAE, and Edwar *et al.* (181) who positively associated detectable viral load with CRAE. Edwar *et al.* (181) specifically showed a decrease in CRAE over a 12-month period in PLWH after initiating ART, but we did not observe a significant change over an 18-month period. Kalyani *et al.* (169) attributed HIV and ART associated effects on CRAE to changes in haematocrit, age and history of hypertension. In our study, age was not significantly associated with CRAE and our HIV+ART study population had mostly blood pressure in the normal range, which may account, in part at least, for differential effects observed between our and other studies.

Viral load, an indicator of HIV disease progression, in HIV+ART in both cross-sectional and longitudinal statistical analyses was inversely associated with AVR, while ART duration was positively associated with AVR. The non-significant difference observed between HIV-free and HIV+ART in terms of AVR in our study supports Haddow *et al.* (180) who also did not observe significant differences between study groups. Our findings also support Tan *et al.* (15) who found an inverse association between viral load and AVR. Gangaputra *et al.* (159) furthermore showed that a 0.1 decrease in AVR was associated with a 12% increased risk of mortality in their HIV study population. Haddow *et al.* (180) in particular found that a smaller AVR in PLWH was associated with SBP, history of stroke and history of a heart attack. These results suggest that viral load in our study population may indicate an increased risk for CVD and mortality in our HIV+ART study population. On the other hand, the positive association between ART duration and AVR may indicate a decrease in HIV-associated mortality and cardiovascular risk. However, the present study did not measure CVD mortality outcomes; therefore, more studies on the relationship between AVR and mortality risk in our cohort are necessary.

HIV+ART-associated cardiometabolic risk factors that were significantly different between HIV-free and HIV+ART groups, and also independently associated with retinal vessel calibres included: (i) GGT, which inversely correlated and independently associated with CRAE; (ii) DBP, which inversely correlated and independently associated with CRAE and AVR; (iii) HbA1c, which positively correlated and independently associated with CRAE; and (iv) HDL, which inversely correlated and independently associated with CRVE and positively associated with AVR. These results suggest that HIV and ART-associated GGT, DBP, HbA1c and HDL cholesterol may be involved in changes in retinal vessel calibre in our study population. HDL cholesterol in particular appeared to play a significant role in our findings, and it can be speculated that the higher levels of cardioprotective and anti-atherosclerotic HDL cholesterol observed in our HIV+ART study population compared to HIV-free may have contributed to smaller CRVE calibre compared to controls. HDL cholesterol was also positively associated with AVR, which may furthermore indicate a lower risk for CVD

and mortality in PLWH (on ART) as previously reported (159). These findings may imply that the specific ART regimes are exerting cardioprotective effects in our study population. However, in depth qualitative analyses of HDL and its sub-fractions in PLWH should be considered in future studies.

In terms of other cardiovascular risk factors, our cross-sectional data showed a positive association between glycated haemoglobin (HbA1c), a marker of medium-term blood glucose level handling, and CRAE in HIV+ART and the total population. These findings are in line with other reports that also showed a positive association between retinal vessel calibre and diabetes (165,166). Also, the inverse association between SBP and CRAE observed in our cross-sectional study, and DBP with AVR observed in our longitudinal study, has previously been reported by others (159–164,167–169,172–174) These reports suggest that a possible mechanistic pathway involved between blood pressure and narrower vessel diameters include shear stress on the vascular wall, which may lead to a vasoconstrictive vascular response and/or decreased nitric oxide bioavailability as a result of possible endothelial dysfunction associated with hypertension. Additionally, the positive association between systemic inflammation, as indicated by hsCRP, and vessel diameter indicated by CRAE in the total study population and CRVE in the total and HIV+ART study populations is in line with the general consensus that inflammation is associated with larger vessel calibres (170,176) A possible mechanistic pathway that may explain increasing vessel diameters may include inflammation as an obesogenic glucose profile, increased glucose levels, is commonly associated with systemic inflammation as indicated by hsCRP levels.

Overall, various factors may have contributed to differential findings between reports, but our findings indicate that CRVE and AVR may be markers of the effects of HIV, ART, and HIV- and ART associated cardiometabolic risk factors in our study population. We postulate that higher levels of HDL cholesterol in HIV+ART compared to HIV-free may be a candidate mechanism involved in HIV+ART-associated beneficial effects on vessel calibre. More research in terms of specific mechanistic pathways involved is needed.

5.2. Discussion: Retinal vessel network features

Compared to retinal vessel calibre, retinal vessel network features are generally less commonly reported in literature, with most studies focusing on fractal analyses and vessel tortuosity. Understanding complex retinal vessel network features may be challenging, but to simplify the interpretation of vessel network features one should understand that these parameters are broadly a reflection of retinal vessel density (e.g., branch point, end points, vessel length and diameter, and lacunarity) and complexity (e.g., tortuosity and fractal dimensions). Physiologically, the network architecture aims to achieve maximum structural and regulatory complexity, maximum vessel length and perform maximum transport efficiency with minimum genetic information, tissue mass and cardiac power required to maintain homeostasis (182,183). Thus, the following section will be discussed accordingly.

In our cross-sectional analyses, vessel network features did not significantly differ between study groups and markers of HIV and ART were not significantly associated with retinal network features however, the

longitudinal study data**)** showed various HIV- and ART-related associations with retinal vessel features (**Figure 5.2.**).

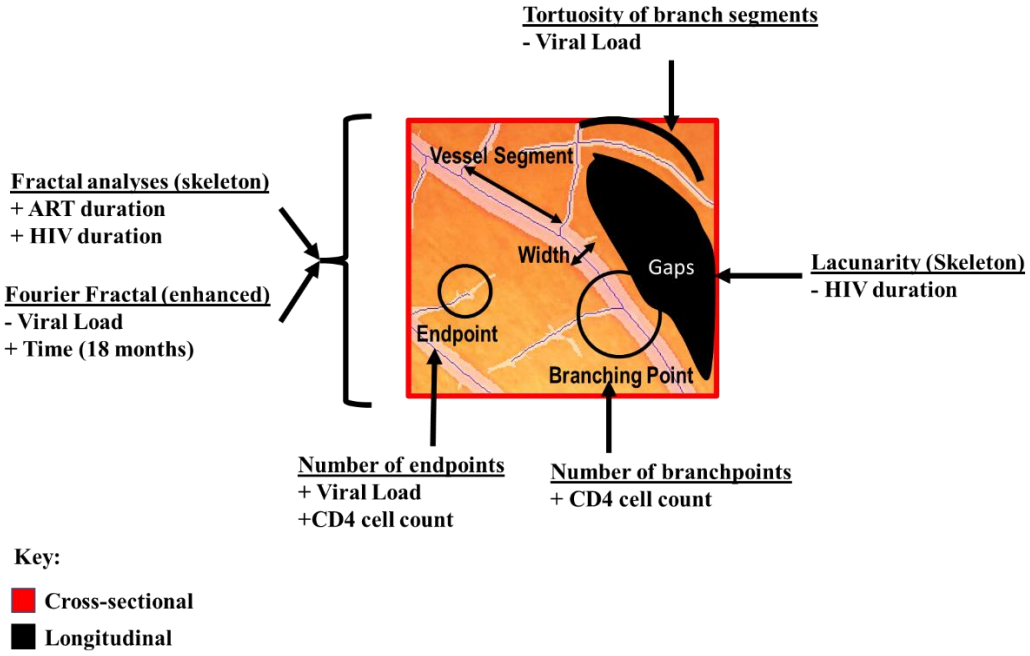

Figure 5.2*. Summary of main findings related to retinal vessel network features.*

These results suggest that the longitudinal effects of HIV and ART may be more pronounced compared to cross-sectional statistical effects, and longitudinal repeated measures offer more statistical power.

In our study, HIV disease progression, as indicated by viral load, was inversely associated with vessel tortuosity and Fourier fractal, implying a less complex vessel network, while factors related to time such as ART duration, HIV duration and an 18-month period were positively associated with fractal dimensions (implying a denser and complex vessel network). A previous study reported a positive association between tortuosity and increased cardiovascular risk and that lower fractal dimensions are associated with degenerative disorders, including age (147). In contrast to our findings, Tan *et al.* (15,206,207) reported that HIV+ART was positively associated with tortuosity and fractal dimensions, which indicate cardiovascular risk. These results suggest that HIV disease progression as indicated by high viral load, may be associated with increased cardiovascular risk, and that over time, the cardiovascular risk may increase in our study population. It could be speculated that the 18-month ART treatment period in our HIV+ART study population may have displayed cardioprotective or beneficial effects, but more investigation is needed to confirm this hypothesis.

Both immune function-higher CD4 cell count associated with more vessel branch and endpoints. and HIV disease progression/duration-higher viral loads was associated with more branchpoints and a longer HIV-duration with smaller gaps between vessels-were associated with a denser vessel network. A less dense vessel network indicated by high lacunarity has been associated with cardiovascular risk factors such as hypertension (201,202), diabetes (201,203) and degenerative disorders (204). These results suggest that HIV+ART over time, may be associated with vascular geometric features that may have beneficial effects on the retinal microvasculature.

HIV- and ART-associated cardiometabolic risk factors in the current HIV+ART study population that were also associated with retinal vessel network features included BMI, significantly lower in HIV+ART compared to HIV-free, and DBP, significantly lower in HIV+ART compared to HIV-free inversely correlated with D0 and D1. Our longitudinal study supports the findings of other studies (197,198), that also showed a positive correlation and independent association between BMI and a less dense vessel network, indicated by lacunarity, and more complexity, indicated by Fourier fractal dimensions. In addition, DBP was associated with a higher vessel complexity, fractal analyses, as observed by other studies (192). These results suggest that BMI and DBP, commonly positively associated with each other, may play an intermediate role in HIV- and ART-associated effects on retinal vessel network features observed in the current study. Furthermore, these results may suggest possible cardioprotection due to the more favourable BMI and DBP profile seen in our HIV population compared to our control. Literature has shown that the association of HIV with risk factors such as obesity and hypertension together with endothelial dysfunction may have various adverse effects on vasculature (238). Obesity in itself is associated with various mechanistic pathways that may contribute to alterations in microvascular architecture. Obesity, for example, is associated with decreased bioavailability of nitric oxide, which may lead to a decrease in vascular reactivity and relaxation (239). This may contribute to narrower vessels and thus a lower network density. A decrease in vessel diameters may furthermore decrease blood supply to cells/tissue, which may lead to hypoxia (240). Obesity-associated inflammation may be another mechanistic pathway that may contribute to thickening of vessel walls that may lead to vessel stiffness and contribute to hypertension (241). These effects may lead to increases in vessel diameter. The specific pathophysiological pathways involved in results observed in the current study needs more investigation.

Overall, our results suggest that the longitudinal effects of HIV and ART on retinal vessel network features are more pronounced than cross-sectional analyses. HIV appeared to be associated with a less dense vessel network, but these effects seem to be reversed over time. As previously discussed, BMI and DBP may be important cardiometabolic factors that contribute to the effects observed. More investigation related to possible mechanistic pathways involved is needed.

5.3. Discussion: Retinal vessel branching features

Retinal vessel branching features are least commonly reported in literature compared to other retinal microvascular geometric parameters. According to literature, retinal vessel branching features are closely related to the efficiency of blood circulation, power required for blood circulation and drag experienced during blood flow (211–214). Therefore, branching features have previously been reported as markers of cardiac function (221). Branching features are also considered as long-term markers for vascular modeling and cardiovascular risk as opposed to short term markers since branching changes become more pronounced over a longer period of time (171,211). As studies in terms of HIV and retinal vessel branching features are scarce, our results related to branching features will be discussed in relation to the aforementioned factors that relates to vessel branching features and blood flow efficiency.

Although no standardised protocol for the quantification of retinal vessel branching features has been set, the protocol used in our study (**Chapter 2**) to quantify branching features showed various significant associations between markers of HIV- and ART and may thus be considered as a protocol in future studies, although validation and comparisons to other protocols are still required (**Figure 5.3.**).

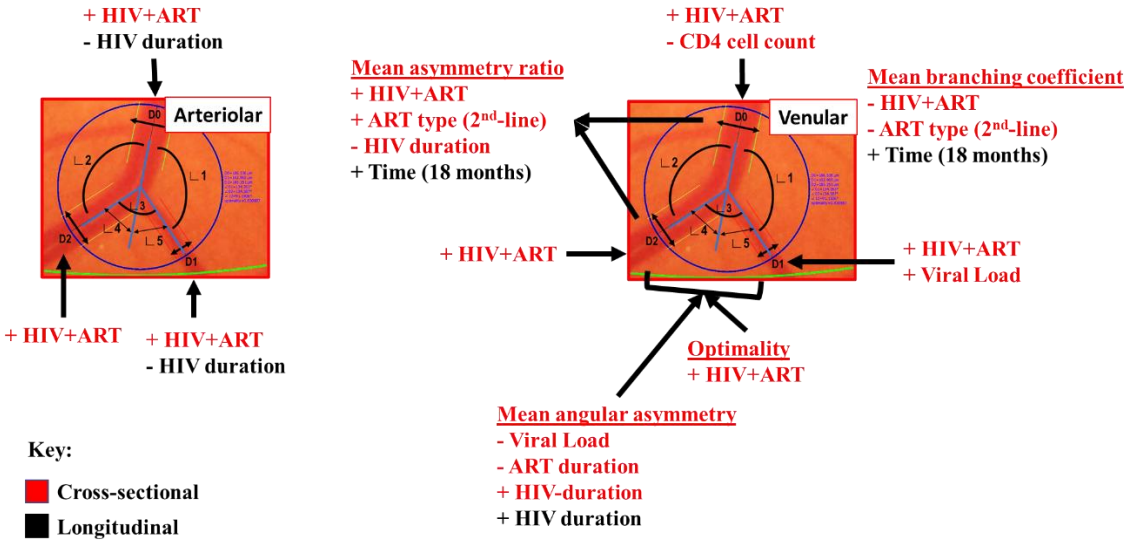

Figure 5.3*. Summary of main findings related to retinal vessel branching features.*

In our study population, venular branches appeared to be more susceptible to the effects of HIV and ART compared to arterioles. In contrast to our retinal calibre results, HIV+ART *vs.* HIV-free was associated with larger arteriolar and venular vessel diameters, D0, D1 and D2, in the bifurcation area. Our results support Dunn *et al*. (229) who showed that HIV+ART is at lower risk for vessel occlusion compared to controls. As vessel occlusion, narrower vessels in the bifurcation area, are associated with increased cardiovascular risk, these results suggest that our HIV+ART study population compared to HIV-free may present with more efficient blood circulation and that ART may exhibit cardioprotective effects on our HIV+ART study population.

Although HIV duration in our cross-sectional analysis did not show any significant associations within the HIV+ART study population, it was associated with arteriolar narrowing of D0 and D1 in the bifurcation area in our longitudinal analyses. This result suggests that despite the beneficial effects HIV+ART *vs.* HIV-free exhibited on vessel diameters, a longer period (≥ 5 years) of HIV-infection in our HIV+ART study population, may be associated with a less effective arteriolar blood flow and this increases cardiovascular risk.

In our cross-sectional analyses in the HIV population, restoration of immune function indicated by CD4 cell counts was associated with a smaller venular D0, while HIV disease progression indicated by viral load was associated with a larger D1. A negative association between GGT, significantly higher in HIV+ART *vs.* HIV-free, and venular D0 was also observed. It can therefore be speculated that elevated GGT may indicate higher risk for the development of liver diseases over time in our HIV+ART population, but a longer period of follow-up is needed. Similarly, a significant positive association between HbA1c, significantly higher in HIV+ART *vs.* HIV-free, and venular D1 in the HIV+ART study population was observed, which may suggest that poor glucose regulation was associated with narrower D1. Longitudinal statistical analyses did not show any

significant associations between markers of HIV and ART and venular branching features. These findings suggest that an 18-month period may not be enough for longitudinal HIV and ART effects to become pronounced.

Markers of HIV and ART were not significantly associated with arteriolar branching features related to angle. This finding is in contrast to Tan *et al.* (207) who found that each 1° increase in arteriolar branching angle was significantly associated with a subsequent 3.74 cells/ul decrease in CD4 count ($p = 0.001$).

Various significant associations between markers of HIV and ART and retinal venular branching angle features were observed. In the total cross-sectional study population, HIV+ART *vs.* HIV-free was associated with a larger venular branching optimality, larger asymmetry ratio and a smaller branching coefficient. These results suggest that HIV+ART compared to HIV-free may be associated with a more efficient blood circulation. An 18-month time period in our longitudinal HIV+ART study population was positively associated with venular branching coefficient and asymmetry ratio. The significant positive and negative association between age and venular branching coefficient and asymmetry ratio suggest that the longitudinal effects observed may be age-related, but more investigation is needed.

In contrast to the aforementioned beneficial effects, in our longitudinal and cross-sectional statistical analyses, longer HIV duration (≥ 5 years) was positively associated with venular angular asymmetry, and inversely associated with asymmetry ratio in cross-sectional analyses. These results suggest that over time, HIV may be associated with a less efficient micro-circulation, which may contribute to increased cardiovascular risk.

In terms of cardiometabolic variables, GGT in our cross-sectional analyses was significantly higher in HIV+ART *vs.* HIV-free and also positively associated with venular angle optimality in the total and HIV+ART study populations, which may suggest possible mechanistic involvement, but more investigation is needed. The negative and positive associations between ART type (2^{nd}-line *vs.* 1^{st}-line) and asymmetry ratio and branching coefficient in the HIV+ART study population observed in our cross-sectional analyses suggest that compared to 1^{st}-line ART, consisting of TDF+3TC/FTC+EFV, 2^{nd}-line ART, consisting of 3TC+AZT+LPV/r, may be associated with beneficial effects on the efficiency of blood circulation. The significant positive and negative association between age and venular branching coefficient and asymmetry ratio observed in our longitudinal analyses suggest that the longitudinal effects observed may be also age-related. The relationship between HIV- and ART-associated cardiometabolic effects and retinal branching angle features need more investigation.

Huang *et al.* (2020) showed a close relationship between cardiac structure/function and retinal arteriolar branching angles (222). Nadal *et al.* (2019) showed a close relationship between cerebral microcirculation and retinal vessel branching features (223). In the larger picture, these results suggest that HIV and ART in our study population may not contribute to increased cardiovascular and cerebrovascular risk, but these relationships in our study populations needs to be further explored.

Other cardiovascular and cardiometabolic risk factors such as smoking, hypertension, diabetes, hyperlipidaemia and hypercholesterolaemia, and hyperuricemia have previously been associated with ocular

vessel occlusion (221,224,225). In line with these reports, triglyceride levels in our total and HIV+ART study populations were inversely associated with arteriolar D0 and D1. As observed in the retinal vessel calibre results, systemic inflammation indicated by hsCRP was positively associated with venular branching D0 vessel diameter in the total and HIV+ART study population. In line with findings by Huang *et al.* (2020) who reported a close relationship between cardiac structure/function and arteriolar branching features, heart rate in our HIV+ART and total study population was positively associated with arteriolar branching coefficient and asymmetry ratio.

Overall, venular as opposed to arteriolar branching features, appeared to be mostly affected by HIV and ART in the current study population. It is possible that the venules are more susceptible to the effects of HIV/ART due to structural differences between arterioles and venules, for example, vascular wall is structurally stronger in arteries than veins, but more focused investigation is needed. HIV+ART appeared to display beneficial effects on retinal vessel branching features, as it was associated with larger arteriolar and venular branching vessel diameters. HIV+ART was also associated with better branching angle, optimality, and asymmetry. These beneficial effects appear to decrease over time. Blood pressure and GGT appeared to be possible cardiometabolic risk factors involved in effects observed in retinal vessel branching features. More investigation is needed to clarify specific mechanistic pathways involved.

Chapter 6
Conclusion

6.1. Final conclusion

South Africa is in the midst of epidemiological transition from a high prevalence of communicable disease such as HIV/AIDS to a high prevalence of non-communicable diseases such as CVD. The current study investigated the intersection between HIV/AIDS and CVD in PLWH in SA and whether retinal imaging may be a potential useful tool in assessing cardiovascular risk in this population. Therefore, the overarching aim of the study was to investigate the association between retinal microvascular geometric morphology, HIV, ART, and HIV- and ART-associated cardiometabolic risk factors in an HIV study population from the Western Cape Province.

Retinal microvascular geometric features included vessel calibre (arterioles and venules, respectively), vessel network features and vessel branching features (arterioles and venules, respectively). To our knowledge, results in terms of retinal vessel network and branching features are novel in SA and no studies in SA population were found in literature. Markers of HIV and ART included HIV+ART status *vs*. HIV-free in the total study population and viral load, CD4 cell count, ART duration (weeks), ART type (1^{st}-line *vs.* 2^{nd}-line) and HIV duration (< 5 years *vs.* ≥ 5 years in the HIV+ART study population. To evaluate possible associations, we conducted cross-section statistical analyses in the total (HIV-free and HIV+ART study groups combined) and HIV+ART study populations. To evaluate the temporal effects, we additionally conducted a longitudinal statistical analysis only in the HIV+ART group.

Our results showed that all markers of HIV and ART were associated with at least one retinal microvascular geometric feature. We also showed that various HIV- and ART-associated cardiometabolic risk factors such as HDL, HbA1c, GGT, and blood pressure in our study population were correlated and/or independently associated with retinal vessel geometric features. These results show that retinal microvascular imaging may be a useful tool in assessing cardiovascular risk, not only in our HIV study population, but also in the general population.

There is limited literature on the relationship between HIV/ART and retinal geometric morphology, therefore, we offered a general discussion in relation to trends/changes in vessel features previous studies associated with cardiovascular risk/protection in mostly HIV-free study populations. In terms of these previously reported findings, associations observed between markers of HIV and ART in our study appeared to mostly be cardioprotective especially compared to our HIV-free population, however, our longitudinal results did indicate some increase in cardiovascular risk over time. To validate whether statistical effects reflect cardiovascular risk/protection in our study population, future studies should include a more comprehensive panel of markers of cardiovascular risk/protection. Possible mechanistic pathways between cardiovascular risk factors and changes in retinal vessel geometric features are also limited. Therefore, future research should also

include biochemical markers of mechanistic pathways that may be involved, such as markers of endothelial function, atherosclerosis, inflammation, and oxidative stress.

Moreover, reports on the effects of cardiovascular risk factors on retinal vessel features differ. Several factors such as differences in ART combinations, duration of ART and HIV exposure, demographic and socioeconomic profiles, and external environmental factors may account for different findings in reports. Similarly, differences in statistical models/analyses, software and algorithms used to quantify retinal vessel features may account for different findings in reports. The influence of these aforementioned factors still needs to be clearly looked at.

Nonetheless, our results contribute significantly to the sparse body of evidence, especially in terms of network and branching features, that investigated the relationship between retinal vessel geometric morphology and HIV and ART. Our results also underline the potential that retinal microvascular imaging offers as a useful tool to non-invasively assess cardiovascular risk in research setting, clinical setting, in PLWH and the general population. As retinal images are digital, they can also be obtained and sent for further assessment remotely. This could be especially useful in the African setting, where medical resources are limited.

6.2. Strengths, limitations, and future directions

Results for the current study are presented with a number of strengths and limitations. Since retinal vessel calibre is commonly reported in literature, the inclusion of retinal vessel network and branching features in our study contribute to the limited body of evidence in the literature. Our study is also one of a few studies related to retinal microvascular imaging in South Africa. Although most studies related to retinal imaging consists of large sample sizes, our study found significant findings in a relatively small study population, but a larger study population is advised for future studies. Our study mostly represents a study population of mixed ancestry in the Cape Town area. As the South African population is diverse in terms of regions, demographic, cultural, social and lifestyle factors, future studies should also explore the relationship between retinal vessel features and these factors. This would also allow for the inclusion of more confounding factors in statistical models and statistical analyses would have more statistical power. The inclusion of ART naïve HIV+ participants would have given more insight into the specific role of ART; however, it is not possible due to guidelines that patients are immediately placed on ART upon diagnosis.

We relied solely on participants' word regarding ART compliance, future studies could conduct pharmacokinetic studies to verify the levels of ART in blood. Covid-19 interrupted data collection period, resulting in loss of patients to follow-up which reduced our sample size. Some retinal images were unanalysable which resulted in a further reduction of our sample size. Financial restrictions prevented the analyses of biomarkers.

As previously mentioned, evidence from literature that investigate possible mechanistic pathways involved between cardiovascular risk factors and changes/effects on retinal microvascular features are scarce. Therefore, our study contributes specifically to CVD risk in PLWH. Our study shows the potential of retinal imaging in the context of low resource environments such as SSA and telemedicine. Future studies should add

biochemical markers involved in possible mechanistic pathways. Retinal vessel features have also been associated with various morbidities. Future studies, especially in SA, should also explore the relationship between these morbidities and retinal vessel features. Although the follow-up period of 18 months in our longitudinal statistical analyses did show significant associations, no significant changes over a period of 18 months in retinal vessel features were observed, significant changes may become more pronounced in a period beyond 18 months.

Retinal images can also be used to assess other retinal pathologies such as vessel nicking and cutting, vascular oedema and cotton wool spots. Our images and those of future studies can also be used to assess these pathologies. Retinal imaging has also been shown to be useful in other fields of medical research such as, neuroscience and cerebrovascular diseases. Future studies could thus consider expanding the scope of their research.

6.3. Active role the M.Sc. candidate played in research activities

Although the current study formed part of a larger parent study, the M.Sc. candidate played an active role in all aspects of research activities and aims and objectives of the current study as specified below:

- Played an active role in field work to obtain data from all study participants. This included travelling to research sites/clinics in the Cape Town and the Worcester area.
- Assisted in laboratory work, including sample collection, processing, sample storage and sample delivery to the NHLS for further analyses.
- Obtaining retinal images from her study, analysing all retinal images, and processing and capturing of retinal data.
- With the guidance of her supervisors, performed all statistical analyses on her own, presented the results and interpreted the results.
- Took part in general research activities of the parent study, for example preparations for field work, assisting with other clinical assessment techniques such as flow-mediated dilatation, data capturing, data calculations, data verification and data capturing.

6.4. Research outputs produced during the course of the study

The M.Sc. candidate produced a number of research outputs over the 2-year period of her MSc. as listed below:

First-authored peer reviewed conference outputs:

- **Kgokane B**, Everson F, Kamau F, De Boever P, Nawrot TS, Goswami N, Webster I, Williams C, and Strijdom H. Effects of HIV and first-line antiretroviral therapy on retinal microvascular calibre in a HIV population from the Western Cape. Annual Research Day, Faculty of Medicine and Health Sciences, Stellenbosch University, August 2020.

- **Kgokane B**, Kamau F, Everson F, Webster I, De Boever P, Nawrot TS, Goswami N, Charania S, Dinnie Y and Strijdom H. HIV-infected individuals are predisposed to endothelial dysfunction: Results from the EndoAfrica study. Physiology Society of Southern Africa Congress, September 2021.
- **Kgokane B**, Everson F, Kamau F, Webster I, De Boever P, Goswami N, Nawrot TS, Dinnie Y and Strijdom H. An investigation into the relationship between HIV and antiretroviral Therapy (ART)-dependent parameters and retinal vessel branching features in a Western Cape study population. Annual Research Day, Faculty of Medicine and Health Sciences, Stellenbosch University, August 2021.

Co-authored peer reviewed conference outputs:

- Williams C, Kamau F, Everson F, **Kgokane B**, De Boever P, Nawrot TS, Goswami N, Webster I and Strijdom H. Viral load in people living with HIV is associated with altered ventricular depolarisation/repolarisation: data from the EndoAfrica study. Annual Research Day, Faculty of Medicine and Health Sciences, Stellenbosch University, August 2020.
- Dinnie Y, Everson F, Kamau F, Webster I, **Kgokane B**, De Boever P, Goswami N, Nawrot TS and Strijdom H. Investigating the Cardiometabolic Effects of HIV/AIDS and Antiretroviral Therapy in a Western Cape Study Population. Annual Research Day, Faculty of Medicine and Health Sciences, Stellenbosch University, August 2021.
- Everson F, Webster I, Kamau F, **Kgokane B**, De Boever P, Goswami N, Nawrot TS, Dinnie Y and Strijdom H. Cardiometabolic risk and systemic inflation (hsCRP): Is retinal vessel calibre a marker of effect? Annual Research Day, Faculty of Medicine and Health Sciences, Stellenbosch University, August 2021.
- Everson F, De Boever P, Martens DS, Nawrot TS, Goswami N, Webster I, Charania S, Kamau F, **Kgokane B** and Strijdom H. Personal NO2 and BTEX exposure contribute to an increased cardiovascular risk profile in women in the Cape Town Area. Physiology Society of Southern Africa Congress, September 2021.
- F. Everson, P. De Boever, T.S. Nawrot, N. Goswami, I. Webster, F. Kamau. **B. Kgokane**, S. Charania, H. Strijdom. Urinary 1-hydroxypyrene concentration independently predicts endothelial function in a Cape Town study population. Stellenbosch University AAD 2020.
- Festus Kamau, **Boipelo Kgokane**, Eva Mthethwa, Nyiko Mashele, Frans Everson, Nandu Goswami, Patrick De Boever, Tim Nawrot, Sana Charania, Ingrid Webster, Hans Strijdom. HIV -infected individual as predisposed to proatherosclerotic biochemical changes. European Atherosclerosis Society Conference, 2020.
- F. Everson, P. De Boever, T.S. Nawrot, N. Goswami, I. Webster, S. Charania, F. Kamau, **B. Kgokane**, Y. Dinnie, H. Strijdom. A first-line fixed-dose combination ART regimen containing Efavirenz/Emtricitabine/Tenofovir exhibit beneficial effects on retinal microvascular calibre in a South African HIV-infected study population. SA-MRC annual BRIP Symposium, 2021.

Co-authored peer reviewed journal publication:

- Williams C, Kamau F, Everson F, **Kgokane B**, De Boever P, Goswami N, Webster I and Strijdom H. HIV and antiretroviral therapy are independently associated with cardiometabolic variables and cardiac electrical activity in adults from the Western Cape region of South Africa. Journal of Clinical Medicine, 2021.

7. References

1. WHO. Cardiovascular disease. Available from: https://www.who.int/health-topics/cardiovascular-diseases (accessed 12 March 2020).
2. Murray CJL, Lopez AD, WHO. The global burden of disease: a comprehensive assessment of mortality and disability from diseases, injuries, and risk factors in 1990 and projected to 2020: Available from: https://apps.who.int/iris/bitstream/handle/10665/41864/0965546608_eng.pdf. (accessed on 12 March 2020).
3. Mensah GA, Sampson UKA, Roth GA, Forouzanfar MH, Naghavi M, Murray CJL, et al. Mortality from cardiovascular diseases in sub-Saharan Africa, 1990–2013: a systematic analysis of data from the Global Burden of Disease Study 2013. Cardiovasc J Afr. 2015;26(2 H3Africa Suppl):S6.
4. Arthur M. Institute for Health Metrics and Evaluation. Available from: http://rcnpublishing.com/doi/abs/10.7748/ns.28.42.32.s33. (accessed 26 March 2020).
5. Gaziano TA. Reducing the growing burden of cardiovascular disease in the developing world. Health Aff. 2007;26(1):13–24.
6. Lim SS, Vos T, Flaxman AD, Danaei G, Shibuya K, Adair-Rohani H, et al. A comparative risk assessment of burden of disease and injury attributable to 67 risk factors and risk factor clusters in 21 regions, 1990-2010: A systematic analysis for the Global Burden of Disease Study 2010. Lancet. 2012;380(9859):2224–60.
7. Steyn K, Damasceno A. Lifestyle and related risk factors for chronic diseases. Dis Mortal sub-Saharan Africa. 2006;2:247–65.
8. Durand M, Sheehy O, Baril JG, Lelorier J, Tremblay CL. Association between HIV infection, antiretroviral therapy, and risk of acute myocardial infarction: A cohort and nested case-control study using Québec's Public Health Insurance database. J Acquir Immune Defic Syndr. 2011;57(3):245–53.
9. Freiberg MS, Chang C-CH, Kuller LH, Skanderson M, Lowy E, Kraemer KL, et al. HIV infection and the risk of acute myocardial infarction. JAMA Intern Med. 2013;173(8):614–22.
10. Triant VA, Lee H, Hadigan C, Grinspoon SK. Increased acute myocardial infarction rates and cardiovascular risk factors among patients with human immunodeficiency virus disease. J Clin Endocrinol Metab. 2007;92(7):2506–12.
11. Worm SWW, Sabin C, Weber R, Reiss P, El-sadr W, Dabis F, et al. Risk of Myocardial Infarction in Patients with HIV Infection Exposed to Specific Individual Antiretroviral Drugs from the 3 Major Drug Classes : The Data Collection on Adverse Events of Anti-HIV Drugs (D : A : D) Study. JID. 2010;201(3):318–30.
12. Unaids J. Fact sheet—latest global and regional statistics on the status of the AIDS epidemic. Available from: https://www.unaids.org/sites/default/files/media_asset/UNAIDS_FactSheet_en.pdf. (accessed 5

April 2020).

13. UNAIDS. South Africa. Available from: https://www.unaids.org/en/regionscountries/countries/southafrica. (accessed 15 March 2020).

14. Boccara F, Lang S, Meuleman C, Ederhy S, Mary-Krause M, Costagliola D, et al. HIV and coronary heart disease: time for a better understanding. J Am Coll Cardiol. 2013;61(5):511–23.

15. Tan PB, Hee OK, Cheung C, Yeo TK, Agrawal R, Ng J, et al. Retinal vascular parameter variations in patients with human immunodeficiency virus. Investig Ophthalmol Vis Sci. 2013;54(13):7962–7.

16. Lenci LT, Chin EK, Almeida DRP. Central retinal artery occlusion in a young HIV-infected patient on highly active antiretroviral therapy. Retin Cases Br Reports. 2017;11(2):160–2.

17. Pathai S, Shiels PG, Weiss HA, Gilbert CE, Peto T, Bekker L-G, et al. Ocular parameters of biological ageing in HIV-infected individuals in South Africa: Relationship with chronological age and systemic biomarkers of ageing. Mech Ageing Dev. 2013 Sep;134(9):400–6.

18. WHO. Types of cardiovascular disease. Available from: https://www.who.int/news-room/fact-sheets/detail/cardiovascular-diseases-(cvds). (15 March 2020).

19. WHO. A prioritized research agenda for prevention and control of NCDs: CVD, cancer, chronic respiratory disease, diabetes. Available from: http://www.who.int/cardiovascular_diseases/publications/ncd_agenda2011/en/. (accessed 15 March 2020).

20. Go AS, Mozaffarian D, Roger VL, Benjamin EJ, Berry JD, Borden WB, et al. Executive summary: Heart disease and stroke statistics-2013 update: A Report from the American Heart Association. Circulation. 2013;127(1):143–52.

21. Mendis S, Puska P, Norrving B. Global atlas on cardiovascular disease prevention and control. Available from: https://apps.who.int/iris/handle/10665/44701. (accessed 5 April 2020).

22. Kassebaum NJ, Bertozzi-Villa A, Coggeshall MS, Shackelford K a., Steiner C, Heuton KR, et al. Global, regional, and national levels and causes of maternal mortality during 1990-2013: a systematic analysis for the Global Burden of Disease Study 2013. Lancet. 2014;6736(14):1–25.

23. Ross R. Inflammation or Atherogenesis. N Engl J Med. 1999;340(2):115–26.

24. Mudau M, Genis A, Lochner A, Strijdom H. Endothelial dysfunction: the early predictor of atherosclerosis. Cardiovasc J Afr. 2012;23(4):222.

25. Plutzky J. The vascular biology of atherosclerosis. Am J Med. 2003;115(8 SUPPL. 1):55–61.

26. WHO. Cardiovascular diseases (CVDs): WHO key facts. Available from: https://www.who.int/health-topics/cardiovascular-diseases#tab=tab_1. (accessed 30 March 2020).

27. Alwan A. Global status report on noncommunicable diseases 2010. Available from:

http://whqlibdoc.who.int/publications. (accessed 30 March 2020).

28. Stevens G, Mascarenhas M, Mathers C. Global health risks: Progress and challenges. Vol. 87, Bulletin of the WHO. 2009. p. 646.

29. Mathers CD, Loncar D. Projections of global mortality and burden of disease from 2002 to 2030. PLoS Med. 2006;3(11):2011–30.

30. Mathers Loncar, D. CD. Updated projections of global mortality and burden of disease, 2002-2030: data sources, methods and results. WHO. 2005;(October):1–130.

31. Narayan KMV, Ali MK, Ch B, Koplan JP. Global Noncommunicable Diseases — Where Worlds Meet. N Engl J Med. 2010;363(13):1196–8.

32. Yusuf S, Reddy S OSA. Global Burden of Cardiovascular Diseases. Circulation. 2001;104(22):2746–53.

33. Dalal S, Beunza JJ, Volmink J, Adebamowo C, Bajunirwe F, Njelekela M, et al. Non-communicable diseases in sub-Saharan Africa: What we know now. Int J Epidemiol. 2011;40(4):885–901.

34. Adeboye B, Bermano G, Rolland C. Obesity and its health impact in Africa: a systematic review. Cardiovasc J Afr. 2012;23(9):512–21.

35. Tibazarwa K, Ntyintyane L, Sliwa K, Gerntholtz T, Carrington M, Wilkinson D, et al. A time bomb of cardiovascular risk factors in South Africa: Results from the Heart of Soweto Study "Heart Awareness Days." Int J Cardiol. 2009;132(2):233–9.

36. Malaza A, Mossong J, Bärnighausen T, Newell M-L. Hypertension and obesity in adults living in a high HIV prevalence rural area in South Africa. Myer L, editor. PLoS One. 2012 Oct;7(10):e47761.

37. Mayosi BM, Flisher AJ, Lalloo UG, Sitas F, Tollman SM, Bradshaw D. The burden of non-communicable diseases in South Africa. Lancet. 2009;374(9693):934–47.

38. Norman R, Bradshaw D, Schneider M, Pieterse D, Groenewald P. Revised Burden of Disease Estimates for the Comparative Risk Factor Assessment , South Africa 2000. Cape Town: South African Medical Research Council, 2006. 2006.

39. Bradshaw D, Groenewald P, Laubscher R, Nannan N, Nojilana B, Norman R, et al. Initial burden of disease estimates for South Africa, 2000. South African Med J. 2003 Jul;93(9):682–8.

40. Sliwa K, Damasceno A, Mayosi BM. Epidemiology and etiology of cardiomyopathy in Africa. Circulation. 2005;112(23):3577–83.

41. Heart and Stroke Foundation South Africa. Cardiovascular Disease Statistics Reference Document. Available from: https://www.heartfoundation.co.za/. (accessed 12 April 2020).

42. Dougan S. Mortality and causes of death in South Africa, 1997-2003: findings from death notifications. Available from: https://www.statssa.gov.za/publications/P03093/P030932018.pdf. (accessed 16 April

2020).

43. Watkins D a, Sebitloane M, Engel ME, Mayosi BM. The burden of antenatal heart disease in South Africa: a systematic review. BMC Cardiovasc Disord. 2012;12(1):23.

44. Murphy JFA. The global burden of disease. Available from: https://www.who.int/healthinfo/global_burden_disease/GBD_report_2004update_full.pdf. (accessed 30 April 2020).

45. Lakatta EG, Levy D. Arterial and Cardiac Aging : Major Shareholders in Cardiovascular Disease Enterprises Part II : The Aging Heart in Health : Links to Heart Disease. Circulation. 2003;107(2):139–46.

46. Lakatta EG. Age-associated cardiovascular changes in health: impact on cardiovascular disease in older persons. Hear Fail. 2002;7(1):29–49.

47. Wood D. Established and emerging cardiovascular risk factors. Am Heart J. 2001;141(2 Suppl):S49-57.

48. Winham SJ, de Andrade M, Miller VM. Genetics of cardiovascular disease: Importance of sex and ethnicity. Atherosclerosis. 2014;241(1):219–28.

49. Cooper RS. Social inequality, ethnicity and cardiovascular disease. Int J Epidemiol. 2001;30 Suppl 1:S48-52.

50. Spence JD, Pilote L. Importance of sex and gender in atherosclerosis and cardiovascular disease. Atherosclerosis. 2015;241(1):208–10.

51. World Heart Federation. State of the Heart: Cardiovascular Disease Report. Available from: https://world-heart-federation.org/resource/state-heart-cvd-report/. (accessed 7 June 2020).

52. Sidhu MS, Farkouh ME. Diabetes and cardiovascular disease. In: Cardiology Secrets. 2017. p. 387–93.

53. Abel ED, O'Shea KM, Ramasamy R. Insulin resistance: Metabolic mechanisms and consequences in the heart. Arterioscler Thromb Vasc Biol. 2012;32(9):2068–76.

54. Heart and Stroke Foundation South Africa. Diabetes. Available from: http://www.heartfoundation.co.za/diabetes/. (accessed 15 June 2020).

55. Cárceles CM, Fernández-Varón E, Marín P, Escudero E. Tissue disposition of azithromycin after intravenous and intramuscular administration to rabbits. Vet J. 2007;174(1):154–9.

56. Jurgoński A, Juśkiewicz J, Zduńczyk Z. A high-fat diet differentially affects the gut metabolism and blood lipids of rats depending on the type of dietary fat and carbohydrate. Nutrients. 2014;6(2):616–26.

57. Mozaffari MS, Patel C, Ballas C, Schaffer SW. Effects of excess salt and fat intake on myocardial function and infarct size in rat. Life Sci. 2006;78(16):1808–13.

58. Lozano R, Naghavi M, Foreman K, Lim S, Shibuya K, Aboyans V, et al. Global and regional mortality from 235 causes of death for 20 age groups in 1990 and 2010: a systematic analysis for the Global Burden of Disease Study 2010. Lancet. 2012;380(9859):2095–128.

59. Cecchini M, Sassi F, Lauer J a., Lee YY, Guajardo-Barron V, Chisholm D. Tackling of unhealthy diets, physical inactivity, and obesity: Health effects and cost-effectiveness. Vol. 376, The Lancet. Elsevier Ltd; 2010. p. 1775–84.

60. Anand SS, Yusuf S. Stemming the global tsunami of cardiovascular disease. Lancet. 2011;377(9765):529–32.

61. Lozano R, Naghavi M, Foreman K, Lim S, Shibuya K, Aboyans V, et al. Global and regional mortality from 235 causes of death for 20 age groups in 1990 and 2010 : a systematic analysis for the Global Burden of Disease Study 2010. Lancet. 2010;380:2095–128.

62. Kopelman P. Health risks associated with overweight and obesity. Vol. 8, Obesity Reviews. 2007. p. 13–7.

63. Dietz WH. Health Consequences of Obesity in Youth: Childhood Predictors of Adult Disease. Off J Am Acad Pediatr. 1998;101:518–26.

64. Alexander RW. Hypertension and the pathogenesis of atherosclerosis: Oxidative stress and the mediation of arterial inflammatory response: A new perspective. In: Hypertension. 1995. p. 155–61.

65. Winkleby M a., Jatulis DE, Frank E, Fortmann SP. Socioeconomic status and health: How education, income, and occupation contribute to risk factors for cardiovascular disease. Am J Public Health. 1992;82(6):816–20.

66. WHO. World Health Statistics - Minitoring Health for the Sustainable Development Goals. Available from: https://www.who.int/gho/publications/world_health_statistics/2019/en/. (accessed 24 June 2020).

67. Aiello AE, Kaplan GA. Socioeconomic position and inflammatory and immune biomarkers of cardiovascular disease: applications to the panel study of income dynamics. Biodemography Soc Biol. 2009;55(2):178–205.

68. Gao B. Hepatoprotective and anti-inflammatory cytokines in alcoholic liver disease. J Gastroenterol Hepatol. 2012;27:89–93.

69. Gardner JD, Mouton AJ. Alcohol effects on cardiac function. Compr Physiol. 2011;5(2):791–802.

70. Weidmann H, Touat-Hamici Z, Durand H, Mueller C, Chardonnet S, Pionneau C, et al. SASH1, a new potential link between smoking and atherosclerosis. Atherosclerosis. 2015;242(2):571–9.

71. Csiszar A, Wang M, Lakatta EG, Ungvari Z. Inflammation and endothelial dysfunction during aging: role of NF-kappaB. J Appl Physiol. 2008;105(4):1333–41.

72. North BJ, Sinclair DA. The intersection between aging and cardiovascular disease. Circ Res.

2012;110(8):1097–108.

73. Fedele F, Bruno N, Mancone M. Cardiovascular Risk Factors and HIV Disease. Aids Rev. 2011;13(2):119–29.

74. Bailey AL, Smyth SS. Invasive coronary vasoreactivity testing to diagnose microvascular dysfunction in women. JACC Cardiovasc Interv. 2012;5(6):654–5.

75. Winkleby MA, Cubbin C, Ahn DK, Kraemer HC. Pathways by Which SES and Ethnicity Influence Cardiovascular Disease Risk Factors. Ann N Y Acad Sci. 1999;896(1):191–209.

76. Buchacz K, Baker RK, Palella FJ, Shaw L, Patel P, Lichtenstein K a., et al. Disparities in prevalence of key chronic diseases by gender and race/ethnicity among antiretroviraltreated HIV-infected adults in the US. Antivir Ther. 2013;18(1):65–75.

77. Bannon M. Ethnicity and cardiovascular disease. Q J Med. 2011;104(6):467–8.

78. Friedman-Kien AE. Disseminated Kaposi's sarcoma syndrome in young homosexual men. J Am Acad Dermatol. 1981;5(4):468–71.

79. Barré-Sinoussi F, Chermann J-C, Rey F, Nugeyre MT, Chamaret S, Gruest J, et al. Isolation of a T-lymphotropic retrovirus from a patient at risk for acquired immune deficiency syndrome (AIDS). Science (80-). 1983;220(4599):868–71.

80. Gallo RC, Salahuddin SZ, Popovic M, Shearer GM, Kaplan M, Haynes BF, et al. Frequent detection and isolation of cytopathic retroviruses (HTLV-III) from patients with AIDS and at risk for AIDS. Science (80-). 1984;224(4648):500–3.

81. Sharp PM, Hahn BH. Origins of HIV and the AIDS pandemic. Cold Spring Harb Perspect Med. 2011;1(1):a006841.

82. Fanales-Belasio E, Raimondo M, Suligoi B, Buttò S. HIV virology and pathogenetic mechanisms of infection: a brief overview. Ann Ist Super Sanita. 2010;46:5–14.

83. Kirchhoff F. HIV life cycle: overview. Encycl AIDS. 2013;1–9.

84. Hazenberg MD, Otto SA, van Benthem BHB, Roos MT, Coutinho RA, Lange JMA, et al. Persistent immune activation in HIV-1 infection is associated with progression to AIDS. Aids. 2003;17(13):1881–8.

85. Nelson JA, Ghazal P, Wiley CA. Role of opportunistic viral infections in AIDS. Aids. 1990;4(1):1–10.

86. Clifford GM, Franceschi S. Cancer risk in HIV-infected persons: influence of CD4+ count. Futur Oncol. 2009;5(5):669–78.

87. Yang C, Tang D. Patient-Specific Carotid Plaque Progression Simulation. C Model Eng Sci. 2000;1(2):119–31.

88. WHO. Towards universal access: scaling up priority HIV/AIDS interventions in the health sector:

progress report 2010. Available from: https://www.who.int/hiv/mediacentre/universal_access_progress_report_en.pdf. (accessed 12 April 2020).

89. WHO. World Health Statistics 2011. Available from: https://www.who.int/gho/publications/world_health_statistics/EN_WHS2011_Full.pdf. (accessed 13 August 2020).

90. Anabwani G, Navario P. Nutrition and HIV/AIDS in sub-Saharan Africa: An overview. Vol. 21, Nutrition. 2005. p. 96–9.

91. UNAIDS. Global Rport: UNAIDS report on the global AIDS epidemic 2013. Available from: https://www.unaids.org/sites/default/files/media_asset/UNAIDS_Global_Report_2013_en_1.pdf. (accessed 25 August 2020).

92. Anuurad E, Bremer A, Berglund L. HIV protease inhibitors and obesity. Curr Opin Endocrinol Diabetes Obes. 2010;17(5):478.

93. Houle B, Clark SJ, Gómez-Olivé FX, Kahn K, Tollman SM. The unfolding counter-transition in rural South Africa: Mortality and cause of death, 1994-2009. PLoS One. 2014;9(6).

94. Levitt NS, Steyn K, Dave J, Bradshaw D. Chronic noncommunicable diseases and HIV-AIDS on a collision course: Relevance for health care delivery, particularly in low-resource settings - Insights from South Africa. Am J Clin Nutr. 2011;94(6):1690–6.

95. SANAC. LET OUR ACTIONS COUNT: Reflections on NSP 2012-2016 and moving forward to NSP 2017-2022. Available online: https://sanac.org.za/wpcontent/uploads/2017/06/NSP_FullDocument_FINAL.pdf. (accessed 27 August 2020).

96. Baker J V., Lundgren JD. Cardiovascular implications from untreated human immunodeficiency virus infection. Eur Heart J. 2011;32(8):945–51.

97. Worm SW, Sabin C, Weber R, Reiss P, El-Sadr W, Dabis F, et al. Risk of myocardial infarction in patients with HIV infection exposed to specific individual antiretroviral drugs from the 3 major drug classes: the data collection on adverse events of anti-HIV drugs (D: A: D) study. J Infect Dis. 2010;201(3):318–30.

98. Deeks SG, Tracy R, Douek DC. Systemic Effects of Inflammation on Health during Chronic HIV Infection. Immunity. 2013;39(4):633–45.

99. Baker J V, Duprez D. Biomarkers and HIV-associated cardiovascular disease. Curr Opin HIV AIDS. 2010;5(6):511–6.

100. Mangili A, Polak JF, Quach LA, Gerrior J, Wanke CA. Markers of atherosclerosis and inflammation and mortality in patients with HIV infection. Atherosclerosis. 2011;214(2):468–73.

101. Wang T, Green LA, Gupta SK, Kim C, Wang L, Almodovar S, et al. Transfer of intracellular HIV Nef to endothelium causes endothelial dysfunction. PLoS One. 2014;9(3):e91063.

102. Lo J, Abbara S, Shturman L, Soni A, Wei J, Rocha-Filho J, et al. Increased prevalence of subclinical coronary atherosclerosis detected by coronary computed tomography agiography in HIV-infected men. Aids. 2010;24(2):243–53.

103. Palella Jr FJ, Phair JP. Cardiovascular disease in HIV infection. Curr Opin HIV AIDS. 2011;6(4):266.

104. Fourie CMT, Schutte AE, Smith W, Kruger A, Van Rooyen JM. Endothelial activation and cardiometabolic profiles of treated and never-treated HIV infected Africans. Atherosclerosis. 2015;240(1):154–60.

105. Sinha A, Ma Y, Scherzer R, Hur S, Li D, Ganz P, et al. Role of T-cell dysfunction, inflammation, and coagulation in microvascular disease in HIV. J Am Heart Assoc. 2016;5(12).

106. Levy BI, Ambrosio G, Pries AR, Struijker-Boudier HAJ. Microcirculation in Hypertension. Circulation. 2001 Aug;104(6):735–40.

107. Leung H, Wang JJ, Rochtchina E, Wong TY, Klein R, Mitchell P. Dyslipidaemia and microvascular disease in the retina. Eye (Lond). 2005;19(8):861–8.

108. Mazzuca P, Caruso A, Caccuri F. HIV-1 infection, microenvironment and endothelial cell dysfunction. New Microbiol. 2016;39(3):1121–7138.

109. De Cock KM, Jaffe HW, Curran JW. The evolving epidemiology of HIV/AIDS. Aids. 2012;26(10):1205–13.

110. De Cock KM, Jaffe HW, Curran JW. Reflections on 30 Years of AIDS. Emerg Infect Dis. 2011;17(6):1044–8.

111. Vella S, Schwartländer B, Sow SP, Eholie SP, Murphy RL. The history of antiretroviral therapy and of its implementation in resource-limited areas of the world. AIDS. 2012;26(10):1231–41.

112. Arts EJ, Hazuda DJ. HIV-1 antiretroviral drug therapy. Cold Spring Harb Perspect Med. 2012;2(4):a007161.

113. Palmisano L, Vella S. A brief history of antiretroviral therapy of HIV infection: success and challenges. Ann Ist Super Sanita. 2011;47:44–8.

114. De Clercq E. Antiviral drugs in current clinical use. J Clin Virol. 2004;30(2):115–33.

115. Jochmans D. Novel HIV-1 reverse transcriptase inhibitors. Virus Res. 2008;134(1–2):171–85.

116. WHO. Clinical Guidelines: Antiretroviral Therapy. Available from: https://www.who.int/hiv/pub/arv/chapter4.pdf. (accessed 29 August 2020).

117. Anderson PL, Kakuda TN, Lichtenstein K a. The cellular pharmacology of nucleoside- and nucleotide-analogue reverse-transcriptase inhibitors and its relationship to clinical toxicities. Clin Infect Dis.

2004;38(5):743–53.

118. Brinkman K, Smeitink JA, Romijn JA, Reiss P. Mitochondrial toxicity induced by nucleoside-analogue reverse-transcriptase inhibitors is a key factor in the pathogenesis of antiretroviral-therapy-related lipodystrophy. Lancet. 1999;354(9184):1112–5.

119. AIDS Research Advisory Council. Guidelines for the use of antiretroviral agents in HIV-1-infected adults and adolescents. Available from: https://clinicalinfo.hiv.gov/sites/default/files/guidelines/documents/AdultandAdolescentGL.pdf. (accessed 10 September 2020).

120. Aboud M, Elgalib A, Kulasegaram R, Peters B. Insulin resistance and HIV infection: a review. Int J Clin Pract. 2007;61(3):463–72.

121. Aberg JA. Cardiovascular Complications in HIV Management: Past, Present, and Future Judith. J Acquir Immune Defic Syndr. 2010;50(1):1–5.

122. Pauwels R. New non-nucleoside reverse transcriptase inhibitors (NNRTIs) in development for the treatment of HIV infections. Curr Opin Pharmacol. 2004;4(5):437–46.

123. Pérez SE, Chow SP, Kania A, Goldberg R, Badowski ME. Weighing in on the Role of Integrase Strand Transfer Inhibitors (INSTIs) on Weight Gain: Fact or Fiction? Curr Infect Dis Rep. 2020;22:1–11.

124. Achhra AC, Mocroft A, Reiss P, Sabin C, Ryom L, De Wit S, et al. Short-term weight gain after antiretroviral therapy initiation and subsequent risk of cardiovascular disease and diabetes: the D: A: D study. HIV Med. 2016;17(4):255–68.

125. Gorwood J, Bourgeois C, Pourcher V, Pourcher G, Charlotte F, Mantecon M, et al. The integrase inhibitors dolutegravir and raltegravir exert proadipogenic and profibrotic effects and induce insulin resistance in human/simian adipose tissue and human adipocytes. Clin Infect Dis. 2020;71(10):e549–60.

126. Leonard M, Bourgi K, Koeth J. Pharmacogenetics of weight gain after switch from efavirenz to integrase inhibitors. In: Conference on Retroviruses and Opportunistic Infections, Seattle, WA. 2019.

127. Murray CJL, Ortblad KF, Guinovart C, Lim SS, Wolock TM, Roberts DA, et al. Global, regional, and national incidence and mortality for HIV, tuberculosis, and malaria during 1990-2013: A systematic analysis for the Global Burden of Disease Study 2013. Lancet. 2014;384(9947):1005–70.

128. Delpech V, Gahagan J. The global epidemiology of HIV. Medicine (Baltimore). 2009;37(7):317–20.

129. Pillay-van Wyk V, Msemburi W, Laubscher R, Dorrington RE, Groenewald P, Matzopoulos R, et al. Second National Burden of Disease Study South Africa: national and subnational mortality trends, 1997–2009. Lancet. 2013;381:S113.

130. Shisana O, Rehle T, Simbayi L, Zuma K, Jooste S, Pillay-van-Wyk V, et al. South African national HIV prevalence, incidence, behaviour and communication survey, 2008: A turning tide among

teenagers? Human Sciences Research Council Funded. HSRC Press; 2008. p. 1–120.

131. Hontelez JAC, Lurie MN, Bärnighausen T, Bakker R, Baltussen R, Tanser F, et al. Elimination of HIV in South Africa through expanded access to antiretroviral therapy: A Model Comparison Study. PLoS Med. 2013;10(10):e1001534.

132. Anand SSHDG. Emerging risk factors for atherosclerotic vascular disease: A Critical Review of the Evidence. JAMA J Am Med Assoc. 2003;290(7):932–40.

133. Kannel WB, McGee D, Gordon T. A general cardiovascular risk profile: The Framingham study. Am J Cardiol. 1976;38(1):46–51.

134. Deaton C, Froelicher ES, Wu LH, Ho C, Shishani K, Jaarsma T. The global burden of cardiovascular disease. Eur J Cardiovasc Nurs. 2011;10(SUPPL. 2):S5–13.

135. Brindle P, Beswick A, Fahey T, Ebrahim S. Accuracy and impact of risk assessment in the primary prevention of cardiovascular disease: a systematic review. Heart. 2006;92(12):1752–9.

136. Cooney MT, Dudina AL, Graham IM. Value and Limitations of Existing Scores for the Assessment of Cardiovascular Risk. A Review for Clinicians. J Am Coll Cardiol. 2009;54(14):1209–27.

137. Hadi HA, Carr CS, Al Suwaidi J. Endothelial dysfunction: cardiovascular risk factors, therapy, and outcome. Vasc Heal Risk Manag. 2005;1(3):183–98.

138. D'Agostino RB, Vasan RS, Pencina MJ, Wolf PA, Cobain M, Massaro JM, et al. General cardiovascular risk profile for use in primary care: The Framingham heart study. Circulation. 2008 Feb;117(6):743–53.

139. van Wijk JPH, de Koning EJP, Cabezas MC, Joven J, op't Roodt J, Rabelink TJ, et al. Functional and structural markers of atherosclerosis in human immunodeficiency virus-infected patients. J Am Coll Cardiol. 2006;47(6):1117–23.

140. MBoistat KM, Liew G, Macashill P, Irwig L, Klein R, K. KBE, et al. Retinal Vessel Caliber and Risk for Coronary Heart Disease: A Systematic Review and Meta-Analysis. Ann Intern Med. 2007;151(June 2009):404–13.

141. Badimon L, Romero JC, Cubedo J, Borrell-Pagès M. Circulating Biomarkers. Thromb Res. 2012;130(SUPPL.1):S12–5.

142. Wang TJ. Assessing the role of circulating, genetic, and imaging biomarkers in cardiovascular risk prediction. Circulation. 2011;123(5):551–65.

143. Leung H, Wang JJ, Rochtchina E, Wong TY, Klein R, Mitchell P. Impact of current and past blood pressure on retinal arteriolar diameter in an older population. J Hypertens. 2004;22(8):1543–9.

144. Abramoff MD, Garvin MK, Sonka M. Retinal imaging and image analysis. Vol. 3, IEEE Reviews in Biomedical Engineering. IEEE; 2010. p. 169–208.

145. Sasongko MB, Hodgson LAB, Wong TY, Kawasaki R, Cheung CY, Hsu W, et al. Correlation and reproducibility of retinal vascular geometric measurements for stereoscopic retinal images of the same eyes. Ophthalmic Epidemiol. 2012;19(5):322–7.

146. De Boever P, Louwies T, Provost E, Int Panis L, Nawrot TS. Fundus photography as a convenient tool to study microvascular responses to cardiovascular disease risk factors in epidemiological studies. J Vis Exp. 2014 Oct;(92):e51904.

147. Li L-J, Ikram MK, Wong TY. Retinal vascular imaging in early life: insights into processes and risk of cardiovascular disease. J Physiol. 2016 Apr;594(8):2175–203.

148. Yip W, Tham YC, Hsu W, Lee ML, Klein R, Klein B, et al. Comparison of common retinal vessel caliber measurement software and a conversion algorithm. Transl Vis Sci Technol. 2016 Oct;5(5):11.

149. Wang JJ, Shi Y, Xie J, Tan AG, Hogdson LAB, Lee S, et al. Pupil dilation may affect retinal vessel caliber measures. Ophthalmic Epidemiol. 2018 May;25(3):234–7.

150. Cheung N, Sharrett AR, Klein R, Criqui MH, Islam FMA, Macura KJ, et al. Aortic distensibility and retinal arteriolar narrowing: The multi-ethnic study of atherosclerosis. Hypertension. 2007 Oct;50(4):617–22.

151. Bernardes R, Serranho P, Lobo C. Digital ocular fundus imaging: A review. Ophthalmologica. 2011;226(4):161–81.

152. Wang SB, Mitchell P, Liew G, Wong TY, Phan K, Thiagalingam A, et al. A spectrum of retinal vasculature measures and coronary artery disease. Atherosclerosis. 2017 Jan;268:215–24.

153. Ong YT, De Silva DA, Cheung CY, Chang HM, Chen CP, Wong MC, et al. Microvascular structure and network in the retina of patients with ischemic stroke. Stroke. 2013;44(8):2121–7.

154. Patton N, Aslam TM, MacGillivray T, Deary IJ, Dhillon B, Eikelboom RH, et al. Retinal image analysis: Concepts, applications and potential. Prog Retin Eye Res. 2006 Jan;25(1):99–127.

155. Leung H, Wang JJ, Rochtchina E, Tan AG, Wong TY, Klein R, et al. Relationships between age, blood pressure, and retinal vessel diameters in an older population. Investig Opthalmology Vis Sci. 2003 Jul;44(7):2900–5.

156. Im JC, Shin JP, Kim IT, Park DH. Analysis of factors associated with retinal vascular caliber in normal Korean subjects. J Korean Ophthalmol Soc. 2014;55(4):548.

157. Lammertyn L, Schutte AE, Smith W, Pieters M, Schutte R. Retinal vessel calibres and haemostasis in black and white South Africans. J Hypertens. 2015 Dec;33(12):2483–90.

158. Felicia. The relationship between oxidative stress-related markers and retinal microvascular structure and function in a bi-ethnic population: The SABPA study. North-West University (South Africa) , Potchefstroom Campus; 2016.

159. Gangaputra S, Kalyani PS, Fawzi AA, Van Natta ML, Hubbard LD, Danis RP, et al. Retinal vessel

caliber among people with acquired immunodeficiency syndrome: relationships with disease-associated factors and mortality. Am J Ophthalmol. 2012 Mar;153(3):434-444.e1.

160. Gepstein R, Rosman Y, Rechtman E, Koren-Morag N, Segev S, Assia E, et al. Association of retinal microvascular caliber with blood pressure levels. Blood Press. 2012 Jun;21(3):191–6.

161. Drobnjak D, Munch IC, Glümer C, Faerch K, Kessel L, Larsen M, et al. Retinal vessel diameters and their relationship with cardiovascular risk and all-cause mortality in the inter99 eye study: A 15-year follow-up. J Ophthalmol. 2016;2016.

162. von Hanno T, Bertelsen G, Sjølie AK, Mathiesen EB. Retinal vascular calibres are significantly associated with cardiovascular risk factors: the Tromsø Eye Study. Acta Ophthalmol. 2014 Feb;92(1):40–6.

163. Köchli S, Endes K, Infanger D, Zahner L, Hanssen H. Obesity, blood pressure, and retinal vessels: a meta-analysis. Vol. 141, Pediatrics. American Academy of Pediatrics; 2018. p. e20174090.

164. Taarnhøj NCBB, Larsen M, Sander B, Kyvik KO, Kessel L, Hougaard JL, et al. Heritability of retinal vessel diameters and blood pressure: A twin study. Investig Ophthalmol Vis Sci. 2006 Aug;47(8):3539–44.

165. Kappelgaard P, Holfort SK, Klefter ON, Larsen M. Retinal vessel diameter changes in relation to dark adaptation and acute hyperglycemia. J Ophthalmol. 2018;2018.

166. Crosby-Nwaobi R, Heng LZ, Sivaprasad S. Retinal vascular calibre, geometry and progression of diabetic retinopathy in type 2 diabetes mellitus. Ophthalmologica. 2012 Jul;228(2):84–92.

167. Kaushik S, Kifley A, Mitchell P, Wang JJ. Age, blood pressure, and retinal vessel diameter: Separate effects and interaction of blood pressure and age. Investig Ophthalmol Vis Sci. 2007 Feb;48(2):557–61.

168. Wong TY, Klein R, Klein BEKK, Meuer SM, Hubbard LD. Retinal vessel diameters and their associations with age and blood pressure. Investig Opthalmology Vis Sci. 2003 Nov;44(11):4644–51.

169. Kalyani PS, Fawzi A., Gangaputra S, Van Nata ML, Holland GN. Evaluation of retinal vessel caliber in people with AIDS. IOVS. 2010;51(13):4856.

170. Jabs DA, Van Natta ML, Trang G, Jones N, Milush JM, Cheu R, et al. Association of systemic inflammation with retinal vascular caliber in patients with AIDS. Investig Ophthalmol Vis Sci. 2019 May;60(6):2218–25.

171. Gopinath B, Baur LA, Teber E, Liew G, Wong TY, Mitchell P. Effect of obesity on retinal vascular structure in pre-adolescent children. Int J Pediatr Obes. 2011 Jun;6(2–2).

172. Triantafyllou A, Anyfanti P, Gavriilaki E, Zabulis X, Gkaliagkousi E, Petidis K, et al. Association between retinal vessel caliber and arterial stiffness in a population comprised of normotensive to early-stage hypertensive individuals. Am J Hypertens. 2014 Dec;27(12):1472–8.

173. Klein R, Myers CE, Klein BEK, Zinman B, Gardiner R, Suissa S, et al. Relationship of blood pressure to retinal vessel diameter in type 1 diabetes mellitus. Arch Ophthalmol. 2010 Feb;128(2):198–205.

174. McEvoy CT, Wallace IR, Hamill LL, Neville CE, Hunter SJ, Patterson CC, et al. Increasing fruit and vegetable intake has no effect on retinal vessel caliber in adults at high risk of developing cardiovascular disease. Nutr Metab Cardiovasc Dis. 2016 Apr;26(4):318–25.

175. Yanagi M, Misumi M, Kawasaki R, Takahashi I, Itakura K, Fujiwara S, et al. Is the association between smoking and the retinal venular diameter reversible following smoking cessation? Investig Ophthalmol Vis Sci. 2013 Dec;55(1):405–11.

176. Yim-Lui Cheung C, Wong TY, Lamoureux EL, Sabanayagam C, Li J, Lee J, et al. C-reactive protein and retinal microvascular caliber in a multiethnic Asian population. Am J Epidemiol. 2010;171(2):206–13.

177. Klein R, Klein BEK, Moss SE, Wong TY. Retinal vessel caliber and microvascular and macrovascular disease in type 2 diabetes. XXI: The Wisconsin Epidemiologic Study of Diabetic Retinopathy. Ophthalmology. 2007 Oct;114(10):1884–92.

178. Peto T; Haddow L; Leung I; Laverick R; Williams I; Vera J; et al. Retinal vascular calibres in older HIV-positive men compared to HIV-negative and younger HIV+ controls. Investigative Ophthalmology & Visual Science. 2017 Jun 23;58(8):1493.

179. Pathai S, Weiss H a., Lawn SD, Peto T, D'Costa LM, Cook C, et al. Retinal arterioles narrow with increasing duration of anti-retroviral therapy in HIV infection: a novel estimator of vascular risk in HIV? He W, editor. PLoS One. 2012 Dec;7(12):1–8.

180. Haddow L, Laverick R, Leung I, Post F, Vera J, Gilson R, et al. Measurement of retinal vessels as a biomarker of cerebrovascular aging in older HIV-positive men compared with controls. J Acquir Immune Defic Syndr. 2018 Feb;77(2):199–205.

181. Edwar L, Karim B, Wijaya IP, Ariyanto I, Tanudjaja SA, Estiasari R, et al. Factors affecting the health of retinal vessels in human immunodeficiency virus patients beginning anti-retroviral therapy. AIDS Res Hum Retroviruses. 2019 Jun;35(6):529–35.

182. Cheung N, Liew G, Lindley RI, Liu EY, Wang JJ, Hand P, et al. Retinal fractals and acute lacunar stroke. Ann Neurol. 2010 Mar;68(1):107–11.

183. Masters BR. Fractal analysis of the vascular tree in the human retina. Vol. 6, Annual Review of Biomedical Engineering. 2004. p. 427–52.

184. Ţălu Ş, Giovanzana S. Fractal and multifractal analysis of human retinal vascular network: a review. Int J Bioflux Soc. 2011;3(3):2011.

185. Hart WE, Goldbaum M, Côté B, Kube P, Nelson MR. Measurement and classification of retinal vascular tortuosity. Int J Med Inform. 1999 Feb;53(2–3):239–52.

186. Gould DJ, Vadakkan TJ, Poche RA, Dickinson ME. Multifractal and lacunarity analysis of microvascular morphology and remodeling. Microcirculation. 2011 Feb;18(2):136–51.

187. Ventura LolaCosta E, Albuquerque Nogueira R. Fractal, multifractal and lacunarity analysis applied in retinal regionsof diabetic patients with and without non-proliferative diabetic retinopathy. Fractal Geom Nonlinear Anal Med Biol. 2016;1(3).

188. Wang R, Li P, Pan Q, Li JKJ, Kuebler WM, Pries AR, et al. Investigation into the diversity in the fractal dimensions of arterioles and venules in a microvascular network – A quantitative analysis. Microvasc Res. 2019 Sep;125:103882.

189. Hughes AD, Wong TY, Witt N, Evans R, Thom SAM, Klein BE, et al. Determinants of retinal microvascular architecture in normal subjects. Microcirculation. 2009 Jan;16(2):159–66.

190. Vaes A, Spruit M, Wouters E, Theunis J, De Boever P, Standaert A, et al. Retinal image analysis in patients with COPD. In: Rehabilitation and Chronic Care. European Respiratory Society; 2017. p. OA4869.

191. Liew G, Mitchell P, Rochtchina E, Wong TY, Hsu W, Lee ML, et al. Fractal analysis of retinal microvasculature and coronary heart disease mortality. Eur Heart J. 2011;32(4):422–9.

192. Cheung CY, Thomas GN, Tay W, Ikram MK, Hsu W, Lee ML, et al. Retinal vascular fractal dimension and its relationship with cardiovascular and ocular risk factors. Am J Ophthalmol. 2012 Oct;154(4):663-674.e1.

193. Sng CCAA, Sabanayagam C, Lamoureux EL, Liu E, Lim SCSC, Hamzah H, et al. Fractal analysis of the retinal vasculature and chronic kidney disease. Nephrol Dial Transplant. 2010;25(7):2252–8.

194. Waduthantri S. Eye as a window to the brain in central nervous system diseases. Med J Dr DY Patil Vidyapeeth. 2019;12(4):376.

195. Zhu P, Huang F, Lin F, Li Q, Yuan Y, Gao Z, et al. The relationship of retinal vessel diameters and fractal dimensions with blood pressure and cardiovascular risk factors. Metze K, editor. PLoS One. 2014 Sep;9(9):e106551.

196. Aliahmad B, Kumar DK, Hao H, Unnikrishnan P, Che Azemin MZ, Kawasaki R, et al. Zone specific fractal dimension of retinal images as predictor of stroke incidence. Sci World J. 2014;2014.

197. Cheung CYL, Zheng Y, Hsu W, Lee ML, Lau QP, Mitchell P, et al. Retinal vascular tortuosity, blood pressure, and cardiovascular risk factors. Ophthalmology. 2011 May;118(5):812–8.

198. Tai ELM, Kueh YC, Wan Hitam W-H, Wong TY, Shatriah I. Comparison of retinal vascular geometry in obese and non-obese children. Breslin JW, editor. PLoS One. 2018 Feb;13(2):e0191434.

199. Sasongko MB, Wong TY, Nguyen TT, Cheung CY, Shaw JE, Wang JJ. Retinal vascular tortuosity in persons with diabetes and diabetic retinopathy. Diabetologia. 2011 Sep;54(9):2409–16.

200. Sasongko MB, Wong TY, Donaghue KC, Cheung N, Jenkins AJ, Benitez-Aguirre P, et al. Retinal

arteriolar tortuosity is associated with retinopathy and early kidney dysfunction in type 1 diabetes. Am J Ophthalmol. 2012 Jan;153(1):176-183.e1.

201. Popovic N, Radunovic M, Badnjar J, Popovic T. Fractal dimension and lacunarity analysis of retinal microvascular morphology in hypertension and diabetes. Microvasc Res. 2018 Jul;118:36–43.

202. Wiharto, Suryani E, Kipti MY. Assessment of early hypertensive retinopathy using fractal analysis of retinal fundus image. Telkomnika (Telecommunication Comput Electron Control. 2018;16(1):445–54.

203. Cheng SC, Huang YM. A novel approach to diagnose diabetes based on the fractal characteristics of retinal images. IEEE Trans Inf Technol Biomed. 2003 Sep;7(3):163–70.

204. Arthur E, Somfai GM, Kostic M, Oropesa S, Santiesteban CM, DeBuc DC. Distinguishing cognitive impairment by using singularity spectrum and lacunarity analysis of the retinal vascular network. Neurophotonics. 2019 Sep;6(04):1.

205. Crystal HA, Holman S, Lui YW, Baird AE, Yu H, Klein R, et al. Association of the fractal dimension of retinal arteries and veins with quantitative brain MRI measures in HIV-infected and uninfected women. Ahammer H, editor. PLoS One. 2016 May;11(5):e0154858.

206. Tan P, Hee OK, Cheung CY, Yeo TK, Agrawal R, Ng J, Han C, Lim TH, Wong TY TS. Prospective evaluation of retinal microvascular parametric changes in patients with HIV. Invest Ophthalmol Vis Sci. 2012;53(14):2657.

207. Retinal vascular changes and immune restoration in a cohort of HIV patients on highly active antiretroviral therapy | IOVS | ARVO Journals.

208. Teoh S, Tan P, Cheung C, Li Q, Yeo TK, Agrawal R, Ng J, Hee O, Lim T WT. Evaluation of relationships between retinal microvascular parametric changes and immune status in patients with HIV. Invest Ophthalmol Vis Sci. 2013;54(15):24.

209. Tan P, Hee OK, Cheung CY, Yeo TK, Agrawal R, Ng J, et al. Prospective evaluation of retinal microvascular parametric changes in patients with HIV. Invest Ophthalmol Vis Sci. 2012;53(14):2657.

210. Seo SW, Lee J-M, Im K, Park J-S, Kim S-H, Kim ST, et al. Cardiovascular risk factors cause cortical thinning in cognitively impaired patients: relationships among cardiovascular risk factors, white matter hyperintensities, and cortical atrophy. Alzheimer Dis Assoc Disord. 2012;26(2):106–12.

211. Luo T, Gast TJ, Vermeer TJ, Burns SA. Retinal vascular branching in healthy and diabetic subjects. Investig Ophthalmol Vis Sci. 2017 May;58(5):2685–94.

212. Ţălu Ş. Characterization of retinal vessel networks in human retinal imagery using quantitative descriptors. Hum Vet Med. 2013;5(2):52–7.

213. Hayreh SS. Central retinal vein occlusion. In: Encyclopedia of the Eye. Elsevier; 2010. p. 238–49.

214. Youm DJ, Ha MM, Chang Y, Song SJ. Retinal vessel caliber and risk factors for branch retinal vein occlusion. Curr Eye Res. 2012 Apr;37(4):334–8.

215. Patton N, Maini R, MacGillivary T, Aslam TM, Deary IJ, Dhillon B. Effect of axial length on retinal vascular network geometry. Am J Ophthalmol. 2005 Oct;140(4):648.e1-648.e7.

216. Zamir M, Brown N. Arterial branching in various parts of the cardiovascular system. Am J Anat. 1982 Apr;163(4):295–307.

217. Zamir M, Medeiros JA, Cunningham TK. Arterial bifurcations in the human retina. J Gen Physiol. 1979 Oct;74(4):537–48.

218. Martinez-Perez ME, Hughes AD, Stanton A V., Thom SA, Chapman N, Bharath AA, et al. Retinal vascular tree morphology: A semi-automatic quantification. IEEE Trans Biomed Eng. 2002;49(8):912–7.

219. Ruhrberg C, Gerhardt H, Golding M, Watson R, Ioannidou S, Fujisawa H, et al. Spatially restricted patterning cues provided by heparin-binding VEGF-A control blood vessel branching morphogenesis. Genes Dev. 2002 Oct;16(20):2684–98.

220. De Smet F, Segura I, De Bock K, Hohensinner PJ, Carmeliet P. Mechanisms of vessel branching: Filopodia on endothelial tip cells lead the way. Vol. 29, Arteriosclerosis, Thrombosis, and Vascular Biology. Lippincott Williams & Wilkins; 2009. p. 639–49.

221. Hetzel A. Systemic diseases in non-inflammatory branch and central retinal artery occlusion. An overview of 416 patients.

222. Huang L, Aris IM, Teo LLY, Wong TY, Chen WQ, Koh AS, et al. Exploring associations between cardiac structure and retinal vascular geometry. J Am Heart Assoc. 2020 Apr;9(7):e014654.

223. Nadal J, Deverdun J, Champfleur NM, Carriere I, Creuzot-Garcher C, Delcourt C, et al. Retinal vascular fractal dimension and cerebral blood flow, a pilot study. Acta Ophthalmol. 2020 Feb;98(1):e63–71.

224. Hayreh SS, Podhajsky PA, Zimmerman MB. Retinal artery occlusion. associated systemic and ophthalmic abnormalities. Ophthalmology. 2009 Oct;116(10):1928–36.

225. Youm DJ, Ha MM, Chang Y, Song SJ. Retinal vessel caliber and risk factors for branch retinal vein occlusion. Curr Eye Res. 2012 Apr;37(4):334–8.

226. Li LJ, Lamoureux E, Wong TY, Lek N. Short-term poor glycemic control and retinal microvascular changes in pediatric Type 1 Diabetes patients in Singapore: A pilot study. BMC Ophthalmol. 2017 Jun;17(1):1–6.

227. Kumari N, Cher J, Chua E, Hamzah H, Wong TY, Cheung CY. Association of serum lutein and zeaxanthin with quantitative measures of retinal vascular parameters. PLoS One. 2018;13(9):1–14.

228. Querques G, Cicinelli MV, Querques L, Zucchiatti I, Benatti L, Mazzaferro A, et al. Systemic hypertension. In: Retinal and Choroidal Imaging in Systemic Diseases. Springer Singapore; 2017. p. 217–29.

229. Dunn JP, Yamashita A, Kempen JH, Jabs DA. Retinal vascular occlusion in patients infected with

human immunodeficiency virus. Retina. 2005;25(6):759–66.

230. Conway MD, Tong P, Olk RJ. Branch retinal artery occlusion (BRAO) combined with branch retinal vein occlusion (BRVO) and optic disc neovascularization associated with HIV and CMV retinitis. Int Ophthalmol. 1995;19(4):249–52.

231. Strijdom H, De Boever P, Walzl G, Essop MF, Nawrot TS, Webster I, et al. Cardiovascular risk and endothelial function in people living with HIV/AIDS: design of the multi-site, longitudinal EndoAfrica study in the Western Cape Province of South Africa. BMC Infect Dis. 2017;17(1):41.

232. Marfell-Jones MJ, Stewart AD, De Ridder JH. International standards for anthropometric assessment. 2012.

233. The Heart and Stroke Foundation South Africa. Cholesterol. Available from: https://www.heartfoundation.co.za/cholesterol/. (accessed 22 August 2021).

234. γ-Glutamyltransferase. Available from: http://labogids.sintmaria.be/sites/default/files/files/ggt-2_2017-01_v10.pdf. (accessed 12 May 2020).

235. Association AH. High-sensitivity C-reactive Protein. Available from: https://www.testing.com/tests/high-sensitivity-c-reactive-protein-hs-crp/. (accessed 14 June 2020).

236. Blood and Urine Tests. Available from: https://lifeoptions.org/learn-about-kidney-disease/blood-and-urine-tests/. (accessed 23 July 2020).

237. WHO. HIV/AIDS. Available from: https://www.who.int/health-topics/hiv-aids#tab=tab_1. (accessed 15 June 2020).

238. PapiÅ AM, Albu A, Fodor D, Bondor CI, Itu C, Dumitru CÃ. Markers of preclinical vascular disease and left ventricular diastolic dysfunction in patients with HIV infection. Med Ultrason. 2012;14(1):10–8.

239. Gruber HJ, Mayer C, Mangge H, Fauler G, Grandits N, Wilders-Truschnig M. Obesity reduces the bioavailability of nitric oxide in juveniles. Int J Obes. 2008;32(5):826–31.

240. Netzer N, Gatterer H, Faulhaber M, Burtscher M, Pramsohler S, Pesta D. Hypoxia, oxidative stress and fat. Biomolecules. 2015;5(2):1143–50.

241. Watanabe R, Zhang H, Berry G, Goronzy JJ, Weyand CM. Immune checkpoint dysfunction in large and medium vessel vasculitis. Am J Physiol Circ Physiol. 2017;312(5):H1052–9.

8. Supplementary Material

Supplementary Table 1.1. *Independent associations with CRAE (baseline and follow-up).*

Variables[a]	Change (95% CI)	*p*-value
Age (years)	-8.904 (-33.665 to 15.802)	0.477
Sex (Women)	-0.545 (-5.575 to 4.485)	0.830
Smoking (Yes)	-2.789 (-7.814 to 2.238)	0.274
Alcohol consumption (Yes)	3.256 (-1.041 to 7.552)	0.136
Employment (Yes)	-0.380 (-4.281 to 3.521)	0.847
BMI (kg/m^2)	1.940 (-15.251 to 19.131)	0.822
DBP (mmHg)	-40.938 (-70.475 to -11.563)	0.007
CRVE (µm)	6.380 (4.318 to 8.422)	< 0.001
Viral load (copies mRNA/mL)	-0.001 (-0.003 to 0.001)	0.179
CD4 cell count (cells/mm3)	500 (-250.000 to 1250.000)	0.172
ART type (2^{nd}-line)	-0.507 (-6.387 to 5.374)	0.865
ART duration (weeks)	0.838 (-6.774 to 8.449)	0.828
HIV duration (≥ 5 years)	1.149 (-3.817 to 6.115)	0.648
Timepoint (Timepoint 2 *vs.* 1)	-1.601 (-4.539 to 1.338)	0.282

[a]Estimates expressed as change for each increment change in confounding factors (Age: 9.04 years, BMI: 6.36 kg/m^2, DBP: 12.5 mmHg, CRVE: 19.45 µm, CD4 count: 250 cells/mm^3, virial load: 1000 copies mRNA/mL and ART duration: 166.98 weeks).

Supplementary Table 1.2. *Independent associations with CRVE (baseline and follow-up).*

Variables[a]	Change (95% CI)	*p*-value
Age (years)	0.036 (-3.978 to 4.041)	0.987
Sex (Women)	-0.146 (-7.490 to 7.197)	0.968
Smoking (Yes)	4.909 (-2.277 to 12.095)	0.179
Alcohol consumption (Yes)	-3.823 (-9.951 to 2.304)	0.219
Employment (Yes)	-0.009 (-5.519 to 5.502)	0.997
BMI (kg/m^2)	0.852 (-1.908 to 5.883)	0.311
DBP (mmHg)	0.788 (-2.613 to 4.188)	0.647
CRAE (µm)	8.99 (5.976 to 12.009)	< 0.001
Viral load (copies mRNA/mL)	0.096 (0.017 to 0.175)	0.018
CD4 cell count (cells/mm3)	-2.500 (-6.750 to 1.750)	0.233
ART type (2^{nd}-line)	8.580 (0.353 to 16.808)	0.041
ART duration (weeks)	8.043 (-2.527 to 18.614)	0.135
HIV duration (≥ 5 years)	-2.606 (-9.553 to 4.342)	0.459
Timepoint (Timepoint 2 *vs.* 1)	1.496 (-2.520 to 5.511)	0.461

[a]Estimates expressed as change for each increment change in confounding factors (Age: 9.04 years, BMI: 6.36 kg/m^2, DBP: 12.5 mmHg, CRAE: 14.33 µm, CD4 count: 250 cells/mm^3, virial load: 1000 copies mRNA/mL and ART duration: 166.98 weeks).

Supplementary Table 1.3. *Independent associations with AVR (baseline and follow-up).*

Variables [a]	Change (95% CI)	*p*-value
Age (years)	-0.0009 (-0.018 to 0.009)	0.926
Sex (Women)	-0.001 (-0.026 to 0.024)	0.916
Smoking (Yes)	-0.021 (-0.047 to 0.005)	0.106
Alcohol consumption (Yes)	0.016 (-0.006 to 0.039)	0.147
Employment (Yes)	-0.001 (-0.021 to 0.020)	0.941
BMI (kg/m^2)	-0.0064 (-0.019 to 0.013)	0.604
DBP (mmHg)	-0.013 (-0.025 to 0.0013)	0.019
Viral load (copies mRNA/mL)	-0.0003 (-0.0006 to 0.000003)	0.046
CD4 cell count (cells/mm3)	0.025 (-0.025 to 0.025)	0.105
ART type (2^{nd}-line)	-0.01680 (-0.047 to 0.013)	0.269
ART duration (weeks)	0.015 (-0.056 to 0.025)	0.450
HIV duration (≥ 5 years)	0.012 (-0.015 to 0.037)	0.411
Timepoint (Timepoint 2 *vs.* 1)	-0.009 (-0.025 to 0.008)	0.296

[a]Estimates expressed as change for each increment change in confounding factors (Age: 9.04 years, BMI: 6.36 kg/m^2, DBP: 12.5 mmHg, CD4 count: 250 cells/mm^3, virial load: 1000 copies mRNA/mLand ART duration: 166.98 weeks).

Supplementary Table 1.4. *Independent association with average arterial tree diameter (baseline and follow-up).*

Variables [a]	Change (95% CI)	*p*-value
Age (years)	-0.832 (-2.088 to 0.416)	0.189
Sex (Women)	0.955 (-1.327 to 3.236)	0.408
Smoking (Yes)	-0.117 (-2.526 to 2.291)	0.923
Alcohol consumption (Yes)	-0.106 (-2.017 to 1.805)	0.913
Employment (Yes)	-0.609 (-2.288 to 1.070)	0.474
BMI (kg/m^2)	0.979 (-0.223 to 2.181)	0.108
DBP (mmHg)	-0.613 (-1.638 to 0.413)	0.238
Viral load (copies mRNA/mL)	0.004 (-0.021 to 0.029)	0.749
CD4 cell count (cells/mm3)	-1.000 (-2.500 to 0.250)	0.118
ART type (2^{nd}-line)	1.551 (-0.951 to 4.054)	0.222
ART duration (weeks)	2.244 (-0.880 to 5.367)	0.157
HIV duration (≥ 5 years)	-1.802 (-3.964 to 0.359)	0.101
Timepoint (Timepoint 2 *vs.* 1)	0.281 (-0.945 to 1.508)	0.649

[a]Estimates expressed as change for each increment change in confounding factors (Age: 9.04 years, BMI: 6.36 kg/m^2, DBP: 12.5 mmHg, CD4 count: 250 cells/mm^3, virial load: 1000 copies mRNA/mL and ART duration: 166.98 weeks).

Supplementary Table 1.5. *Independent association with total length of skeletonised tree (baseline and follow-up).*

Variables [a]	Change (95% CI)	*p*-value
Age (years)	-0.289 (-2.224 to 1.636)	0.762
Sex (Women)	-0.256 (-3.732 to 3.220)	0.883
Smoking (Yes)	2.609 (-0.928 toc6.146)	0.146
Alcohol consumption (Yes)	-0.173 (-0.285 to 2.501)	0.898
Employment (Yes)	-1.202 (-3.498 to 1.095)	0.301
BMI (kg/m^2)	-0.242 (-2.003 to 1.520)	0.786
DBP (mmHg)	-0.525 (-1.963 to 0.925)	0.475
Viral load (copies mRNA/mL)	0.002 (-0.032 to 0.037)	0.895
CD4 cell count (cells/mm3)	0.750 (-1.000 to 2.750)	0.411
ART type (2^{nd}-line)	-0.583 (-3.970 to 2.804)	0.733
ART duration (weeks)	-2.590 (-6.794 to 1.614)	0.223
HIV duration (≥ 5 years)	1.129 (-1.855 to 4.114)	0.454
Timepoint (Timepoint 2 *vs.* 1)	-0.878 (-2.503 to 0.747)	0.284

[a]Estimates expressed as change for each increment change in confounding factors (Age: 9.04 years, BMI: 6.36 kg/m^2, DBP: 12.5 mmHg, CD4 count: 250 cells/mm^3, virial load: 1000 copies mRNA/mL and ART duration: 166.98 weeks).

Supplementary Table 1.6. *Independent association with segment tree area (baseline and follow-up).*

Variables [a]	Change (95% CI)	*p*-value
Age (years)	-0.0633 (-0.2079 to 0.0723)	0.347
Sex (Women)	0.0290 (-0.2210 to 0.2790)	0.816
Smoking (Yes)	0.2020 (-0.0450 to 0.4490)	0.108
Alcohol consumption (Yes)	-0.0230 (-0.2030 to 0.1580)	0.803
Employment (Yes)	-0.1160 (-0.2690 to 0.0360)	0.134
BMI (kg/m^2)	0.0254 (-0.1018 to 0.1463)	0.708
DBP (mmHg)	-0.0750 (-0.1750 to 0.0250)	0.113
Viral load (copies mRNA/mL)	0.0004 (-0.0019 to 0.0027)	0.744
CD4 cell count (cells/mm3)	0.0082 (0.0001 to 0.2500)	0.900
ART type (2^{nd}-line)	0.0350 (-0.1880 to 0.2590)	0.756
ART duration (weeks)	-0.0190 (-0.2950 to 0.2580)	0.894
HIV duration (≥ 5 years)	-0.0390 (-0.2400 to 0.1610)	0.696
Timepoint (Timepoint 2 *vs.* 1)	-0.0580 (-0.1650 to 0.0490)	0.286

[a]Estimates expressed as change for each increment change in confounding factors (Age: 9.04 years, BMI: 6.36 kg/m^2, DBP: 12.5 mmHg, CD4 count: 250 cells/mm^3, virial load: 1000 copies mRNA/mL and ART duration: 166.98 weeks).

Supplementary Table 1.7. *Independent association with number of branch points (baseline and follow-up).*

Variables [a]	Change (95% CI)	*p*-value
Age (years)	-0.118 (-2.522 to 2.296)	0.925
Sex (Women)	-3.695 (-8.055 to 0.665)	0.096
Smoking (Yes)	3.753 (-8.435 to 8.349)	0.108
Alcohol consumption (Yes)	2.099 (-1.476 to 5.673)	0.247
Employment (Yes)	-0.771 (-3.894 to 2.353)	0.626
BMI (kg/m^2)	0.464 (-1.813 to 2.754)	0.686
DBP (mmHg)	-0.663 (-2.563 to 1.238)	0.493
Viral load (copies mRNA/mL)	0.034 (-0.013 to 80.352)	0.157
CD4 cell count (cells/mm^3)	3.500 (1.000 to 6.000)	0.006
ART type (2^{nd}-line)	0.054 (-4.616 to 4.724)	0.982
ART duration (weeks)	-0.901 (-6.669 to 4.867)	0.757
HIV duration (≥ 5 years)	0.426 (-3.585 to 4.437)	0.833
Timepoint (Timepoint 2 *vs.* 1)	-1.488 (-3.729 to 0.752)	0.189

[a]Estimates expressed as change for each increment change in confounding factors (Age: 9.04 years, BMI: 6.36 kg/m^2, DBP: 12.5 mmHg, CD4 count: 250 cells/mm^3, virial load: 1000 copies mRNA/mL and ART duration: 166.98 weeks).

Supplementary Table 1.8. *Independent association with number of end points (baseline and follow-up).*

Variables [a]	Change (95% CI)	*p*-value
Age (years)	-0.696 (-2.676 to 1.293)	0.489
Sex (Women)	-2.954 (-6.594 to 0.685)	0.110
Smoking (Yes)	1.534 (-2.432 to 5.501)	0.444
Alcohol consumption (Yes)	0.461 (-2.812 to 3.735)	0.781
Employment (Yes)	-1.363 (-4.342 to 1.615)	0.367
BMI (kg/m^2)	-0.668 (-2.633 to 1.291)	0.499
DBP (mmHg)	0.575 (-1.175 to 2.325)	0.518
Viral load (copies mRNA/mL)	0.042 (-0.002 to 0.086)	0.059
CD4 cell count (cells/mm3)	3.000 (0.750 to 5.250)	0.010
ART type (2^{nd}-line)	-1.196 (-5.700 to 3.307)	0.600
ART duration (weeks)	-2.727 (8.402 to 2.948)	0.343
HIV duration (≥ 5 years)	3.113 (-0.692 to 6.918)	0.108
Timepoint (Timepoint 2 *vs.* 1)	-0.098 (-2.440 to 2.246)	0.934

[a]Estimates expressed as change for each increment change in confounding factors (Age: 9.04 years, BMI: 6.36 kg/m^2, DBP: 12.5 mmHg, CD4 count: 250 $cells/mm^3$, virial load: 1000 copies mRNA/mL and ART duration: 166.98 weeks).

Supplementary Table 1.9. *Independent association with lacunarity (segmented) (baseline and follow-up).*

Variables [a]	Change (95% CI)	*p*-value
Age (years)	0.0009 (-0.00904 to 0.00090)	0.125
Sex (Women)	-0.009 (-0.016 to -0.001)	0.019
Smoking (Yes)	0.009 (0.001 to 0.016)	0.020
Alcohol consumption (Yes)	0.0001 (-0.006 to 0.006)	0.971
Employment (Yes)	0.001 (-0.004 to 0.006)	0.607
BMI (kg/m^2)	0.00636 (0.00064 to 0.00636)	0.036
DBP (mmHg)	0.00125 (0.00125 to 0.00125)	0.236
Viral load (copies mRNA/mL)	0.00003 (-0.00003 to 0.00010)	0.351
CD4 cell count (cells/mm3)	0.025 (0.025 to 0.025)	0.556
ART type (2^{nd}-line)	0.0001 (-0.008 to 0.007)	0.903
ART duration (weeks)	-0.006 (-0.015 to 0.003)	0.208
HIV duration (≥ 5 years)	0.003 (-0.003 to 0.010)	0.300
Timepoint (Timepoint 2 *vs.* 1)	0.0001 (-0.004 to 0.003)	0.866

[a]Estimates expressed as change for each increment change in confounding factors (Age: 9.04 years, BMI: 6.36 kg/m^2, DBP: 12.5 mmHg, CD4 count: 250 $cells/mm^3$, virial load: 1000 copies mRNA/mL and ART duration: 166.98 weeks).

Supplementary Table 1.10. *Independent association with lacunarity (skeletonised) (baseline and follow-up).*

Variables [a]	Change (95% CI)	*p*-value
Age (years)	0.000904 (0.000904 to 0.009040)	0.419
Sex (Women)	0.011 (0.003 to 0.019)	0.006
Smoking (Yes)	-0.010 (-0.018 to -0.001)	0.021
Alcohol consumption (Yes)	-0.002 (-0.008 to 0.005)	0.567
Employment (Yes)	-0.002 (-0.007 to 0.004)	0.574
BMI (kg/m^2)	0.000636 (-0.006360 to 0.000636)	0.296
DBP (mmHg)	0.001250 (0.001250 to 0.001250)	0.655
Viral load (copies mRNA/mL)	-0.000064 (-0.000160 to 0.000003)	0.107
CD4 cell count (cells/mm3)	0.025 (0.025 to 0.025)	0.068
ART type (2nd-line)	-0.002 (-0.012 to 0.007)	0.614
ART duration (weeks)	0.009 (-0.002 to 0.020)	0.093
HIV duration (≥ 5 years)	-0.008 (-0.015 to -0.001)	0.036
Timepoint (Timepoint 2 *vs.* 1)	0.0001 (-0.004 to 0.004)	0.936

[a]Estimates expressed as change for each increment change in confounding factors (Age: 9.04 years, BMI: 6.36 kg/m^2, DBP: 12.5 mmHg, CD4 count: 250 cells/mm^3, virial load: 1000 copies mRNA/mL and ART duration: 166.98 weeks).

Supplementary Table 1.11. *Independent association with fractal analysis (segmented) (baseline and follow-up).*

Variables [a]	Change (95% CI)	*p*-value
Age (years)	0.009 (-0.009 to 0.009)	0.215
Sex (Women)	-0.002 (-0.011 to 0.007)	0.635
Smoking (Yes)	0.010 (0.001 to 0.020)	0.320
Alcohol consumption (Yes)	0.001 (-0.007 to 0.008)	0.828
Employment (Yes)	0.0001 (-0.006 to 0.007)	0.941
BMI (kg/m^2)	0.0064 (0.0064 to 0.0127)	0.021
DBP (mmHg)	0.0013 (-0.0125 to 0.0013)	0.018
Viral load (copies mRNA/mL)	0.0001 (0.0001 to 0.0002)	0.167
CD4 cell count (cells/mm3)	0.025 (-0.250 to 0.025)	0.437
ART type (2nd-line)	0.007 (0.0001 to 0.017)	0.135
ART duration (weeks)	0.009 (-0.002 to 0.021)	0.122
HIV duration (≥ 5 years)	-0.006 (-0.003 to 0.003)	0.179
Timepoint (Timepoint 2 *vs.* 1)	-0.002 (-0.014 to 0.003)	0.428

[a]Estimates expressed as change for each increment change in confounding factors (Age: 9.04 years, BMI: 6.36 kg/m^2, DBP: 12.5 mmHg, CD4 count: 250 cells/mm^3, virial load: 1000 copies mRNA/mL and ART duration: 166.98 weeks).

Supplementary Table 1.12. *Independent association with fractal analysis (skeletonised) (baseline and follow-up).*

Variables [a]	Change (95% CI)	*p*-value
Age (years)	0.0009 (0.0009 to 0.0090)	0.397
Sex (Women)	0.0100 (-0.0019 to 0.0220)	0.097
Smoking (Yes)	-0.020 (-0.032 to -0.007)	0.002
Alcohol consumption (Yes)	-0.007 (-0.017 to 0.002)	0.114
Employment (Yes)	0.001 (-0.009 to 0.007)	0.817
BMI (kg/m^2)	-0.0064 (-0.0127 to 0.0006)	0.066
DBP (mmHg)	0.0125 (0.0013 to 0.0125)	0.167
Viral load (copies mRNA/mL)	-0.0001 (-0.0002 to 0.0001)	0.065
CD4 cell count (cells/mm3)	0.025 (0.025 to 0.025)	0.198
ART type (2^{nd}-line)	-0.0200 (-0.2150 to 0.0020)	0.111
ART duration (weeks)	-0.0220 (-0.0370 to -0.0080)	0.003
HIV duration (≥ 5 years)	0.011 (0.0001 to 0.021)	0.045
Timepoint (Timepoint 2 *vs.* 1)	0.002 (0.004 to 0.007)	0.497

[a]Estimates expressed as change for each increment change in confounding factors (Age: 9.04 years, BMI: 6.36 kg/m^2, DBP: 12.5 mmHg, CD4 count: 250 cells/mm^3, virial load: 1000 copies mRNA/mL and ART duration: 166.98 weeks).

Supplementary Table 1.13. *Independent association with Fourier fractal (enhanced) (baseline and follow-up).*

Variables [a]	Change (95% CI)	*p*-value
Age (years)	-0.04520 (-0.07232 to -0.02712)	< 0.001
Sex (Women)	0.082 (0.038 to 0.126)	< 0.001
Smoking (Yes)	0.001 (-0.049 to 0.050)	0.977
Alcohol consumption (Yes)	0.009 (-0.033 to 0.051)	0.681
Employment (Yes)	0.027 (-0.014 to 0.067)	0.197
BMI (kg/m^2)	0.02544 (0.00064 to 0.05088)	0.033
DBP (mmHg)	0.00125 (-0.02500 to 0.02500)	0.810
Viral load (copies mRNA/mL)	-0.00061 (-0.00122 to -0.00003)	0.043
CD4 cell count (cells/mm3)	0.025 (0.025 to 0.025)	0.080
ART type (2^{nd}-line)	0.034 (-0.029 to 0.097)	0.285
ART duration (weeks)	0.017 (-0.064 to 0.099)	0.678
HIV duration (≥ 5 years)	0.003 (-0.055 to 0.049)	0.910
Timepoint (Timepoint 2 *vs.* 1)	0.041 (0.001 to 0.080)	0.046

[a]Estimates expressed as change for each increment change in confounding factors (Age: 9.04 years, BMI: 6.36 kg/m^2, DBP: 12.5 mmHg, CD4 count: 250 cells/mm^3, virial load: 1000 copies mRNA/mL and ART duration: 166.98 weeks).

Supplementary Table 1.14. *Independent association with tortuosity index (baseline and follow-up).*

Variables [a]	Change (95% CI)	*p*-value
Age (years)	0.0009 (0.0009 to 0.0009)	0.486
Sex (Women)	0.002 (-1.004 to 0.008)	0.486
Smoking (Yes)	-0.005 (-0.011 to 0.001)	0.127
Alcohol consumption (Yes)	0.0001 (-0.005 to 0.005)	0.927
Employment (Yes)	0.005 (0.0001 to 0.010)	0.040
BMI (kg/m^2)	0.00064 (-0.00636 to 0.00064)	0.079
DBP (mmHg)	0.00125 (0.00125 to 0.00125)	0.258
Viral load (copies mRNA/mL)	-0.00006 (-0.00013 to 0.00003)	0.167
CD4 cell count (cells/mm3)	0.025 (0.025 to 0.025)	0.620
ART type (2^{nd}-line)	0.006 (-0.001 to 0.013)	0.104
ART duration (weeks)	0.00300 (-0.00600 to 0.01200)	0.536
HIV duration (≥ 5 years)	-0.001 (-0.007 to 0.005)	0.798
Timepoint (Timepoint 2 *vs.* 1)	0.00010 (-0.00400 to 0.00300)	0.877

[a]Estimates expressed as change for each increment change in confounding factors (Age: 9.04 years, BMI: 6.36 kg/m^2, DBP: 12.5 mmHg, CD4 count: 250 $cells/mm^3$, virial load: 1000 copies mRNA/mL and ART duration: 166.98 weeks).

Supplementary Table 1.15. *Independent association with average tortuosity of branch segments (baseline and follow-up).*

Variables [a]	Change (95% CI)	*p*-value
Age (years)	0.000904 (0.000904 to 0.000904)	0.567
Sex (Women)	0.002 (-0.002 to 0.006)	0.408
Smoking (Yes)	-0.003 (-0.007 to 0.002)	0.288
Alcohol consumption (Yes)	0.001 (-0.003 to 0.005)	0.743
Employment (Yes)	0.003 (-0.001 to 0.007)	0.095
BMI (kg/m^2)	0.000636 (-0.006360 to 0.000636)	0.423
DBP (mmHg)	0.001250 (0.001250 to 0.001250)	0.079
Viral load (copies mRNA/mL)	-0.000064 (-0.000128 to 0.000003)	0.022
CD4 cell count (cells/mm3)	0.025 (0.025 to 0.025)	0.663
ART type (2^{nd}-line)	0.001 (-0.004 to 0.007)	0.602
ART duration (weeks)	0.001 (-0.006 to 0.008)	0.716
HIV duration (≥ 5 years)	0.0001 (-0.004 to 0.005)	0.871
Timepoint (Timepoint 2 *vs.* 1)	-0.001 (-0.004 to 0.002)	0.374

[a]Estimates expressed as change for each increment change in confounding factors (Age: 9.04 years, BMI: 6.36 kg/m^2, DBP: 12.5 mmHg, CD4 count: 250 $cells/mm^3$, virial load: 1000 copies mRNA/mL and ART duration: 166.98 weeks).

Supplementary Table 1.16. *Independent association with D0 (baseline and follow-up).*

Independent predictors	Change	*p*-value
Age (years)	-0.759 (-4.565 to 3.037)	0.683
Sex (Women)	6.344 (-0.644 to 13.332)	0.073
Smoking (Yes)	-9.110 (-16.167 to -2.052)	0.013
Alcohol consumption (Yes)	3.448 (-2.623 to 9.519)	0.261
Employment (Yes)	0.540 (-5.021 to 6.100)	0.847
BMI (kg/m^2)	-0.515 (-4.268 to 3.237)	0.781
DBP (mmHg)	-2.875 (-2.413 to 0.413)	0.085
Viral load (copies mRNA/mL)	-0.051 (-0.131 to 0.029)	0.211
CD4 cell count (cells/mm3)	0.500 (-3.500 to 4.750)	0.797
ART type (2^{nd}-line)	5.293 (-3.013 to 13.600)	0.209
ART duration (weeks)	8.605 (-2.170 to 19.380)	0.116
HIV duration (≥ 5 years)	-7.154 (-14.189 to -0.120)	0.046
Timepoint (Timepoint 2 *vs.* 1)	0.209 (-4.065 to 4.482)	0.923

[a]Estimates expressed as change for each increment change in confounding factors (Age: 9.04 years, BMI: 6.36 kg/m^2, DBP: 12.5 mmHg, CD4 count: 250 cells/mm^3, virial load: 1000 copies mRNA/mL and ART duration: 166.98 weeks).

Supplementary Table 1.17. *Independent association with D1 (baseline and follow-up).*

Independent predictors	Change	*p*-value
Age (years)	-0.588 (-3.761 to 2.576)	0.712
Sex (Women)	4.785 (-1.033 to 10.602)	0.106
Smoking (Yes)	-6.052 (-11.900 to -0.204)	0.043
Alcohol consumption (Yes)	4.533 (-0.466 to 9.532)	0.075
Employment (Yes)	0.829 (-3.725 to 5.382)	0.719
BMI (kg/m^2)	0.585 (-2.531 to 3.702)	0.712
DBP (mmHg)	-1.550 (-4.238 to 1.138)	0.256
Viral load (copies mRNA/mL)	-0.002 (-0.068 to 0.064)	0.950
CD4 cell count (cells/mm3)	-0.750 (-4.250 to 2.500)	0.626
ART type (2^{nd}-line)	5.460 (-1.371 to 12.290)	0.116
ART duration (weeks)	3.944 (-4.778 to 12.666)	0.373
HIV duration (≥ 5 years)	-7.329 (-13.048 to -1.611)	0.012
Timepoint (Timepoint 2 *vs.* 1)	1.750 (-1.601 to 5.101)	0.302

[a]Estimates expressed as change for each increment change in confounding factors (Age: 9.04 years, BMI: 6.36 kg/m^2, DBP: 12.5 mmHg, CD4 count: 250 cells/mm^3, virial load: 1000 copies mRNA/mL and ART duration: 166.98 weeks).

Supplementary Table 1.18. *Independent association with D2 (baseline and follow-up).*

Independent predictors	% Change	*p*-value
Age (years)	0.176% (-2.989 to 3.445)	0.913
Sex (Women)	5.829% (-0.256 to 12.285)	0.060
Smoking (Yes)	-8.002% (-13.679 to -1.951)	0.011
Alcohol consumption (Yes)	6.025% (0.109 to 12.291)	0.046
Employment (Yes)	-1.318% (-6.538 to 4.194)	0.628
BMI (kg/m^2)	0.891% (-2.410 to 4.306)	0.596
DBP (mmHg)	0.033% (-3.208 to 3.383)	0.984
Viral load (copies mRNA/mL)	-0.025% (-0.103 to 0.054)	0.533
CD4 cell count (cells/mm3)	2.392% (-1.568 to 6.537)	0.236
ART type (2^{nd}-line)	3.153% (-4.679 to 11.627)	0.436
ART duration (weeks)	3.579% (-7.624 to 16.141)	0.543
HIV duration (≥ 5 years)	-2.737% (-9.557 to 4.597)	0.450
Timepoint (Timepoint 2 *vs.* 1)	-4.838% (-11.175 to 1.951)	0.156

[a]Estimates expressed as % change for each increment change in confounding factors (Age: 9.04 years, BMI: 6.36 kg/m^2, DBP: 12.5 mmHg, CD4 count: 250 $cells/mm^3$, virial load: 1000 copies mRNA/mL and ART duration: 166.98 weeks).

Supplementary Table 1.19. *Independent association with arteriolar branch angle (baseline and follow-up).*

Independent predictors	Change	*p*-value
Age (years)	1.455 (-1.727 to 4.628)	0.364
Sex (Women)	-0.181 (-6.016 to 5.654)	0.951
Smoking (Yes)	3.868 (-2.208 to 9.944)	0.210
Alcohol consumption (Yes)	-2.926 (-8.167 to 2.315)	0.271
Employment (Yes)	-0.856 (-5.692 to 3.980)	0.727
BMI (kg/m^2)	3.116 (-0.064 to 6.296)	0.054
DBP (mmHg)	-2.250 (-5.025 to 0.538)	0.112
Viral load (copies mRNA/mL)	0.007 (-0.063 to 0.077)	0.839
CD4 cell count (cells/mm3)	-2.000 (-5.500 to 1.750)	0.291
ART type (2^{nd}-line)	6.899 (-0.428 to 14.226)	0.065
ART duration (weeks)	5.309 (-4.029 to 14.646)	0.263
HIV duration (≥ 5 years)	0.712 (-5.343 to 6.767)	0.817
Timepoint (Timepoint 2 *vs.* 1)	-1.856 (-5.575 to 1.864)	0.324

[a]Estimates expressed as change for each increment change in confounding factors (Age: 9.04 years, BMI: 6.36 kg/m^2, DBP: 12.5 mmHg, CD4 count: 250 $cells/mm^3$, virial load: 1000 copies mRNA/mL and ART duration: 166.98 weeks).

Supplementary Table 1.20. *Independent association with arteriolar branching optimality (baseline and follow-up).*

Independent predictors	Change	*p*-value
Age (years)	0.001 (-0.009 to 0.009)	0.447
Sex (Women)	-0.003 (-0.019 to 0.012)	0.677
Smoking (Yes)	0.001 (-0.016 to 0.018)	0.899
Alcohol consumption (Yes)	0.006 (-0.009 to 0.022)	0.393
Employment (Yes)	-0.007 (-0.021 to 0.007)	0.344
BMI (kg/m^2)	0.006 (-0.006 to 0.019)	0.050
DBP (mmHg)	0.001 (0.001 to 0.013)	0.147
Viral load (copies mRNA/mL)	0.0005 (0.0001 to 0.001)	0.110
CD4 cell count (cells/mm3)	0.025 (-0.250 to 0.250)	0.935.
ART type (2^{nd}-line)	0.013 (-0.009 to 0.034)	0.243
ART duration (weeks)	-0.019 (-0.047 to 0.010)	0.192
HIV duration (≥ 5 years)	0.001 (-0.017 to 0.019)	0.932
Timepoint (Timepoint 2 *vs.* 1)	-0.002 (-0.015 to 0.010)	0.703

[a]Estimates expressed as change for each increment change in confounding factors (Age: 9.04 years, BMI: 6.36 kg/m^2, DBP: 12.5 mmHg, CD4 count: 250 cells/mm^3, virial load: 1000 copies mRNA/mL and ART duration: 166.98).

Supplementary Table 1.21. *Independent association with arteriolar branching coefficient (baseline and follow-up).*

Independent predictors	Change	*p*-value
Age (years)	0.002 (-0.012 to 0.016)	0.772
Sex (Women)	0.018 (-0.108 to 0.145)	0.393
Smoking (Yes)	-0.010 (-0.331 to 0.131)	0.905
Alcohol consumption (Yes)	-0.014 (-0.255 to 0.226)	0.614
Employment (Yes)	-0.053 (-0.260 to 0.154)	0.365
BMI (kg/m^2)	-0.087 (-0.278 to 0.103)	0.794
DBP (mmHg)	0.019 (-0.108 to 0.140)	0.568
Viral load (copies mRNA/mL)	0.038 (-0.075 to 0.138)	0.591
CD4 cell count (cells/mm3)	-0.001(-0.004 to 0.002)	0.140
ART type (2^{nd}-line)	0.025 (0.025 to 0.250)	0.895
ART duration (weeks)	-0.019 (-0.310 to 0.271)	0.513
HIV duration (≥ 5 years)	0.120 (-0.243 to 0.484)	0.295
Timepoint (Timepoint 2 *vs.* 1)	0.125 (-0.111 to 0.361)	0.043

[a]Estimates expressed as change for each increment change in confounding factors (Age: 9.04 years, BMI: 6.36 kg/m^2, DBP: 12.5 mmHg, CD4 count: 250 cells/mm^3, virial load: 1000 copies mRNA/mL and ART duration: 166.98 weeks).

Supplementary Table 1.22. *Independent association with arteriolar mean asymmetry ratio (baseline and follow-up).*

Independent predictors	Change	*p*-value
Age (years)	-0.0090 (-0.0362 to 0.0271)	0.747
Sex (Women)	0.007 (-0.054 to 0.067)	0.829
Smoking (Yes)	0.003 (-0.060 to 0.065)	.0.926
Alcohol consumption (Yes)	0.0300 (-0.023 to 0.084)	0.268
Employment (Yes)	0.003 (-0.046 to 0.053)	0.892
BMI (kg/m^2)	0.0064 (-0.0254 to 0.0382)	0.782
DBP (mmHg)	-0.0125 (-0.0250 to 0.0250)	0.950
Viral load (copies mRNA/mL)	0.0002 (-0.0005 to 0.0009)	0.550
CD4 cell count (cells/mm3)	0.025 (0.025 to 0.025)	0.317
ART type (2^{nd}-line)	-0.0110 (-0.0860 to 0.0640)	0.778
ART duration (weeks)	-0.051 (-0.145 to 0.044)	0.292
HIV duration (≥ 5 years)	-0.0159 (-0.0770 to 0.0460)	0.610
Timepoint (Timepoint 2 *vs.* 1)	0.0370 (0.0001 to 0.0740)	0.049

[a]Estimates expressed as change for each increment change in confounding factors (Age: 9.04 years, BMI: 6.36 kg/m^2, DBP: 12.5 mmHg, CD4 count: 250 cells/mm^3, virial load: 1000 copies mRNA/mL and ART duration: 166.98 weeks).

Supplementary Table 1.23. *Independent association with arteriolar mean angular asymmetry (baseline and follow-up).*

Independent predictors	% Change	*p*-value
Age (years)	0.208 (-13.559 to 15.686)	0.936
Sex (Women)	-11.080 (-32.857 to 17.761)	0.406
Smoking (Yes)	10.408 (-17.586 to 47.571)	0.503
Alcohol consumption (Yes)	-16.247 (-34.837 to 7.895)	0.167
Employment (Yes)	-0.688 (-21.837 to 2.329)	0.948
BMI (kg/m^2)	-1.454 (-16.116 to 14.088)	0.823
DBP (mmHg)	2.920 (-10.875 to 18.850)	0.617
Viral load (copies mRNA/mL)	0.111 (-0.228 to 0.443)	0.522
CD4 cell count (cells/mm3)	5.925 (5.925 to 5.925)	0.402
ART type (2^{nd}-line)	4.232 (-33.626 to 38.676)	0.824
ART duration (weeks)	8.393 (-31.609 to 72.187)	0.727
HIV duration (≥ 5 years)	5.925 (-31.451 to 29.718)	0.718
Timepoint (Timepoint 2 *vs.* 1)	15.878 (-6.028 to 43.219)	0.166

[a]Estimates expressed as % change for each increment change in confounding factors (Age: 9.04 years, BMI: 6.36 kg/m^2, DBP: 12.5 mmHg, CD4 count: 250 $cells/mm^3$, virial load: 1000 copies mRNA/mL and ART duration: 166.98 weeks).

Supplementary Table 1.24. *Independent association with venular D0 (baseline and follow-up).*

Independent predictors	Change	*p*-value
Age (years)	3.345 (-1.627 to -1.627)	0.185
Sex (Women)	4.609 (-4.481 to -4.481)	0.316
Smoking (Yes)	3.291 (-5.677 to -5.677)	0.469
Alcohol consumption (Yes)	-4.084 (-11.678 to -11.678)	0.290
Employment (Yes)	-0.070 (-6.938 to -6.938)	0.984
BMI (kg/m^2)	-0.999 (-5.826 to -5.826)	0.681
DBP (mmHg)	1.750 (-2.300 to -2.300)	0.393
Viral load (copies mRNA/mL)	0.043 (-0.056 to -0.248)	0.389
CD4 cell count (cells/mm3)	-2.000 (-7.250 to -7.250)	0.456
ART type (2^{nd}-line)	6.192 (-4.168 to -4.168)	0.239
ART duration (weeks)	5.215 (-7.786 to -7.786)	0.429
HIV duration (≥ 5 years)	-3.270 (-11.821 to -11.821)	0.451
Timepoint (Timepoint 2 *vs.* 1)	1.607 (-3.295 to -3.295)	0.517

[a]Estimates expressed as change for each increment change in confounding factors (Age: 9.04 years, BMI: 6.36 kg/m^2, DBP: 12.5 mmHg, CD4 count: 250 cells/mm^3, virial load: 1000 copies mRNA/mL and ART duration: 166.98 weeks).

Supplementary Table 1.25. *Independent association with venular D1 (baseline and follow-up).*

Independent predictors	Change	*p*-value
Age (years)	-2.893 (-7.675 to 1.681)	0.206
Sex (Women)	0.813 (-7.723 to 9.350)	0.850
Smoking (Yes)	-2.134 (-11.079 to 6.811)	0.637
Alcohol consumption (Yes)	-0.439 (-8.109 to 7.230)	0.910
Employment (Yes)	-5.253 (-12.286 to 1.779)	0.142
BMI (kg/m^2)	2.054 (-2.614 to 6.729)	0.385
DBP (mmHg)	-1.163 (-5.113 to 2.788)	0.559
Viral load (copies mRNA/mL)	0.011 (-0.092 to 0.114)	0.831
CD4 cell count (cells/mm3)	-2.000 (-7.250 to 3.000)	0.420
ART type (2^{nd}-line)	3.081 (-7.800 to 13.962)	0.576
ART duration (weeks)	7.568 (-5.781 to 20.917)	0.264
HIV duration (≥ 5 years)	-6.891 (-15.546 to 1.764)	0.118
Timepoint (Timepoint 2 *vs.* 1)	-0.392 (-5.755 to 4.971)	0.885

[a]Estimates expressed as change for each increment change in confounding factors (Age: 9.04 years, BMI: 6.36 kg/m^2, DBP: 12.5 mmHg, CD4 count: 250 cells/mm^3, virial load: 1000 copies mRNA/mLand ART duration: 166.98 weeks).

Supplementary Table 1.26. *Independent association with D2 (baseline and follow-up).*

Independent predictors	Change	*p*-value
Age (years)	3.399 (-1.483 to 8.281)	0.170
Sex (Women)	4.490 (-4.454 to 13.435)	0.321
Smoking (Yes)	2.378 (-6.571 to 11.327)	0.600
Alcohol consumption (Yes)	-5.307 (-12.924 to 2.310)	0.171
Employment (Yes)	1.410 (-5.510 to 8.331)	0.688
BMI (kg/m^2)	-2.239 (-7.015 to 2.538)	0.355
DBP (mmHg)	2.963 (-1.100 to 7.013)	0.151
Viral load (copies mRNA/mL)	0.036 (-0.064 to 0.136)	0.474
CD4 cell count (cells/mm3)	-2.250 (-7.500 to 3.000)	0.393
ART type (2^{nd}-line)	6.656 (-3.788 to 17.101)	0.210
ART duration (weeks)	4.121 (-9.041 to 17.284)	0.537
HIV duration (≥ 5 years)	-2.769 (-11.400 to 5.861)	0.527
Timepoint (Timepoint 2 *vs.* 1)	0.973 (-4.042 to 5.988)	0.701

[a]Estimates expressed as change for each increment change in confounding factors (Age: 9.04 years, BMI: 6.36 kg/m^2, DBP: 12.5 mmHg, CD4 count: 250 cells/mm^3, virial load: 1000 copies mRNA/mL and ART duration: 166.98 weeks).

Supplementary Table 1.27. *Independent association with venular branching angle (baseline and follow-up).*

Independent predictors	Change	*p*-value
Age (years)	-0.506 (-2.775 to 1.772)	0.661
Sex (Women)	0.718 (-3.474 to 4.909)	0.734
Smoking (Yes)	3.861 (-0.335 to 8.058)	0.071
Alcohol consumption (Yes)	-0.511 (-4.134 to 3.111)	0.780
Employment (Yes)	2.899 (-0.401 to 6.199)	0.085
BMI (kg/m^2)	-0.560 (-2.811 to 1.692)	0.620
DBP (mmHg)	-0.288 (-2.288 to 1.725)	0.780
Viral load (copies mRNA/mL)	-0.007 (-0.055 to 0.040)	0.754
CD4 cell count (cells/mm3)	-0.250 (-2.750 to 2.250)	0.909
ART type (2^{nd}-line)	2.043 (-2.814 to 6.900)	0.406
ART duration (weeks)	2.648 (-3.792 to 9.088)	0.417
HIV duration (≥ 5 years)	-2.142 (-6.381 to 2.097)	0.319
Timepoint (Timepoint 2 *vs.* 1)	0.091 (-2.495 to 2.676)	0.945

[a]Estimates expressed as change for each increment change in confounding factors (Age: 9.04 years, BMI: 6.36 kg/m^2, DBP: 12.5 mmHg, CD4 count: 250 cells/mm^3, virial load: 1000 copies mRNA/mL and ART duration: 166.98 weeks).

Supplementary Table 1.28. *Independent association with venular branching optimality (baseline and follow-up).*

Independent predictors	Change	*p*-value
Age (years)	-0.00904 (-0.01808 to 0.00090)	0.166
Sex (Women)	-0.00100 (-0.01800 to 0.01700)	0.947
Smoking (Yes)	-0.00300 (-0.02100 to 0.01490)	0.741
Alcohol consumption (Yes)	-0.00500 (-0.02000 to 0.01100)	0.558
Employment (Yes)	-0.00100 (-0.01500 to 0.01300)	0.901
BMI (kg/m^2)	0.00064 (-0.01272 to 0.00636)	0.867
DBP (mmHg)	0.00125 (-0.01250 to 0.01250)	0.883
Viral load (copies mRNA/mL)	-0.00003 (-0.00026 to 0.00016)	0.702
CD4 cell count (cells/mm3)	0.02500 (0.02500 to 0.02500)	0.227
ART type (2^{nd}-line)	0.00800 (-0.01400 to 0.02900)	0.488
ART duration (weeks)	0.01300 (-0.01400 to 0.04000)	0.348
HIV duration (≥ 5 years)	-0.00900 (-0.02700 to 0.00900)	0.318
Timepoint (Timepoint 2 *vs.* 1)	-0.00300 (-0.01400 to 0.00800)	0.572

[a]Estimates expressed as change for each increment change in confounding factors (Age: 9.04 years, BMI: 6.36 kg/m^2, DBP: 12.5 mmHg, CD4 count: 250 cells/mm^3, virial load: 1000 copies mRNA/mL and ART duration: 166.98 weeks).

Supplementary Table 1.29. *Independent association with venular mean branching coefficient (baseline and follow-up).*

Independent predictors	Change	*p*-value
Age (years)	0.235 (0.018 to 0.443)	0.034
Sex (Women)	0.124 (-0.269 to 0.516)	0.533
Smoking (Yes)	0.238 (-0.165 to 0.641)	0.245
Alcohol consumption (Yes)	-0.079 (-0.425 to 0.267)	0.652
Employment (Yes)	0.267 (-0.049 to 0.584)	0.097
BMI (kg/m^2)	-0.108 (-0.318 to 0.108)	0.321
DBP (mmHg)	0.125 (-0.063 to 0.300)	0.198
Viral load (copies mRNA/mL)	-0.001 (-0.006 to 0.004)	0.673
CD4 cell count (cells/mm3)	0.025 (-0.250 to 0.250)	0.580
ART type (2^{nd}-line)	-0.016 (-0.496 to 0.464)	0.946
ART duration (weeks)	-0.087 (-0.693 to 0.520)	0.778
HIV duration (≥ 5 years)	0.198 (-0.197 to 0.593)	0.324
Timepoint (Timepoint 2 *vs.* 1)	-0.005 (-0.241 to 0.230)	0.964

[a]Estimates expressed as change for each increment change in confounding factors (Age: 9.04 years, BMI: 6.36 kg/m^2, DBP: 12.5 mmHg, CD4 count: 250 cells/mm^3, virial load: 1000 copies mRNA/mL and ART duration: 166.98 weeks).

Table 6.30. *Independent association with venular mean asymmetry ratio (baseline and follow-up).*

Independent predictors	Change	*p*-value
Age (years)	-0.04520 (-0.08136 to -9.04100)	0.027
Sex (Women)	-0.013 (-0.085 to -0.941)	0.719
Smoking (Yes)	-0.009 (-0.078 to -0.941)	0.784
Alcohol consumption (Yes)	0.014 (-0.043 to -0.929)	0.635
Employment (Yes)	-0.052 (-0.103 to -1.001)	0.045
BMI (kg/m^2)	0.03180 (-0.00636 to -6.34900)	0.080
DBP (mmHg)	-0.025 (-0.050 to -12.49990)	0.111
Viral load (copies mRNA/mL)	0.00003 (-0.00070 to -0.00800)	0.930
CD4 cell count (cells/mm3)	0.025 (0.025 to 0.025)	0.527
ART type (2^{nd}-line)	0.025 (-0.052 to -0.898)	0.518
ART duration (weeks)	0.050 (-0.045 to 0.146)	0.298
HIV duration (≥ 5 years)	-0.022 (-0.085 to -0.959)	0.486
Timepoint (Timepoint 2 *vs.* 1)	-0.005 (-0.040 to -0.970)	0.787

[a]Estimates expressed as change for each increment change in confounding factors (Age: 9.04 years, BMI: 6.36 kg/m^2, DBP: 12.5 mmHg, CD4 count: 250 cells/mm^3, virial load: 1000 copies mRNA/mL and ART duration: 166.98 weeks).

Supplementary Table 1.31. *Independent association with venular mean angular asymmetry (baseline and follow-up).*

Independent predictors	Change	*p*-value
Age (years)	0.859 (-4.402 to 6.129)	0.745
Sex (Women)	-4.698 (-14.298 to 4.902)	0.333
Smoking (Yes)	-2.166 (-11.552 to 7.221)	0.649
Alcohol consumption (Yes)	-1.499 (-9.398 to 6.400)	0.708
Employment (Yes)	0.920 (-6.195 to 8.034)	0.799
BMI (kg/m^2)	-1.730 (-6.799 to 3.333)	0.499
DBP (mmHg)	0.200 (-3.963 to 4.350)	0.927
Viral load (copies mRNA/mL)	-0.030 (-0.133 to 0.073)	0.562
CD4 cell count (cells/mm3)	-1.750 (-70.500 to 3.750)	0.543
ART type (2^{nd}-line)	5.388 (-5.431 to 16.207)	0.326
ART duration (weeks)	-1.308 (-14.659 to 12.043)	0.847
HIV duration (≥ 5 years)	11.804 (3.024 to 20.584)	0.009
Timepoint (Timepoint 2 *vs.* 1)	-0.667 (-5.670 to 4.337)	0.792

[a]Estimates expressed as change for each increment change in confounding factors (Age: 9.04 years, BMI: 6.36 kg/m^2, DBP: 12.5 mmHg, CD4 count: 250 cells/mm^3, virial load: 1000 copies mRNA/mL and ART duration: 166.98 weeks).